Università degli Studi di Milano

Scuola di Dottorato in Medicina Molecolare

Dipartimento di Scienze e Tecnologie Biomediche

Curriculum di *Genomica, Proteomica e Tecnologie Correlate*

Ciclo XXIV

Settore Disciplinare: BIO-10

Anno Accademico 2010/2011

Dottorando: Dr.ssa Valentina TINAGLIA

Matricola: R08079

INTEGRATED GENOMICS ANALYSIS OF GENE AND MICRORNA EXPRESSION PROFILES IN CLEAR CELL RENAL CARCINOMA CELL LINES

Direttore della Scuola: Ch.mo Prof. Mario Clerici

Tutore: Prof.ssa Cristina Battaglia

Un grazie speciale a Mamma, Papà ed Enzo
per la loro infinita pazienza e il loro amore.

CONTENTS

SOMMARIO

Il carcinoma renale (RCC) è la neoplasia più frequente tra quelle che colpiscono il rene in età adulta e rappresenta il 2-3% di tutti i carcinomi umani. Il carcinoma renale a cellule chiare (ccRCC) è l'istotipo più frequente (75-80%), invasivo e metastatico tra i sottotipi di RCC. Il gene von Hippel-Lindau (*VHL*), che è il principale oncosoppressore coinvolto negli stadi iniziali della tumorigenesi dell'RCC, è soggetto ad inattivazione completa, per effetto combinato di mutazioni, delezioni e metilazione del promotore, nella maggior parte dei ccRCC sporadici e in tutte le forme ereditarie. Definire la prognosi dei casi di carcinoma renale è importante per operare scelte cliniche riguardo il trattamento dei pazienti, ma a volte la diagnosi differenziale risulta piuttosto difficile perché gli istotipi di RCC possono avere caratteristiche istopatologiche sovrapponibili, risultando quindi indistinguibili all'indagine microscopica. In questi ultimi anni, nell'ambito di diverse patologie neoplastiche, i profili di espressione genica ottenuti tramite tecnologia *microarray* si sono rivelati un potente strumento per classificare meglio i sottotipi tumorali e identificare nuovi marcatori molecolari potenzialmente utili per applicazioni cliniche. Infatti, studiando il profilo trascrittomico del tumore si possono mettere in luce geni funzionalmente correlati al decorso clinico dei pazienti, alla risposta alla terapia e alla sopravvivenza. Recentemente è stato dimostrato che anche i microRNA (miRNA) sono coinvolti nella tumorigenesi, suggerendo che essi potrebbero funzionare sia come oncosoppressori che come oncogeni. I miRNA sono piccole molecole di RNA a singolo filamento non codificanti, che funzionano come regolatori post-trascrizionali negativi dell'espressione genica in animali, piante e virus, e sono coinvolti in molti processi biologici, come il differenziamento delle cellule ematopoietiche, l'apoptosi, la proliferazione cellulare e lo sviluppo degli organi. I profili di espressione dei geni e dei miRNA sono strettamente correlati, in quanto essi lavorano cooperativamente per creare reti regolatrici. Pertanto, l'approccio di analisi genomica integrata potrebbe essere un utile strumento per chiarire le complesse relazioni che stanno alla base di queste reti.

Lo scopo del mio progetto di dottorato è stato quello di ricostruire reti di regolazione post-trascrizionale miRNA-geni coinvolte nella biologia del ccRCC, utilizzando i profili di espressione dei geni e dei miRNA, ottenuti tramite tecnologia *microarray* ad alta densità Affymetrix, di tre linee cellulari di carcinoma renale confrontati con quelli di una linea cellulare renale normale. Mediante un'analisi di arricchimento funzionale, abbiamo individuato geni e miRNA espressi in modo differenziale che risultano associati all'RCC e sono coinvolti in *pathway* rilevanti per questa patologia, come l'ipossia, il meccanismo di trasduzione del segnale mediato da p53, l'adesione focale, l'angiogenesi e il *pathway* di mTOR. Mediante l'analisi integrata dei profili di espressione di geni e miRNA, abbiamo ricostruito reti di regolazione potenzialmente attive che coinvolgono miRNA e i loro geni bersaglio. Mediante PCR quantitativa, abbiamo validato i livelli di espressione di alcune coppie miRNA-gene, confermando così la loro anti-correlazione.

I risultati di questo studio hanno dimostrato che le linee cellulari di carcinoma renale possono essere un buon modello *in vitro* per lo studio dell'RCC, in quanto i profili di espressione di geni e miRNA di queste linee sono comparabili ai dati pubblici ottenuti su tessuti tumorali renali. In questo contesto, l'approccio di analisi genomica integrata potrebbe aiutare ad identificare reti di regolazione post-trascrizionale e quindi potenziali marcatori funzionalmente rilevanti per la patologia. Ad ogni modo, chiarire il ruolo effettivo delle reti miRNA-geni nel contesto della progressione dell'RCC necessiterà sicuramente di ulteriori indagini.

ABSTRACT

Renal cell carcinoma (RCC) is the most common neoplasm of the adult kidney, accounting for a total of 2-3% of adult neoplasias, and it arises from the renal epithelium. Clear cell renal cell carcinoma (ccRCC) is the most common, invasive and metastatic among RCC subtypes, representing 75-80% of kidney primary malignancies. The von Hippel-Lindau (*VHL*) gene, which is the main tumor suppressor gene involved in early steps of RCC tumorigenesis, undergoes complete inactivation by mutation, deletion, and promoter methylation in the majority of sporadic ccRCCs and in all inherited forms. Defining the prognosis for RCC cases is important for both decision-making and counseling patients, but sometimes the diagnosis is difficult because tumor subtypes have overlapping histo-pathological features, thus resulting undistinguishable by microscopy investigation. In recent years, in several human cancers, microarray gene expression profiling proved to be a powerful tool to better classify tumor subtypes and to identify novel molecular biomarkers potentially useful for clinical applications. In fact, tumor transcriptomic profiling may identify patterns of genes that are functionally related to patients' prognosis, response to therapy and overall survival. Recent evidences have shown that microRNA (miRNA) molecules are involved in tumorigenesis, indicating that miRNAs might function as both tumor suppressors and oncogenes, and their role in RCC pathogenesis is now emerging. miRNAs are small single-stranded non-protein-coding RNA molecules, that function as negative post-transcriptional gene regulators in animals, plants and viruses, and are involved in many biological processes, also including haematopoietic cell differentiation, apoptosis, cell proliferation and organ development. miRNA and gene expression patterns are closely related, since they cooperatively work to create gene regulatory networks. Therefore, integrative genomics approach might be a useful tool to elucidate the complex relationships underlying these networks.

The aim of my PhD fellowship work was to reconstruct miRNA-gene post-transcriptional regulatory networks involved in RCC biology, using miRNA and gene expression profiles of three RCC cell lines compared to a normal one, obtained by Affymetrix high-density microarray technology. We calculated differentially expressed genes and miRNAs, and, by functional enrichment analysis, we identified genes and miRNAs that were already known to be associated with RCC and involved in relevant pathways for this pathology, such as hypoxia, p53 signaling, focal adhesion, angiogenesis and mTOR signaling. Through integrated analysis of miRNA-gene expression profiles, we reconstructed potentially active regulatory networks involving miRNAs and their predicted target genes. We validated some miRNA-gene pairs by quantitative PCR, thus confirming their anti-correlated expression levels.

Our results demonstrated that RCC cell lines can be an useful *in vitro* model for RCC pathology, since they showed gene and miRNA expression profiles similar to renal tumoral tissues, as obtained by comparing our results with published data. The analysis of the correlations between gene and miRNA expression profiles using a genome-wide integrative approach could help the identification of both post-transcriptional regulatory networks and novel candidate markers functionally relevant for RCC pathology. However, further investigations are necessary to elucidate the actual role of miRNA-gene networks in the context of RCC progression and outcome.

1 INTRODUCTION

1.1 Renal Cell Carcinoma

1.1.1 Epidemiology

Kidney cancer is one of the major human malignancies and leading cause of cancer mortality, with approximately 280,000 new cases diagnosed in worldwide in 2008 (Ferlay *et al.*, 2010b; Ljungberg *et al.*, 2011). Renal cell carcinoma (RCC) is the most common type of kidney cancer (80-90%), accounting for a total of 2-3% of adult neoplasias (Cohen and McGovern, 2005a; Hansel, 2006). The incidence of kidney cancer is various, the highest rates are in Europe, North America and Australia, while rates are low in Japan, India, Africa and China. In the 27 European Union countries, the age-standardized kidney cancer incidence per 100,000 Europeans are 15,8 for males and 7,1 for females; in particular, in Italy the estimated incidence rate is 15,2 for males and 6,1 for females (Levi *et al.*, 2008h). In regards to the mortality rates, there is the same tendency: the highest in North America, Europe, Australia/New Zealand, whereas the lowest rates are in Africa and Asia. Globally, in 2008, 116,000 deaths were reported, and specifically, the rates were about double in men than in women (Ferlay *et al.*, 2010b). A male predominance exists (male:female ratio = 1,6:1,0) and the peak incidence is in advanced age (60-70 years). Overall, approximately 2-3% of RCCs are familial, affecting patients at younger ages, while the most RCC are sporadic (Cohen and McGovern, 2005a; Ljungberg *et al.*, 2011). The differences about the incidence of RCC among these populations may be due to differences in frequency of diagnostic imaging, genetic background, lifestyle and environmental risk factors. Established risk factors for RCC are tobacco (Hunt *et al.*, 2005b; Parker *et al.*, 2003a), overweight (Chow *et al.*, 2000; Renehan *et al.*, 2008), hypertension and use of antihypertensive medications (Chow *et al.*, 2000), acquired renal cystic disease (Nouh *et al.*, 2010), reproductive-related factors, among women, including the use of oral contraceptives and hormone replacement therapy (Kabat *et al.*, 2007). Lifestyle, especially nutritional factors and diet, are very important in the RCC development, and, nevertheless RCC is not an occupational disease, some exposure might increase RCC risk, for example exposure to trichloroethylene, perchloroethylene and arsenic compounds (Kelsh *et al.*, 2010; Ljungberg *et al.*, 2011). These last factors have been implicated in renal cell cancer risk, but the evidence remains inconclusive.

1.1.2 Clinical features

The cases of RCCs are symptomatic, with a wide spectrum of symptoms, including flank pain, flank mass and hematuria. There are also nonspecific symptoms, such as fatigue, weight loss and abdominal pain. Occasionally, patients may present with paraneoplastic syndromes, such as hypercalcemia, gynecomastia, and polycythemia. Surgical excision (nefrectomy) of the tumor at a localized stage remains the mainstay for curative therapy, but a quarter of the patients present with advanced disease, including locally invasive or metastatic renal cell carcinoma, and die following the removal of a confined tumor (Hansel, 2006). The median survival period for a patient in advanced disease is about 13 months and a 5-year survival rate of less than 20% (Banumathy and Cairns, 2010; Cohen and McGovern, 2005a). Lung, bone, followed by regional lymphonodes, liver and brain are the most common sites of metastases. Unusual sites of metastases, including the thyroid gland, heart, spleen and pancreas may be involved many years after initial diagnosis (Hansel, 2006).

Defining the prognosis of RCC is important for both decision-making and counseling patients, but sometimes the diagnosis is difficult because tumor subtypes have overlapping microscopic characteristics. The actual renal tumor classification system is based on morphology and genetic differences, therefore, it's necessary to use molecular methods to optimize diagnosis and clinical management. Prognosis is closely related to the stage of disease, in fact, nowadays, the tumor stage at the presentation is the most available predictor of the post-operative clinical course of a localized RCC. To date the staging system used only for RCC is the TNM (tumor, node, metastasis) staging system developed by the Union for International Cancer Control (UICC) (**Figure 1**) (Guinan *et al.*, 1997). The categories included in this system are: T, referred to the time of diagnosis (from T1 to T4 based on the increasing size of the primary tumor mass), N, related to the tumor spreading to regional lymph nodes (N0: no lymph node metastasis, N1-N3: increase number of regional lymph nodes), M, that is the presence of distant metastases (M0 and M1 indicate absence and presence of distant metastases, respectively). The American Joint Committee on Cancer (AJCC) defined four stages to classify RCC at the time of diagnosis using the TNM system: Stage I, small tumor (< 7 cm in diameter) limited to one kidney, no evidence of lymph node involvement nor metastatic disease; Stage II, larger tumor (> 7 cm in diameter) limited to one kidney, no evidence of lymph node involvement nor metastatic disease; Stage III, tumor invades major veins or adrenal gland, one regional lymph node involved, no distant metastases; Stage IV, large tumor that extend into surrounding tissues, more than one regional lymph node involved and/or metastases to distant locations (Guinan *et al.*, 1997). After tumor stage, the second most important prognostic parameter is the nuclear differentiation grade, proposed by Fuhrman (Fuhrman *et al.*, 1982). Nuclear features are scored as follows: Grade I, small and uniform nuclei; Grade II, granular open chromatin without conspicuous nucleoli; Grade III, prominent nucleoli identified at 10x magnification; Grade IV, nuclear pleomorphism and macronucleoli.

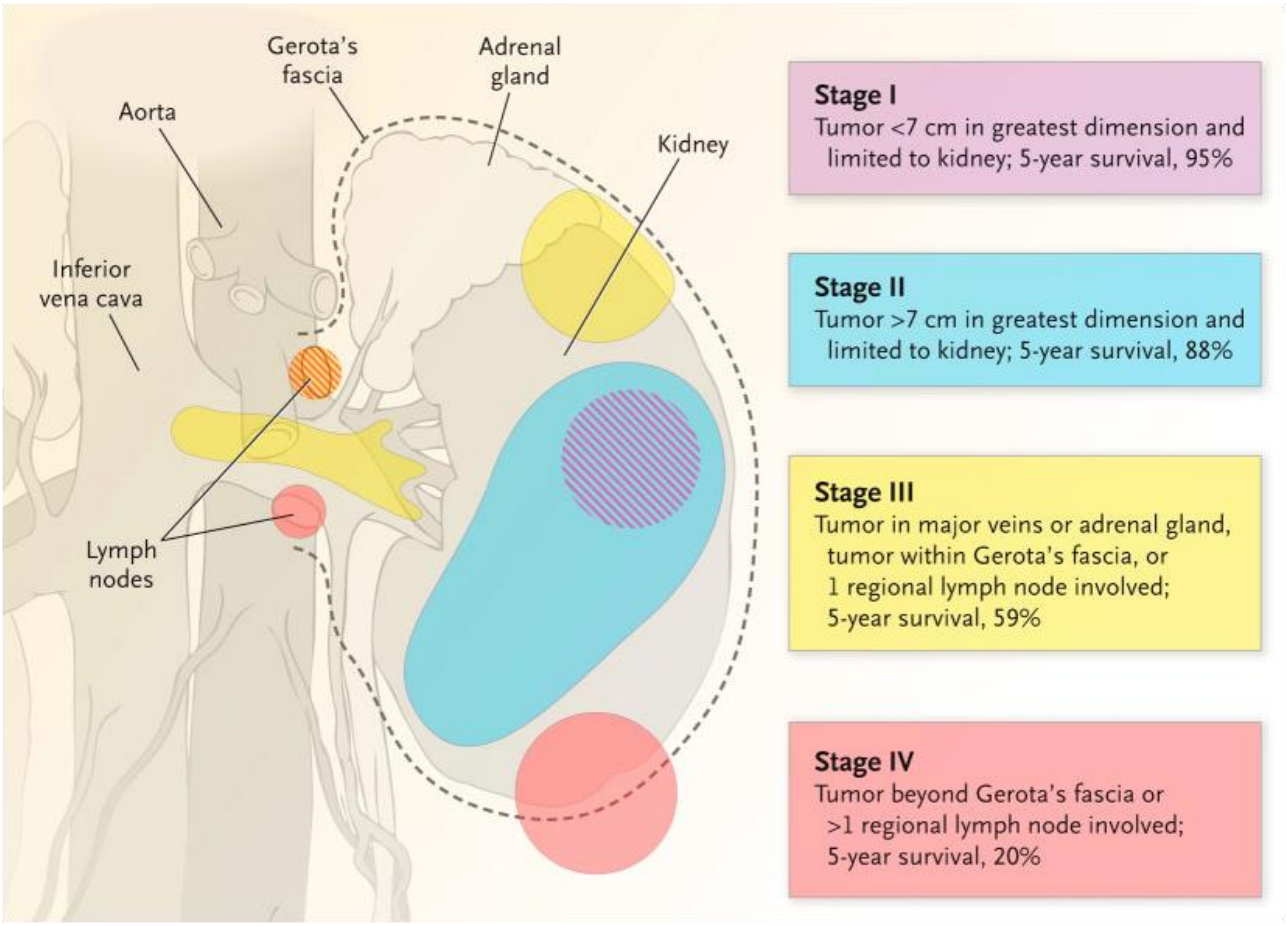

Figure 1. Staging overview and 5-year survival rates for renal cancer. Survival data are based on the 1997 tumor-node-metastasis (TNM) staging guidelines (Adapted from Cohen and McGovern, NEJM, 2005).

1.1.3 Clinical cytogenetic and molecular characteristics of renal tumors

RCC arises from the renal epithelium, it is a heterogeneus pathology, with several morphological subtypes, each subtype has morphologic and molecular features different from the others, and it's associated to a peculiar clinical course, malignant potential and response to therapy. The current World Health Organization (WHO) classification of RCC distinguishes five sporadic subtypes: clear cell (also called conventional, 75-80%), papillary (10%), chromophobe (5%), oncocytoma (5%), collecting duct (<1%), and unclassified. This classification correlates with tumor progression, while the histologic type is very important to predict the clinical and biological features associated with the progression of RCC tumors (Thoenes *et al.*, 1986). As mentioned above, RCC differential diagnosis is sometimes difficult due to heterogeneous histologic features and overlapped microscopic characteristics among subtypes, thus, the role of molecular diagnostics is very important in clinical management (Kovacs, 1993c). Generally, tumors with numerous chromosomal changes tend to be more aggressive than are those with a single abnormality.

The classification system approved by the WHO distinguishes sporadic RCCs in the following major subtypes (Cohen and McGovern, 2005; Hansel, 2006; Meloni-Ehrig, 2002):

Clear cell renal cell carcinoma (ccRCC) that is the most common, invasive and metastatic malignancy subtype, representing 75-80% of primary malignancies of the kidney. Primarily solitary lesion arises within the cortex of the kidney and the proximal renal tubule cell is the cell of origin. It can be familial, associated to

the von Hippel-Lindau (VHL) disease, or in most cases, sporadic. Gross examination reveals a rounded, fairly well-circumscribed yellow-orange lesion with multifocal hemorrhage and necrosis. Microscopic examination demonstrates a variety of growth patterns, including alveolar, solid and acinar patterns surrounded by thin-walled blood vessels. Cells tipically have a clear cytoplasm containing lipids and glycogen; occasionally, eosinophilic granular cytoplasm may be detected. The typical genomic signature of this histotype includes a deletion or unbalanced translocation involving the short arm of chromosome (chr) 3 and resulting in loss of specific small regions, including 3p25-26, spanning the *VHL* gene, 3p21-22, and 3p13-14. Deletions of chr 3p are highly specific for ccRCC and are not observed in any other subtypes. Additional loci affected by deletion are chromosomal arms 3p, 6q, 8p, 9p, 14q and by amplification are chrs 5q and 7 (Cohen and McGovern, 2005; Hansel, 2006). Alteration of the *VHL*, which is a tumor suppressor gene, by mutation, loss of heterozygosity (LOH), and promoter methylation, occurs in a majority of sporadic ccRCCs and in all inherited forms (Gordan *et al.*, 2008). During my PhD fellowship work, I focused my research activity on this hystologic subtype of RCC;

Papillary renal cell carcinoma (pRCC), which is a malignant neoplasm that presents similarly to ccRCC and is primarily distinguished on a pathologic basis, arising from cells of the proximal renal tubule. It's frequently sporadic, but pRCC is rarely found as a component of hereditary papillary renal cancer, hereditary leiomyomatosis and RCC, and Birt-Hogg-Dubè syndrome. This subtype is more commonly multifocal and bilateral than other subtypes of RCC. On gross examination, pRCC appears well-circumscribed and yellow-brown with multiple regions of hemorrhage and necrosis; commonly, cystic degeneration and papillary structures may be identified. Microscopic examination reveals papillary or tubopapillary growth patterns. Cells usually show reduced cytoplasm with granular chromatin. Frequently, foamy and hemosiderin-laden macrophages are observed within the papillae. In recent years, pRCC has been subdivided into type 1 and type 2 lesions, based on cellular morphology and patient outcome, although this classification remains somewhat controversial. Type 1 lesions contain a single layer of small cells with little cytoplasm that rest on the underlying fibrovascular cores, whereas type 2 lesions contain pseudostratified cells with abundant eosinophilic cytoplasm and nuclear atypia. Overall, type 2 lesions demonstrate poorer patient survival. The most common alterations are trisomy 7 and 17 and loss of chromosome Y Chromosome 7 harbors the *MET* proto-oncogene (hepatocyte growth factor receptor), that is duplicated in 75% of sporadic papillary cases;

Chromofobe renal cell carcinoma (chRCC) has a mortality rate of less than 10% and only rare distant metastases. It arises from the intercalated cells of the renal collecting duct and may occur in association with Birt-Hogg-Dubè syndrome. Generally, chRCC presents with similar features to ccRCC. Gross examination reveals a slightly lobulated, light brown cut surface with small areas of hemorrhage. A distinguishing feature is the transition to a gray coloration of the lesion following fixation. Microscopic examination identifies compact growth pattern and tumor cells admixed with broad septa and thick-walled, hyalinized blood vessels. Cells appear as a mixture of large and polygonal elements, with pale cytoplasm and prominent cell membranes, and smaller ones, containing a granular, eosinophilic cytoplasm. Binucleated cells are occasionally seen. Nuclei commonly demonstrate a wrinkled appearance with perinuclear halos. A Hale's colloidal iron stain reveals a blue cytoplasmic staining pattern of the lesional cells and is helpful in the diagnosis. Despite the good prognosis generally associated with chromophobe RCC, these lesions demonstrate a surprisingly extensive loss of chromosomes, including chrs -1, -2, -6, -10, -13, -17, and -21,

resulting in strong hypodiploid DNA content. Additionally, mutations of p53, loss of heterozygosity (LOH) of 10q23.3 in the region of *PTEN* (phosphatase and tensin homolog), and telomere shortening have been reported in these lesions;

Oncocytoma is a benign neoplasm, arising from the intercalated cells of the kidney. This neoplasm occurs sporadically, as well as part of Birt-Hogg-Dubè syndrome. Similarly to other malignant renal neoplasms, these lesions occur in adulthood. On gross examination, it appears as a well-circumscribed, brown lesion with a central scar in one third of cases. On microscopic analysis, the lesion contains nests, acini or tubular structures, comprised of round or polygonal cells with dense eosinophilic cytoplasm filled with mitochondria. Genetic analysis reveals a mixture of cells with normal and abnormal karyotypes. Regarding genetic features, rarely, loss of chrs 1 and 14 and translocation between chromosomal arm 11q13 and other chromosomes (e.g. chr 5q35);

Collecting-duct renal cell carcinoma accounts for less than 1% of all cases of RCC and is typically an aggressive tumor. It arises from the epithelium of the ducts of Bellini in the distal nephron. This tumor affects younger patients and has a survival time ranging from 7 to 18 months. Caused by their medullary localization and the associated hyperplastic and dysplastic epithelial lesions of collecting ducts in the vicinity of the tumor, papillary carcinomas have been classified as collecting-duct RCC. Cytogenetic studies have shown chromosome changes that differ from the ones seen in pRCC (i.e., chrs +7 and +17) as well as from those seen in nonpapillary renal tumors (i.e., del(3p)).

1.1.3.1 Familial renal cell carcinoma

Although the majority of RCCs occurs sporadically, approximately 1 to 4% of all RCCs diagnosed are familial forms. Generally, RCCs arising in the context of heritable syndromes occur at younger ages and are often bilateral and multiple, in contrast to the sporadic forms, which are often solitary. The genetic abnormalities underlying familial renal neoplasms are often distinct from those identified in sporadic forms, with the exception of 3p loss, which encompasses the *VHL* gene locus, in ccRCC. These familial cases have been very useful to understand genetic aspects at the origin of renal carcinogenesis.

The major forms of familial renal cell carcinoma include VHL syndrome, hereditary clear cell renal carcinoma and hereditary papillary renal cell carcinoma.

von Hippel-Lindau (VHL) syndrome: is the most frequent cause of familial RCC, with an incidence of approximately 1/36,000 live births. It's a rare, autosomal dominant, familial cancer syndrome, characterized by hemangioblastomas of the central nervous system and retina, clear cell RCC, renal cysts, pancreatic cysts and neuroendocrine tumors, and inner ear tumors. The risk of ccRCC in VHL disease is more than 70% by the age of 60 years and is the most common cause of death in these patients (Maher and Kaelin, 1997). This syndrome is caused by germline loss-of-function mutations of the *VHL* tumor suppressor gene on chr 3p25-26. Inactivating mutations of the *VHL* gene were observed in 100% of ccRCCs associated to the VHL disease and in 50-60% of sporadic ccRCC cases, thus suggesting its crucial role in the origin of this malignancy. Germline mutations of the *VHL* gene have been found in almost all families with VHL disease, and somatic inactivation of *VHL* by promoter methylation (5% to 19% cases) or mutation (33% to 66%) has been reported in up to 91% of patients with sporadic ccRCC (Choueiri *et al.*, 2008; Linehan *et al.*, 2010).

Loss of the remaining *VHL* allele (LOH) leads to decrease in functional VHL protein (pVHL) and, subsequently, to the induction of hypoxia-regulated genes including potent pro-angiogenic proteins. There are strong genotype-phenotype correlations in VHL disease. Distinct mutation events in hereditary VHL disease lead to four separate phenotypes, classified as follows: type 1, low risk of pheochromocytoma; type 2, high risk of pheochromocytoma, and in particular, type 2A, low risk of RCC; type 2B, high risk of RCC; type 2C, familial pheochromocytoma without hemangioblastoma and ccRCC. Large deletion events with premature protein truncation or complete protein loss occur in type 1 patients, and missense mutations commonly occur in type 2 patients (Cowey and Rathmell, 2009). In all affected cases, inherited germline mutations affecting one *VHL* allele are followed by mutation, methylation, or loss of the remaining wild-type allele, according to Knudson's "two-hits model". Detection of *VHL* gene alterations proved that the vast majority of histologically confirmed ccRCC tumors possesses genetic or epigenetic alteration of the *VHL* gene and support the hypothesis that *VHL* alteration is an early event in ccRCC carcinogenesis. Thus, *VHL* mutations might have important implications for disease prognosis and as a potential predictive marker for response to therapy.

1.1.3.1.1 VHL gene

The *VHL* gene, cloned in 1993 by an international cooperative study (Latif *et al.*, 1993b), lies on chromosome 3p26-p25 and encodes for a 213-aminoacids tumor suppressor protein (pVHL). This gene is composed by three exons of, respectively, 340, 123 and 179 bp, with two translation initiation sites resulting in two protein isoforms of 172 and 213 aminoacids, pVHL30 and pVHL19, both seeming to have tumor suppressor activity. While no alterations occur in the first half of exon 1, 50% of mutations mapped on the second half of exon 1, 31% in exon 2 and 19% in exon 3; frameshift mutations, due to deletions or insertions, are the most common alterations (68%), followed by missense and nonsense nucleotide substitutions. In the familial cases, germline mutations are followed by mutation, methylation, or loss of the remaining wild-type *VHL* allele in the tumor, and in sporadic cases, the biallelic loss-of-function occurs through a combination of somatic allele loss, mutation and/or methylation (Banks *et al.*, 2006).

This gene is an important regulator of the hypoxia pathway via the hypoxia-inducible factors (HIFs), which is vital to tumor survival in low-oxygen conditions. pVHL functions as part of an E3 ubiquitin ligase that ubiquitylates the family of HIFs proteins and targets them for degradation by the proteasome. Defective pVHL causes an accumulation of HIFs and the activation of the hypoxic pathway of gene expression (Cohen and McGovern, 2005a; Cowey and Rathmell, 2009; Gordan *et al.*, 2008; Iwai *et al.*, 1999). pVHL normally functions as the substrate recognition component of a multisubunit ubiquitin ligase complex that also contains elongin B, elongin C, Cul2, and Rbx1 (also called Roc1) (**Figure 2**). *VHL* is inactivated in most of the sporadic ccRCCs, explaining its high vascularity. Hypoxia-inducible factor has a main role in renal tumorigenesis by acting as a transcriptional factor for genes involved in angiogenesis, tumor cell proliferation, cell survival and progression, metastatic spread, apoptosis, and glucose metabolism. HIFs are heterodimeric basic helix-loop-helix/PAS proteins composed by an α subunit (HIF-1α, HIF-2α and also HIF-3α subunits) and a β subunit (HIF-1β or ARNT, aryl hydrocarbon receptor nuclear translocator). HIF-1β is constitutively present, while the HIF-α members are highly instable, except under low oxygen concentrations.

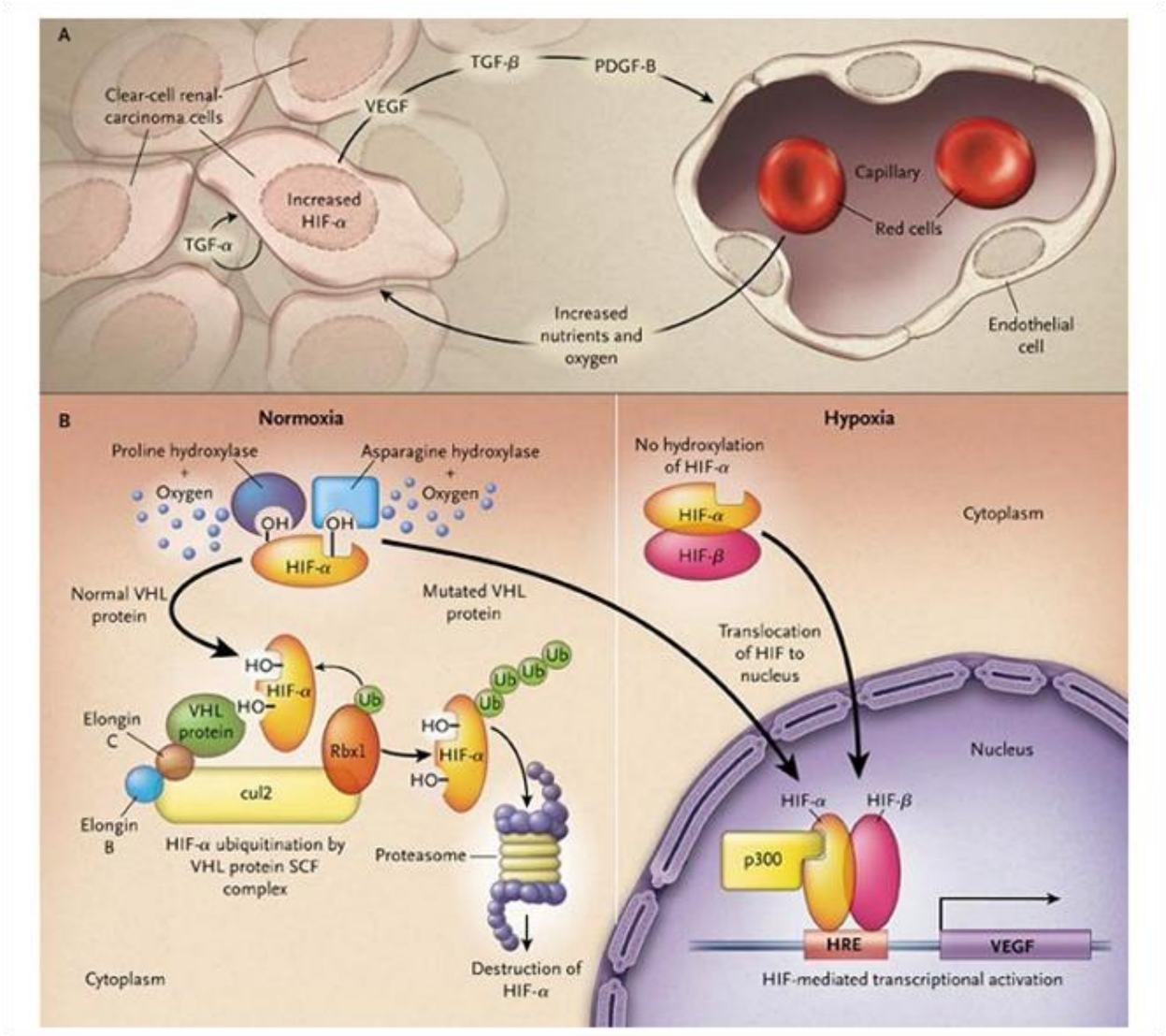

Figure 2. Molecular mechanism of the development of clear cell renal carcinoma (ccRCC). Panel A shows the pathologic cooperativity between ccRCC cells and adjacent vasculature: HIF-α accumulation results in the over-expression of proteins that are normally inducible by hypoxia, such as TGF-α and TGF-β, VEGF, and PDGF-B. The over-expressed VEGF, PDGF-B, and TGF-β act on neighboring vascular cells to promote tumor angiogenesis. The augmented tumor vasculature provides additional nutrients and oxygen to promote the growth of tumor cells. TGF-α acts in an autocrine manner on the tumor cells by signaling through the epidermal growth factor receptor, which promotes tumor cell proliferation and survival. Panel B shows the role of VHL protein in ccRCC and in controlling the expression of the HIF-α transcription factors. Under normoxic conditions, HIF-α is hydroxylated on two proline residues by a proline hydroxylase and on an asparagine residue by an asparagine hydroxylase. Hydroxylation (OH) by proline hydroxylase permits binding of HIF-α to VHL protein, which promotes the ubiquitination (Ub) and destruction of HIF-α by the proteasome pathway. Hydroxylation by asparagine hydroxylase blocks the interaction of HIF-α with transcriptional coactivator p300. VHL protein, with elongin proteins C and B, binds Cul2 protein. Rbx1 serves as the ubiquitin transferase for the VHL skp-cullin-F-box protein (SCF) complex. In cells that lack functional pVHL or that are exposed to low oxygen (hypoxia), unhydroxylated HIF-α accumulates and is able to heterodimerize with HIF-β and activate transcription at hypoxia-response elements (HREs), which are found in genes such as VEGF. In hypoxic conditions, HIF-α is not hydroxylated and so cannot bind VHL protein (Adapted from Cohen and McGovern, NEJM, 2005).

Under normoxic conditions, HIF-α is hydroxilated by specific prolyl hydroxylases on two proline residues and on an asparagine residue by an asparagine hydroxylase. Hydroxylation by proline hydroxylase permits binding of HIF-α to VHL protein, which promotes the ubiquitination and destruction of HIF-α by the proteasome pathway. Hydroxylation by asparagine hydroxylase blocks the interaction of HIF-α with transcriptional coactivator p300. VHL protein, with elongin proteins C and B, binds Cul2 protein (a member of the cullin family of ubiquitin ligase proteins). RING-box protein Rbx1 serves as the ubiquitin transferase for the VHL skp-cullin-F-box protein (SCF) complex. Under hypoxic (low oxygen concentrations) conditions, HIF-α hydroxylation is prevented and therefore unhydroxylated HIF-α accumulates in the cell. HIF-1α and HIF-2α translocate to the nucleus and are able to heterodimerize with HIF-β, activating transcription at hypoxia-response elements (HREs), which are found in genes involved in angiogenesis (e.g., vascular endothelial growth factor, *VEGF*; platelet-derived growth factor, *PDGF*; erythropoietin, *EPO*; placental growth factor, *PLGF*; cyclooxygenase-2, *COX*-2), extracellular matrix formation and turnover (e.g., matrix metalloproteinase 1, *MMP1*; lysyl oxidase, *LOX*), chemotaxis (e.g., stromal cell-derived factor 1, *SDF1*; and chemochine receptors, *CXCR*), cell proliferation and/or survival (e.g., transforming growth factor-α, *TGF*-α; insulin-like growth factor, *IGF*; epidermal growth factor receptor, *EGFR*), pH control (e.g., carbonic anhydrase IX, *CAIX*, and XII, *CAXII*), glucose uptake and metabolism (e.g., glucose transporters, *GLUT-1*; 6-phosphofructokinase 1, *PFKM*; pyruvate dehydrogenase kinase, *PDK1*) (Baldewijns *et al.*, 2010). Similar to hypoxia, *VHL* loss-of-function leads, under aerobic conditions, to HIF-α-dependent metabolic reprogramming from oxidative to glycolytic metabolism, through increased glucose uptake, glycolysis, and lactate production accompanied by a reciprocal decrease in mitochondrial respiration (Warburg effect). Therefore, loss of pVHL function and HIF-α activation induce a transcriptional program that alters diverse aspects of cellular behaviour, including growth factor production, induction of angiogenesis, promotion of invasion and metastasis, adaptation of cellular metabolism, and possibly promotion of cancer stem cell activity (Frew and Krek, 2007; Godinot *et al.*, 2007). Distinct domains of pVHL are illustrated in **Figure 3**.

HIF, may also be activated by interaction with reactive oxygen species (ROS), probably via inhibition of prolyl hydroxylases hydroxylation. Furthermore, recent studies have shown that HIF-1α degradation may occur in a *VHL*-independent manner (Baldewijns *et al.*, 2010).

However, *VHL* has also been implicated in a variety of other cellular processes including cell cycle regulation, extracellular matrix assembly, cytoskeleton stability, epithelial cell differentiation, reduction of matrix metalloproteases secretion and down-regulation of *CXCR4* (i.e. a chemokine receptor implicated in metastatic spread), and there is evidence that some activities are HIF-independent (Baldewijns *et al.*, 2010; Frew and Krek, 2007).

Thus, HIF is the key regulator of the hypoxic response in organisms, while pVHL has a central role in oxygen sensing.

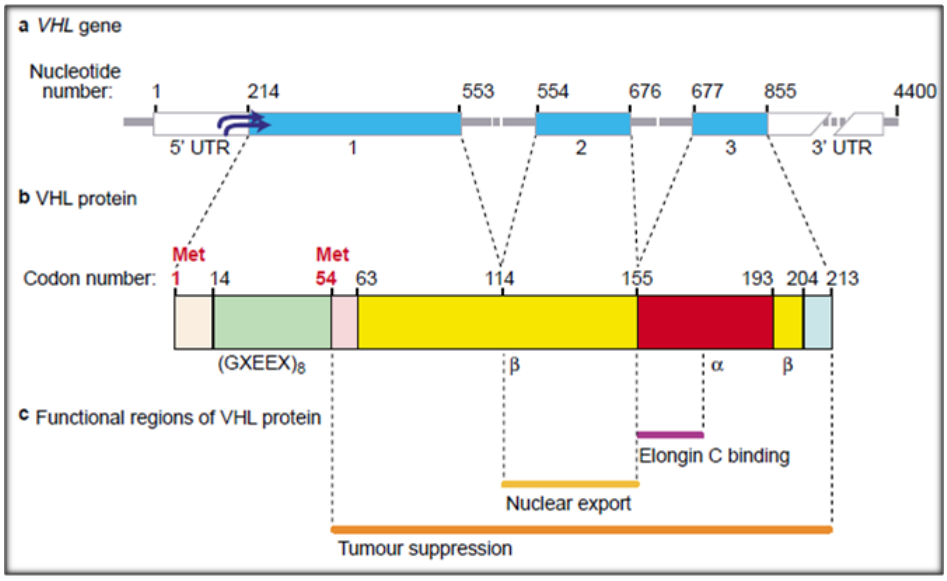

Figure 3. von Hippel–Lindau (VHL) gene and protein structure and function. (a) The VHL gene structure (nucleotides 1–4400) comprises three exons (blue). 5' and 3' untranslated regions (UTRs), and several transcription start sites (curved arrows), are shown. (b) The α- and β-domains structure of the VHL protein (codon numbers 1–213), and the two methionine (Met) start codons (at codons 1 and 54), are shown; the $(GXEEX)_8$ region is a pentameric repeat motif with unknown functional significance. (c) Regions of the protein required for different functions are indicated. (Adapted from Richards, ERMM, 2001).

1.1.3.1.2 Other genes implicated in ccRCC

VHL loss alone is not sufficient for ccRCC tumorigenesis. The Catalogue Of Somatic Mutations In Cancer (COSMIC, http://www.sanger.ac.uk/genetics/CGP/CellLines/), that stores and displays somatic mutation information and related details and contains information relating to human cancers, reported that 37% (1,166) out of 3,149 primary kidney tissues analyzed show a mutated *VHL*. Furthermore, this database displays other genes associated to ccRCC (**Figure 4**).

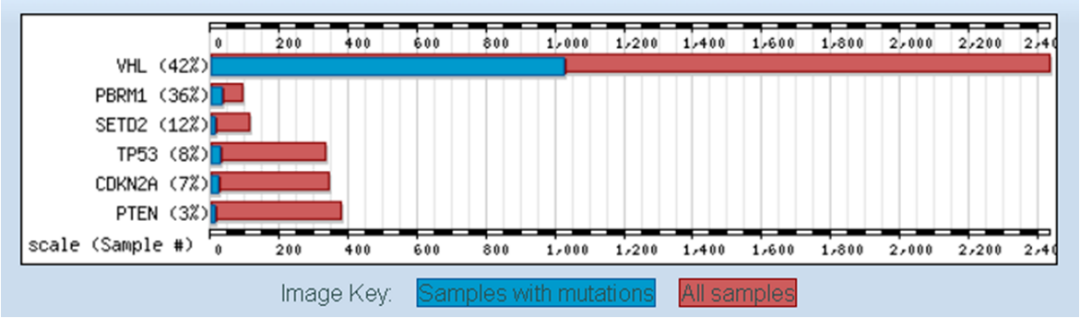

Figure 4. The most significantly mutated genes associated to ccRCC in COSMIC database are here reported. Percentages of mutated samples are given in parentheses (Adapted from COSMIC database).

PBRM1 (polybromo 1) maps on chromosome 3p21, and is recently identified as the second mostly mutated gene in ccRCC samples, after *VHL* (Varela *et al.*, 2011). This gene is involved in regulation of pathways associated with chromosomal instability and cellular proliferation. By exome sequencing, the authors found frequent mutations on *PBRM1*, including truncating mutations in 41% (92/227) of cases. Suggesting *PBRM1* as a second major ccRCC cancer gene (Varela *et al.*, 2011).

Recently, it has been reported that inactivation of the histone H3 lysine 36 methyltransferase gene *SETD2* (SET domain containing 2), located on 3p21.31, is a common event in ccRCC cells. Aberrant expression of histone-modifying enzymes, such as *SETD2*, could result in altered chromatin configuration and disruption of normal transcriptional programs, driving the cell to cancer development, suggesting *SETD2* as a new tumor suppressor gene involved in the development of ccRCC (Duns *et al.*, 2010). Systematic sequencing revealed inactivating mutations in other two genes encoding enzymes involved in histone modification, i.e. *JARID1C* (lysine (K)-specific demethylase 5C), a histone H3 lysine 4 demethylase, and *UTX* (lysine (K)-specific demethylase 6A), a histone H3 lysine 27 demethylase (Dalgliesh *et al.*, 2010).

Mutations on *p53* occur in about 50% of all human cancers, but, in RCC, this is a rare event. *p53* is activated by cellular or genotoxic stress, functioning as a transcription factor to promote cell cycle arrest and DNA repair, or apoptosis if the normal cellular conditions are not restored. However, in cancers with rare *p53* mutations, *p53*/*MDM2* (the negative regulator of *p53*) expression patterns could be related to disease progression/outcomes (Noon *et al.*, 2010, 2011).

Alterations of *CDKN2A* (cyclin-dependent kinase inhibitor 2A) on 9p21 through mutations and/or deletions have been reported in RCC cell lines and in primary ccRCCs, and chromosome 9p loss of heterozygosity was associated with short tumor-specific survival in ccRCC tumors. *CDKN2A* contributes to cell cycle arrest, but its role in RCC is still unclear (Schraml *et al.*, 2001).

PTEN, which is a tumor suppressor gene, maps on 10q23, a region of frequent genetic deletions in ccRCC. *PTEN* seems to be involved in tumor progression in several human cancers, including RCC (Velickovic *et al.*, 2002).

Hereditary clear cell renal carcinoma: a familial disease that predisposes to develop multiple and bilateral ccRCCs, without additional systemic manifestations. This disease is also named “syndrome of constitutional chromosome 3 translocations”. Distinct from von Hippel-Lindau syndrome, familial clear cell renal cancer has been reported in patients with translocations of chromosome 3p at a fragile site at 3p14. The multiple genetic abnormalities underlying this syndrome are unified by heritable patterns of ccRCC associated with breakpoints along the p and q arms of chromosome 3 (Cohen *et al.*, 1979d). Loss of the translocated chr 3p probably implicates VHL protein in the development of these tumors, nevertheless patients do not present systemic manifestations associated with the VHL syndrome. Additional translocations of chromosome 3 have been associated with ccRCC as well (Cohen and McGovern, 2005; Hansel, 2006).

Hereditary papillary renal carcinoma (HPRC): is an autosomal dominant disorder associated with multifocal pRCC with type 1 histologic features. Activating mutations of the *MET* gene, which encodes a receptor tyrosine kinase that binds hepatocyte growth factor (*HGF*), underlie the pathogenesis of this disorder. *MET* is a proto-oncogene and lies on chromosome 7q31-34 (Schmidt *et al.*, 1997). In HPRC, the *MET* receptor tyrosine kinase domain undergoes auto-activating aminoacid-substitution mutations, which promote cellular proliferation and cell migration in response to *HGF*. Subsequently, chromosome 7 harboring the *MET* mutation is duplicated, thus, increasing the gene dose. Mutations of the *MET* gene underlie progression and metastatic spread of numerous epithelial carcinomas, including breast and colon cancers (Jeffers *et al.*, 1997). Only a small percentage of the cases of the sporadic papillary type has *MET* mutations. Thus, the pathogenesis of HPRC is usually different from that of sporadic pRCC (Schmidt *et al.*, 1997).

1.1.4 Clinical utility of molecular profiling in cancer

A better understanding of the oncogenesis and basic biology of RCCs has helped to identify key molecular pathways and proteins underlying their development and growth. Furthermore, this facilitates the discovery of prognostic factors that can stratify patients and predictive biomarkers that can help individualize treatment selection and predict a patient's response to therapy. Morphologic and clinical parameters are not accurate enough for individualized clinical decisions, thus, molecular profiling of cancer has emerged as the solution for individualized diagnosis, prognosis and treatment. Molecular profiling can be established at multiple levels, such as genomic, transcriptomic, proteomic; and to do this, the development of biotechnology, such as microarray and bioinformatics, is very important. Tumor markers can be applied for screening, diagnosing, estimating prognosis, predicting therapeutic response, or monitoring recurrence and progression. As mentioned above, the differential diagnosis in RCC is very important, since each subtype shows a peculiar clinical course, malignant potential and response to therapy, and many tumors are histo-pathologically variegated (Ribal, 2011). According to guidelines, recently published, a tumor marker is only usefuf (1) if its results are appropriate precisely for the required application (i.e., risk assessment, screening, diagnosis, prognosis, prediction, or post-treatment monitoring), (2) if its results allow to separate patients into two or more categories that will become clinically relevant and different, and finally, (3) if the estimate of the separation in outcomes marker positivity and negativity is reliable. Because tumor markers are often used to monitor cancer patients for long time periods, assessment of long-term assay stability at other analyte concentrations is also advisable (Sturgeon *et al.*, 2008a). The identification of diagnostic and therapeutic candidate biomarkers for RCC is the major goal of the RCC research. RCC is known to release several hormones and biologically active substances that induce syndromes and produce metabolic damage in the host. The detection of elevated levels of these substances may be useful in the diagnosis and follow-up of this malignancy. According to the definition by Mejean *et al.* (Mejean *et al.*, 2003a), tumor markers are substances that may be found in the blood or urine of someone with RCC.

The characteristics of an ideal marker include the following (Kashyap *et al.*, 2005):

- to be secreted by malignant cells;
- to be detected when a tumour becomes active, i.e. well differentiated;
- to be simple and detected by a simple method;
- to have increased capability of diagnosis of tumours in the primary stage;
- to detect the recurrence of a tumour;
- to establish the success of the administered therapy;
- to have a positive correlation with the clinical stage of a tumour;
- to predict the outcome of the patients;
- to be socially accepted with the least possible discomfort to patients;
- to be independent of subjective factors such as methodology and examiner experience.

In RCCs, the prediction of metastasis via tumor prognostic markers remains the major problem. In addition, one of the most important challenges of cancer research is the prediction of the invasiveness and metastatic potential of the tumor at an early stage. Therefore, much effort is needed towards the identification of some reliable tumor markers for RCC.

1.1.5 Gene expression studies

Gene expression profiling is a promising approach, in fact expression microarrays can resolve certain tumors into diagnostic, prognostic and therapeutic subclasses. Transcriptional profiling can define a unique gene expression signature for each tumor that may prove useful for classification and prognosis (Chin *et al.*, 2011). For example, renal tumor subtypes can be classified diagnostically using microarrays, on the basis of distinct and reproducible gene expression profiles, as shown in many studies (Boer *et al.*, 2001; Gieseg *et al.*, 2002; Higgins *et al.*, 2003b; Schuetz *et al.*, 2005; Takahashi *et al.*, 2003; Young *et al.*, 2001).

In the last few years, in several types of human cancer, gene expression profiles by microarray have been used as a tool to classify tumors and to identify novel molecular biomarkers (Schuetz *et al.*, 2005). Tumor transcriptomic profiling may identify patterns of genes that are correlated to patients, prognosis, response to therapy and survival (Zhao *et al.*, 2006f). To identify more effective biomarkers in RCC, gene expression profiling studies have been extensively performed; in particular, we will focus on ccRCC. In 2001, Takahashi *et al.* identified a gene signature that could classify tumors based on 5-year disease-specific survival, so gene expression studies could be used to predict outcome in ccRCC, unfortunately, the results have not been validated (Takahashi *et al.*, 2001g). Two years later, Vasselli *et al.* examining 51 metastatic ccRCCs identified 45 survival genes, whose the most predictive was *VCAM-1* (vascular cell adhesion molecule-1) (Vasselli *et al.*, 2003). Subsequently, *VCAM-1* undergone validation as a prognostic biomarker in two other studies (Shioi *et al.*, 2006; Yao *et al.*, 2008). Interestingly, high expression of *VCAM-1* predicted for better overall survival in both clear cell and papillary tumors, suggesting that the expression of this molecule may generally indicate tumor cells with lower metastatic potential. Another study described a gene signature for RCC progression, including genes already associated to RCC aggression and/or survival, such as caveolin-1 (*CAV1*), lysyl oxidase (*LOX*) and annexin A4 (*ANXA4*) (Jones *et al.*, 2005c). Sültmann *et al.* hybridized 19 ccRCCs that had metastasis at the time of diagnosis and 17 that did not have metastasis to cDNA microarrays containing 4,207 probes. They found 85 gene probes statistically significantly associated with metastasis (Sültmann *et al.*, 2005). Kosari *et al.*, examining 28 ccRCCs found 35 differentially expressed genes between non-aggressive and aggressive tumors (Kosari *et al.*, 2005). The largest study included 177 ccRCCs and identified 340 transcripts (including *VCAM-1*) that could be used to assign a risk score to a patient, with a significant correlation with stage, grade, and performance status. This group saw five different subgroups within two larger groups of ccRCC, with significant survival differences as well as predicted biological pathways distinctions (Zhao *et al.*, 2006f). Gene expression analysis and also cytogenetics study on single nucleotide polymorphisms (SNPs) on 54 cases of sporadic ccRCC and 36 tumors from 12 patients with VHL disease demonstrated that ccRCC tumors, either sporadic and VHL disease, have overall similar profiles, but sporadic ccRCCs are more heterogeneous and contain a higher number of genetic events per tumor. This study didn't identify any biomarkers, neither for prognosis nor predictive, but probably VHL disease that induces ccRCC and sporadic ccRCCs might be targeted with the same treatments, since they

are so similar (Beroukhim *et al.*, 2009). Another study was performed by Skubitz *et al.* to identify biologic differences of ccRCCs using 16 tumors, they found tumors with more highly over-expressed metabolic genes or more higly over-expressed extracellular matrix and cell adhesion genes (Skubitz *et al.*, 2006). The aim of another study (Tun *et al.*, 2010) was to define a biological pathway signature and a cellular differentiation program in ccRCC; stressing, however, that genes that don't seem differentially expressed at a statistically significant level may reveal biologically significant changes when studied in ontology groups.

A large number of potential biomarkers have emerged from all these gene expression studies, but, surely, they require external validation in larger sample sizes before they can be implemented.

VHL mutation might have important implications for disease prognosis. In fact, the presence and type of *VHL* mutations in tumors have been consistently considered as possible biomarkers (Cowey and Rathmell, 2009). When *VHL* is inactivated and HIF is constitutively expressed, a number of other genes is transcriptionally up-regulated. One HIF target is *VEGF*, the vascular epithelial growth factor, that is significantly up-regulated in RCCs compared with its elevated expression in many other cancers (Gordan *et al.*, 2007). It seems that *VEGF* may be predictive for response to *VEGF*-targeted therapy. Another HIF target is *CAIX*, its serum levels are elevated in ccRCC patients, with a significant association between *CAIX* serum levels and tumor size and occurrence of metastases (Zhou *et al.*, 2010). *CAIX*, as a target of HIF transcriptional activation, may be an indicator of functional *VHL* loss, indicating *VHL* events that impart a significant failure of HIF suppression. There have been very few studies regarding *VHL* gene alteration as a potential predictive marker for response to therapy, so, further evaluations of the role of this gene as a biomarker may be needed (Cowey and Rathmell, 2009).

Using unsupervised consensus clustering algorithms, Brannon *et al.* distinguished two distinct molecular subtypes of ccRCC (ccA and ccB), characterized by divergent biological pathways and a highly significant association with survival outcomes. In fact, ccA patients have a better prognosis respect to ccB patients, probably due to the over-expression of genes involved in hypoxia, angiogenesis, fatty acid metabolism and organic acid metabolism, while ccB patients showed the over-expression of genes related to EMT, cell cycle and wound healing. Thus, defining a tumor as ccA or ccB could be an important prognostic indicator for predicting outcome in patients affected by ccRCC (Brannon *et al.*, 2010). Subsequently, in another study it has been reported that in ccA subset tumors two distinct subgroups emerged along gender lines, with males'tumors which over-expressed many immune or inflammatory gene sets, whereas females'tumors which over-expressed catabolic process-related genes. This gender disparity may provide additional disease informations (Brannon *et al.*, 2011).

1.1.6 Signaling pathways in renal cell carcinoma and therapy

Kidney cancer comprises a number of different types of cancer that occur in the kidney, it's not a single disease. Each of these tumors has different histological features and clinical course, which respond differently to therapy and is often caused by mutation in different genes. It has been suggested to define renal cancer as a metabolic disease, in fact, each of the inherited kidney cancer syndromes caused by germline mutations in the kidney cancer genes identified to date represents disorders in metabolic pathways involved in oxygen, iron, nutrient and energy sensing. Thus, targeting the metabolic defects in these pathways might be a possible way to develop kidney cancer gene-specific therapies (Linehan *et al.*, 2010).

Generally, RCC is highly resistant to conventional chemotherapy and radiation therapy. Recently, a number of drugs have been developed, they act by blocking critical signaling pathways involved in RCC, such as angiogenesis, PI3K/AKT/mTOR, Wnt/β-catenin, Epithelial to Mesenchymal Transition (EMT), which will be described below (**Figure 5**) (Banumathy and Cairns, 2010).

Angiogenesis is due primarily to loss-of-function mutation of the *VHL* gene on chromosome 3. RCC tends to be a highly vascular tumor with high expression of *VEGF*, VEGF receptor (*VEGFR*), PDGF receptor (*PDGFR*), and basic fibroblast growth factor (*bFGF*) (Finley *et al.*, 2011). In fact, kidney tumors are frequently characterized by hypoxic conditions, so, hypoxia and compensatory hyperactivation of angiogenesis are thought to be very important in RCC. In hypoxic conditions, in the absence of *VHL*, HIF-α proteins remain constitutively expressed thereby inducing *VEGF* and other HIF targets. Increased expression of many of the HIF target genes is implicating in promoting cancer, inducing both changes within the tumor (cell-intrinsic) and changes in the growth of adjacent endothelial cells to promote blood vessel growth. In particular, *VEGF* and *PDGF*, the most-studied HIF targets, are potential endothelial cell mitogens. The expression level of *VEGF* strongly correlates with microvessel density, that is a measure of the degree of angiogenesis. *VEGFR* and *PDGFR* are up-regulated on endothelial cells in angiogenesis (Kluger *et al.*, 2008). Other HIF targets include genes involved in glucose metabolism (endoglin, *ENG*; *GLUT-1*), cell proliferation and survival (*TGF-α* and epidermal growth factor receptor, *EGFR*) and metastasis (mucin 1, *MUC1*) (Semenza, 2010a). Another HIF-α target is the carbonic anhydrase IX (*CAIX*) gene, that has been extensively studied as a prognostic marker for RCC (Stillebroer *et al.*, 2010a). Furthermore, also the miR-210 has been reported up-regulated in hypoxia and its expression can be induced by both HIF-1α and HIF-2α (Huang *et al.*, 2009b).

PI3K/AKT/mTOR Pathway: protein kinase B (Akt) and mammalian target of rapamycin (mTOR) are hubs for key oncogenic processes including angiogenesis, cell proliferation and survival. Autocrine binding of *VEGF* and *PDGF* to their receptor tyrosine kinases (*VEGFR*, *PDGFR*, *KIT*) on RCC tumor cells activates *PI3K*, which promotes the generation of *PIP3* (phosphatidylinositol-3,4,5-triphosphate). *PIP3* recruits the cytoplasmic kinase *AKT* to the cell membrane, where it is activated by phosphorylation at two independent sites mediated by *PDK1* and mTOR (TORC2), respectively (Linehan *et al.*, 2010). *AKT* activation inhibits apoptosis, by inactivating proapoptotic proteins (e.g., the bcl2 family member *BAD*, procaspase-9, apoptosis signal regulating kinase 1 *ASK1*). *AKT* inactivates also *GSK-3β* (glycogen synthase kinase 3 beta), that normally phosphorilates and induces the degradation of cell cycle promoting proteins (e.g., cyclin D1, *CCND1*) and proliferation-promoting transcription factors (e.g., c-Myc, β-catenin, c-Jun, Notch). *VEGF* and *PDGF* activate mTOR through *AKT* (Banumathy and Cairns, 2010). mTOR is part of two distinct signaling complexes. The rapamycin-sensitive complex mTORC1 regulates cell growth and protein synthesis in response to growth factor stimulation by phosphorylating S6 kinase and the eukaryotic translation factor 4E-binding protein 1 (4E-BP1) to modulate key regulators of messenger RNA (mRNA) translation. The other complex, mTORC2, regulates actin cytoskeleton organization through phosphorylation of protein kinase Cα and also phosphorylates the serine-threonine protein kinase Akt to activate the Akt-mTORC1 pathway. mTORC2 is insensitive to rapamycin (Linehan *et al.*, 2010; Wullschleger *et al.*, 2006). The *PTEN* negatively regulates numerous growth factor receptor-mediated signal transductions by dephosphorylating *PIP3*, that is a substrate of activated *PI3K* enzymes. Loss-of-function of *PTEN* leads to constitutive activation of *PI3K* downstream components including *AKT* and mTOR kinases (Dahinden *et al.*, 2010b).

Wnt/β-catenin Signaling: Wnts are a family of secreted glycoproteins that regulate cell proliferation, differentiation and cell migration. The final effector of Wnt signaling is the β-catenin, a transcriptional coactivator. In normal quiescent cells, β-catenin is trapped in a highly processive enzyme complex containing casein kinase 1 (*CK1*), glycogen synthase kinase 3β (*GSK-3β*), adenomatosis polyposis coli protein (*APC*) and axin. β-catenin is phosphorylated at serine and threonine residues by this complex and targeted for proteosomal degradation (Barker and Clevers, 2006). Wnt positively regulates and stabilizes β-catenin, inhibiting its phosphorylation, ubiquitination and degradation. Stabilized β-catenin translocates into the nucleus and, together with a member of the LEF-TCF (lymphoid enhancer-binding factor 1-T cell specific transcription factor 7) family of transcription factors, activates target genes such as the *MYC* oncogene (Furge *et al.*, 2007). Wnt probably mediates its effect on cell growth and tumor promotion by activating the mTOR pathway through inhibition of *GSK-3β* (Inoki *et al.*, 2006). Thus, Wnt induces transcription throygh activation of β-catenin and also stimulates translation and cell growth through activation of the mTOR pathway (Linehan *et al.*, 2009a).

Epithelial to Mesenchymal Transition (EMT): EMT is an essential process before metastasis can occur. Epithelial cell-cell adhesion is mediated by intercellular junctional complexes of tight junctions, adherens junctions and desmosomes. E-cadherin (*CDH1*) is the principal component of adherens junctions and desmosomes, and if it lost, cells acquire invasive and metastatic properties. *VHL* loss-of-function leading to HIF-1α gain-of-function, which induces the increased expression of the *CDH1* repressors (e.g., *SLUG*, *SNAIL*, *TCF3*, *ZEB1*, *ZEB2*). These repressors bind the proximal promoter of *CDH1*, repressing its transcription, and induce the epithelial to mesenchymal transition (Krishnamachary *et al.*, 2006). Noticeably, *CDH1* is hypermethylated in 11% of primary RCC (Dulaimi *et al.*, 2004). Thus, hypoxia is also involved in tumor metastasis. The kidney is mesenchymal in origin and develops through mesenchymal to epithelial transition (MET). In cancer this transition is reversed, resulting in EMT and dedifferentiation. Another interesting gene implicated in EMT is *TGF-β*, a multifunctional cytokine which plays different roles in normal and cancerous cells. In normal and pre-malignant cells *TGF-β* acts as a tumor suppressor, in malignant cells it's over-expressed because these tumor cells often become resistant to the growth inhibitor effects of *TGF-β*. A different tumor microenvironment can induce *TGF-β* to function as a tumor promoter (Wendt *et al.*, 2009).

Localized RCC can be successfully treated by surgical resection alone. Cytokine or the newer targeted therapies are used to treat patients with locally advanced or metastatic disease. Unfortunately, response rates are very low. Drug resistance may be due to the expression of the multidrug resistance transporter in proximal-tubule cells. Immunomodulatory therapies involve the use of cytokines, such as interferon α (IFNα) and interleukin-2 (IL-2), high dose of these cytokines work effectively only in a minority of ccRCC patients, and median overall survival with these agents ranges from 10 to 15 months (Biswas and Eisen, 2009b; Cohen and McGovern, 2005a; Motzer and Molina, 2009b). The current targeted therapies have focused on targeting the genes that are transcriptionally up-regulated by HIFs, such as *VEGF*, *VEGFR*, *PDGFR*, and the serine-threonine protein kinase mTOR. A number of drugs have recently been approved by the FDA (Food and Drug Administration) that target either the HIF targets or inhibit mTORC1 (Linehan *et al.*, 2010). Briefly, bevacizumab is an antibody that targets *VEGF*; sorafenib is a small molecule multikinase inhibitor that targets *VEGFR* and *PDGFR*; sunitib also inhibits *VEGFR* and *PDGFR*, and is often used in advanced

ccRCCs; temsirolimus and everolimus inhibit mTORC1 complex. These therapies mainly inhibit angiogenesis and exhibit antitumor activity by blocking the supply of oxygen and nutrients to the tumor cells.

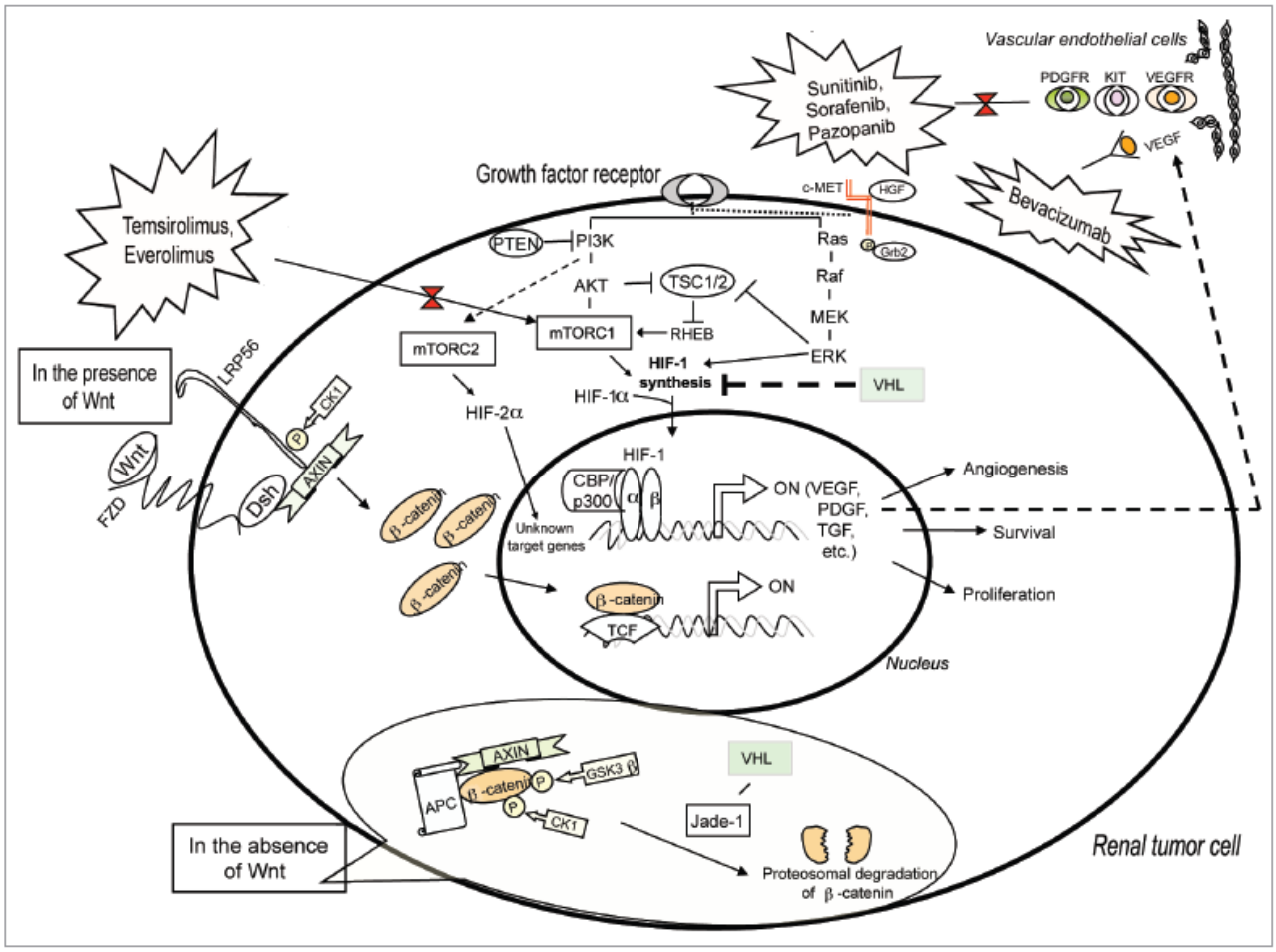

Figure 5. Schematic representation of selected signaling pathways and the current targeted therapies related to RCC. Angiogenic and cell proliferating signaling cascades are up-regulated in RCC tumor cells. VEGF and other related growth factors secreted by tumor cells stimulate angiogenic signaling in the surrounding vascular endothelial cells. In response to growth factor signaling mediated through VEGF, PDGF and KIT receptors, PI-3-kinase and Ras effectors activate HIF transcription factors, which in turn switch on gene expression needed for angiogenesis and cell proliferation in endothelial cells. In addition to the angiogenic pathway, the Wnt and HGF pathways are also up-regulated in RCC tumor cells. While VEGF-targeted therapy for metastatic RCC is focused on blocking angiogenic signaling in vascular endothelial cells surrounding the tumor, mTOR inhibitors act directly on the tumor cells to suppress growth (Adapted from Banumathy and Cairns., Cancer Biology & Therapy, 2010).

1.2 MICRORNA

1.2.1 microRNAs and mechanism of action

MicroRNAs (miRNAs) are small single-stranded non-protein-coding RNA molecules, of about 22-25 nucleotides in length, generated from endogenous hairpin-shaped transcripts (Ambros *et al.*, 2003d; Cullen 2004). At first, they were discovered in *Caenorhabditis elegans*, where they control the ontogenetic development and the differentiation (Lee *et al.*, 1993). They function as negative post-transcriptional gene regulators in animals, plants and viruses (Ambros, 2003a; Lai, 2003). Recent evidences showed that miRNA expression has been implicated in tumorigenesis, indicating that miRNAs might function as tumor suppressors and oncogenes (Esquela-Kerscher and Slack, 2006). Many studies have revealed that miRNAs can regulate many pathways, also including haematopoietic cell differentiation, apoptosis, cell proliferation and organ development. They belong to a highly conserved class of RNA, in fact, some components of this system have been found in archaea and eubacteria (Ambros, 2004; Bartel, 2004f). miRNAs are believed to account for >3% of all human genes (Bentwich *et al.*, 2005a), in fact, at now over 1,000 were identified in human species. These RNA molecules negatively regulate gene expression by recognizing and binding sequences within the 3' untranslated region (UTR) of target mRNAs: the degree of complementarity to miRNA seems to determine the fate of targets. Thus, partially complementarity leads to translational repression, while fully complementarity targets are directed to cleavage (Ambros, 2003a; Lai, 2003). The complementarity is usually restricted to 2-8 nucleotides present at the 5' end of miRNAs. These nucleotides form the so-called "miRNA seed" that binds the target, called "seed match". The 5' end seems to be important for stability and for the loading of the same miRNA in the RISC complex (Khvorova *et al.*, 2003), and is also crucial to carry out biological function. The nucleotides of the "seed" can pair up not completely to the target, or in a non-canonical base-pair (e.g., pairing G:U) (Brennecke *et al.*, 2005a; Doench *et al.*, 2003). Using specific algorithms, it has been seen that a single miRNA can bind up to 200 target genes and that they may have different biological functions, such as transcription factors, receptors and transporters (Grosshans *et al.*, 2005; Lewis *et al.*, 2005a; Lim *et al.*, 2003, 2005). This means that miRNAs can control the expression of approximately one third of human messengers. On the other hand, a few experiments have indicated possible target sites in the 5'UTR. Lee *et al.* reported that, based on both hybridization energy and sequence matches, many endogenous motifs within human 5'UTRs specific to the 3' ends of miRNAs exist. They showed combinatory interactions between a single miRNA and both end regions of a mRNA, based on the fact that many miRNAs contain significant interaction sites with mRNA 5'UTR and 3'UTR motifs through their 3' and 5' end sequences, respectively. Thus, a new miRNA target class has been proposed containing simultaneous 5' and 3' UTR interaction sites and that studies with full 5'UTR sequences may reveal further miRNA functions within this new targets class (Lee *et al.*, 2009).

A single miRNA can bind to and regulate many different targets and, conversely, several different miRNAs can bind to and cooperatively control a single mRNA target (Lewis *et al.*, 2003). All metazoan eukaryotes encode miRNAs, which may be expressed in more than 1,000 copies per cell and many miRNAs have a tissue-specific and/or a stage-specific expression patterns (Bartel, 2004f). Different tissues have distinctive patterns of miRNome expression (defined as the full complement of miRNAs in a cell) with each tissue presenting a specific signature. By combining tissue-specific expression of miRNAs and their targets, a

complex network of interactions regulates cell-specific functions. It is therefore plausible that miRNA function may vary depending on cell type, because of differences in “cell-specific” gene targets (Liu *et al.*, 2004). Defining cell-specific miRNA expression may be important in order to assess miRNA function. Over 250 small RNA cDNA libraries obtained by cloning and sequencing from 26 distinct organ systems and cell types of human and/or rodents were analyzed. Results of this study demonstrated that the miRNA expression varied from highly specific to ubiquitous, and that very few miRNAs were exclusively found in individual tissues or cell types, and only a third of the analyzed miRNAs were expressed with a higher degree of tissue specificity (**Figure 6**) (Landgraf *et al.*, 2007a).

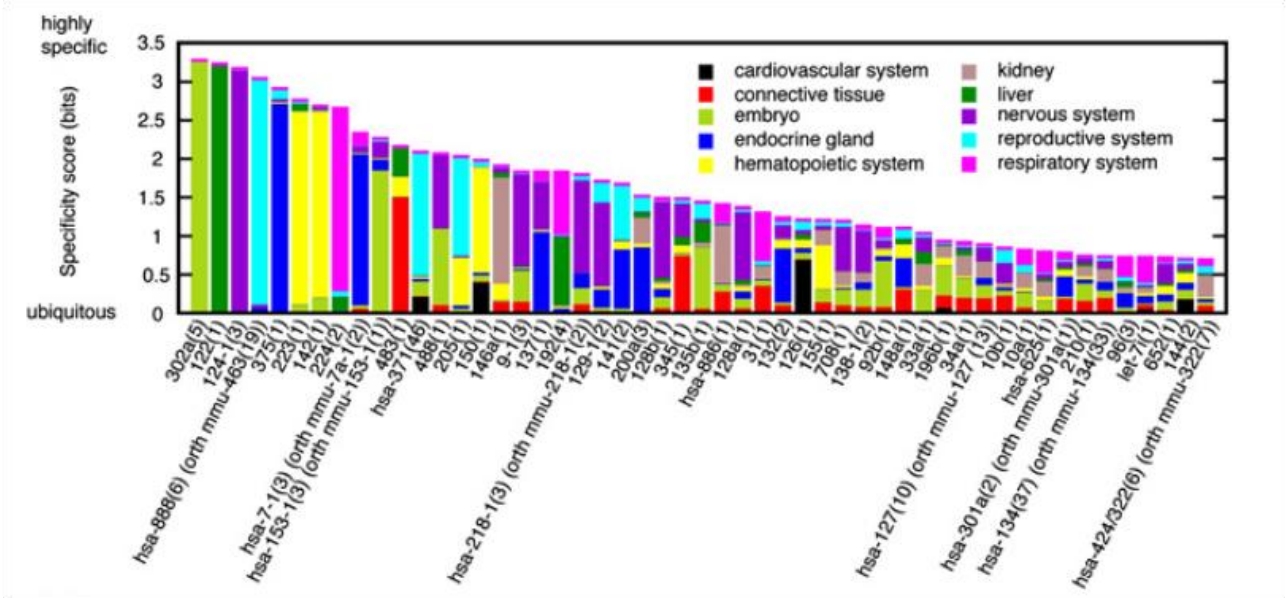

Figure 6. The 51 most specific miRNA precursor clusters for human are here illustrated. The total height of each bar represents the information content reflecting tissue specificity, while the relative heights for each of the tissues are proportional to the clones of a miRNA precursor cluster in a given tissue type relative to all tissue types (Adapted from Landgraf P., Cell, 2007a).

Recently, the tissue-specificity of miRNAs has been demonstrated also in NCI-60 cell panel, composed by 59 human cancer cell lines derived from 9 different tissues of origin: melanoma, leukemia, kidney, ovary, breast, lung, central nervous system, colon and prostate. A higher correlation between the cell line-specific signature has been observed, suggesting that cell line-specific miRNA profiles are robust. Data suggested also a strong and consistent tissue-specific signature in different tissues, in fact some miRNAs were preferentially expressed in cell lines originating from one tissue compared with the rest of cell lines. For example, the authors detected an interesting pattern in the expression of miR-200 in renal cell lines (Søkilde *et al.*, 2011).

1.2.2 Genomic localization

Most miRNA genes are located in introns and/or exons, they may be in sense or antisense orientation. About 30% of miRNA genes are located in intergenic regions. They are often located in critical chromosomal areas (Kim, 2005). Furthermore, many miRNA genes are transcribed as independent transcriptional units (Lau *et al.*, 2001, Lagos-Quintana *et al.*, 2001), but it has been observed that about 50% of known miRNAs is located near other miRNAs. It is assumed that these clusters may be transcribed as a single polycistronic

transcriptional unit (Lau *et al.*, 2001; Mourelatos *et al.*, 2002). The genes that encode for miRNAs can be localized not only in exons or introns of independent transcriptional units that do not encode proteins (Rodriguez *et al.*, 2004), but also in protein-coding genes (Smalheiser, 2003). It is unclear whether these miRNA genes are functionally related to their guests: the splicing process may be unable to issue an intron that is accessible to a miRNA. In addition, splicing and processing by miRNAs might be coupled, and so miRNAs and mRNAs could be processed simultaneously. Studies on expression levels of miRNAs and messengers have revealed that miRNAs are frequently co-expressed with their host genes (Baskerville and Bartel, 2005). miRNAs can be grouped into families based on sequence homology at the 5' end of their mature forms, but it was still not clear whether members of a family monitor the same biological processes (Esquela-Kerscher and Slack, 2006).

1.2.3 miRNA biogenesis

miRNA biogenesis is a multi-step process (**Figure 7**), that begins in the nucleus and ends in the cytoplasm. miRNA genes are transcribed by RNA Polymerase II (Pol II), although it cannot be excluded that a small number of these genes can be transcribed by other RNA polymerases (Cai *et al.*, 2004; Lee *et al.*, 2004). Primary transcripts (pri-miRNAs) are single-stranded RNA molecules folded in on themselves to form a loop structure flanked by two free sequences, not folded, and present a cap of 7-methylguanine at the 5' end and a poly-A tail at the 3' end, features of mRNAs coding for proteins. Subsequently, pri-miRNAs are processed by the endonuclease RNase III Drosha, and its cofactor Pasha, to release the pre-miRNA precursor product of about 70 nucleotides in length. Then, these precursors are transported by the exportin 5 into the cytoplasm, where they are processed by another RNase III enzyme, Dicer, to generate a transient miRNA:miRNA* duplex of about 22 nucleotides in length. This duplex is then loaded into the miRNA-containing RNA-induced silencing complex (miRISC), which includes the Argonaute (Ago) proteins, and the mature miRNA is retained in this complex, while the other strand is cleaved. Then, the mature miRNA can bind to its target sites. It is believed that the thermodynamic stability of the two ends of the duplex determines which strand should be selected. The strand with less stability at the paired bases at the 5' end is typically incorporated (e.g., G:U instead of G:C) (Esquela-Kerscher and Slack, 2006).

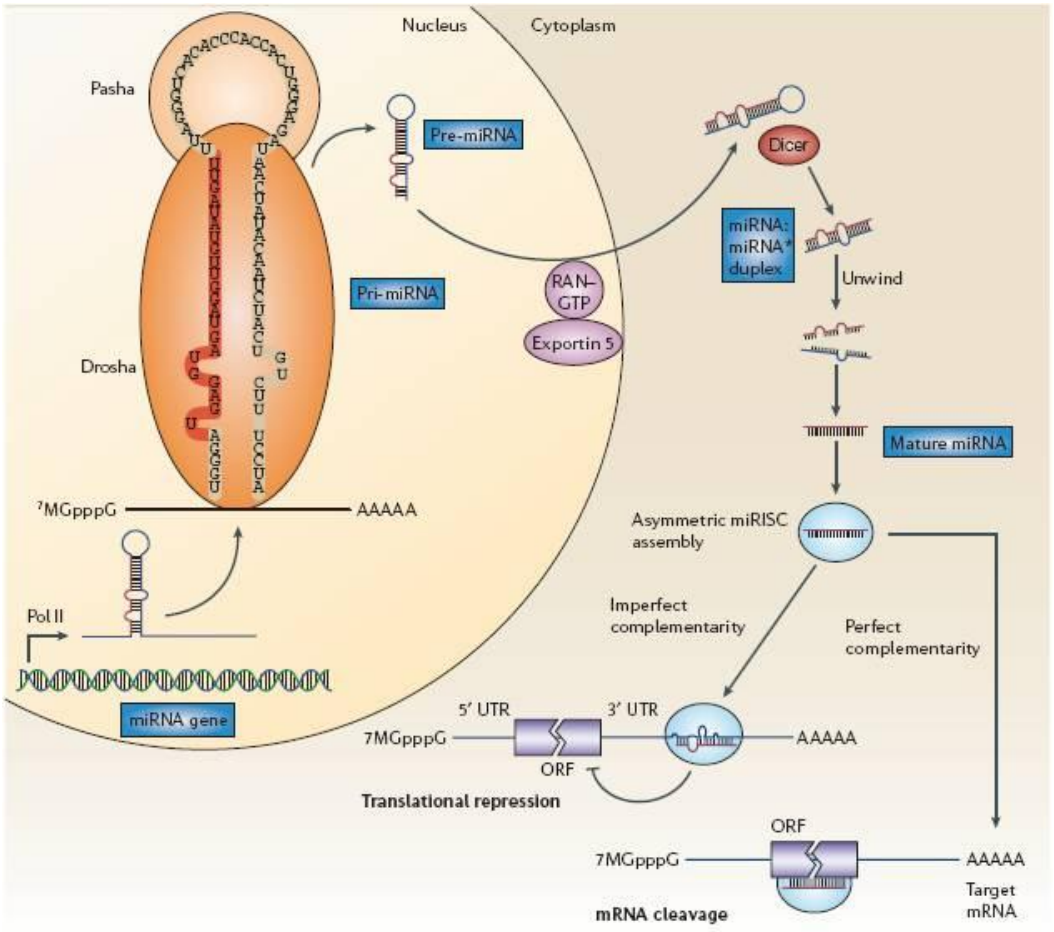

Figure 7. The biogenesis of microRNAs (Adapted from Esquela-Kerscher and Slack, Nat Rev Cancer, 2006).

1.2.4 Target prediction and new miRNAs discovered

In the last few years computational methods have been developed to identify miRNA targets (Enright *et al.*, 2003, Lewis *et al.*, 2003, Stark *et al.*, 2003). These methods search for conserved regions in the 3'UTR that are complementary to miRNAs. Identification of mRNA targets is more difficult in animals than in plants, since there are few mRNAs perfectly complementary to miRNAs in animals (Rajewsky, 2006a). The analysis of the miRNA binding sites, which must be experimentally validated, is based on several criteria: (1) a perfect complementarity between the 3'UTR of mRNA targets and the first 8 nucleotides of miRNAs from their 5'UTR end (within this region pairing G:U are allowed), (2) the formation of a heteroduplex structurally and thermodynamically stable, and (3) the evolutionary conservation of target sites among vertebrates (Stark *et al.*, 2003). Several independent groups have formulated algorithms to predict miRNA targets (Enright *et al.*, 2003; John *et al.*, 2004; Kertesz *et al.*, 2007; Kiriakidou *et al.*, 2004; Krek *et al.*, 2005; Lewis *et al.*, 2005a). However, the binding of multiple miRNAs to a single mRNA complicates the target prediction (Krek *et al.*, 2005).

The Sanger Center miRBase (http://www.mirbase.org/) provides the central repository for microRNA sequence information. miRBase has a role in defining the nomenclature for miRNA genes and assigning names to novel miRNAs for publication in peer-reviewed journals. The online miRBase database is a resource containing all published miRNA sequences, together with textual annotation and links to the

primary literature and to other secondary databases (Griffiths-Jones, 2004, 2010). At now, the miRBase Targets database, has been rebranded as MicroCosm (http://www.ebi.ac.uk/enright-srv/microcosm/htdocs/targets/v5/), containing computationally predicted targets for microRNAs across many species. The miRNA sequences are obtained from the miRNA Registry and analyzed with the 3'UTR sequences of all human genes.

Several algorithms for computational mapping of miRNA targets have been published (Ioshikhes *et al.*, 2007). Some of the most popular algorithms for miRNA target prediction are described below.

TargetScan (http://www.TargetScan.org/) combines models based on thermodynamics of the interaction between miRNA and mRNA with sequence analysis to predict conserved targets in many genomes. Given a sequence of a conserved miRNA gene in multiple vertebrates and a set of orthologous 3'UTR sequences of these organisms, TargetScan looks for UTRs for segments with the perfect complementarity of Watson-Crick between 2 and 8 bases of a miRNA starting from the 5' end (the seed match). The conservation of target sites is required in at least five genomes (human, mouse, rat, dog and chicken). The program extends the seed match in each direction, including G:U pairing but stopping in the presence of a wrong pairing. The algorithm assigns a score to each interaction in agreement with the binding energy and conservation among species (Lewis *et al.*, 2005a).

Pic Tar (http://pictar.mdc-berlin.de/) is one of the programs that most successfully predicts targets for miRNAs (Krek *et al.*, 2005). The approach of this program provides a comparison between the different species using multiple sequence alignment between orthologous 3'UTR sequences. A score with maximum likelihood is given to each candidate sequence for each species separately. The program looks for conserved segments of 3'UTR containing a minimum of perfect and imperfect pairing for a given set of user-specified miRNAs. Thus, a length of the putative binding site for the length of the corresponding miRNA seed is established, taking a score based on Hidden Markov Model (HMM) for each 3'UTR sequence.

Diana-microT (http://diana.pcbi.upenn.edu/cgi-bin/micro_t.cgi) is an algorithm that first identifies putative interactions miRNA/mRNA-based energy between the two RNA-binding imperfectly matched (Kiriakidou *et al.*, 2004). In a first phase, the program evaluates whether there are at least three consecutive canonical pairing between the two sequences: it calculates the minimum free energy required for the connection between the two sequences, using two nucleotides at a time to calculate the pairing between a miRNA and its putative target. DIANA-microT method allows a weak binding at 5' seed, involving 6 consecutively paired nucleotides or G:U wobble pairs, if there exists additional base paring between the miRNA 3' end and target gene (Kiriakidou *et al.*, 2004). This method was reported to show the precision levels of 66%, which is the highest among several prediction programs (Min and Yoon, 2010a).

miRanda (http://www.micro-RNA.org/): this method was originally developed to predict miRNA target genes in *D. melanogaster* (Enright *et al.*, 2003), but is also used to predict human miRNA targets. For each miRNA, miRanda selects target genes on the basis of three properties: sequence complementarity using a position-weighted local alignment algorithm, free energies of RNA-RNA duplexes, and conservation of target sites in related genomes (Enright *et al.*, 2003). John *et al.* (John *et al.*, 2004) improved the method by implementing a strict model for the binding sites that require almost perfect complementarity in the seed region allowing a single wobble pairing. The potential targets are identified by the use of a modified Smith-Waterman local

alignment program (Smith and Waterman, 1981a). The score for each alignment is based on the complementary sequence and not the identity. Based on these alignments, the thermodynamic stability of these RNA duplexes is also estimated.

PITA (http://genie.weizmann.ac.il/pubs/mir07/mir07_prediction.html) estimates the free energy cost to unfold the mRNA secondary structure that surrounds the target site. This algorithm combines this free energy cost with the ΔG of miRNA-target pairing to measure ΔΔG. The algorithm finds seed matches (allowing a user-specified number of mismatches), and calculates ΔΔG for each match, irrespective of conservation. PITA starts by scanning the UTR for potential microRNA targets (using the supplied seed matching tools) and then scores each site using the method described in Kertesz *et al.* (Kertesz *et al.*, 2007). Although designed and tested for 3'UTRs, PITA can predict miRNA recognition elements outside the 3'UTR (Kertesz *et al.*, 2007).

Some features allow users to define whether an identified molecule is a true microRNA: (1) a mature miRNA should be expressed as a transcript of about 22 nucleotides in length, (2) it must derive from a precursor with a characteristic secondary structure (hairpin structure without large loops) and (3) should cover the portion of the stem of the hairpin and (4) be processed by Dicer. Another commonly used criterion concerns the conservation of sequence and hairpin structure of a predicted miRNA in different species. A “perfect” miRNA should satisfy all these criteria, only one of these criteria is not sufficient to establish that a gene is a new candidate miRNA (Ambros *et al.*, 2003d).

1.2.5 miRNA and cancer

Recent studies have shown that the expression of microRNAs may be involved in the process of tumorigenesis, functioning as tumor suppressors or oncogenes (Esquela-Kerscher and Slack, 2006). miRNAs associated with cancer are called "oncomirs". The expression of miRNAs is associated with various types of cancer. About 50% of human miRNAs is found in regions of the genome known as fragile sites, which are associated with cancer, indicating that they have an important role in tumor progression. The first indication of a possible role of miRNA as tumor suppressor resulted from a study by Calin *et al.* in which it has been shown that patients with B-cell chronic lymphocytic leukemia (CLL), the form of adult leukemia, often had deletions or reduction of expression of two miRNA genes in a cluster: mir-15a and mir-16-1. Deletions within the 13q14 locus have been found in more than 65% of cases of CLL, and also in 50% of cases of mantle cell lymphoma, in 16-40% of patients with multiple myeloma, and finally in 60% cases of prostate cancer. So, it was thought that a tumor suppressor gene may be located in this region of the genome of about 30 kb. In addition, it was found that mir-15a and mir-16-1 are located within the intron of a non-protein-coding RNA gene of unknown function, called *LEU2*. In patients with CLL, who have these deletions, a more favorable prognosis was found than in patients with an abnormal karyotype or deletions at other loci such as 11q23 and 17p13. This can be explained by the fact that homologues of mir-15a and mir-16-1 have been found in a cluster on chromosome 3 (mir-15b and mir-16-2, respectively) and expressed at low levels in patients with CLL (so, in any case, the deletions do not involve a complete elimination of these miRNA families) (Calin *et al.*, 2002, 2004b).

Then, Cimmino and his collaborators showed that miR-15a and miR-16-1 negatively regulate *BCL2*, which is an anti-apoptotic gene and is often over-expressed in many types of cancer in humans, including leukemias and lymphomas. Therefore, it was thought that the deletion or deregulation of mir-15a and mir-16-1 leads to

an increased expression of *BCL2*, promoting leukaemogenesis and lymphomagenesis in hematopoietic cells (Cimmino *et al.*, 2005).

Other studies have shown a strong correlation between a decreased expression of some miRNAs and oncogenesis (Iorio *et al*., 2005; Michael *et al.,* 2003).

Different expression profiles of miRNAs have been observed in certain organs emphasizing the importance of miRNAs in the maintenance of stem cells and in directing the differentiation of certain cell types during development. The miRNA profiles are surprisingly informative, reflecting the lines of development and state of differentiation of tumors (Lu *et al.*, 2005c). Some researchers are now using the expression profiles of miRNAs as a distinctive character in order to classify the different types of cancer, defining miRNA as markers that may predict a favorable prognosis (Calin *et al.* 2004b; Calin *et al.*, 2005; Chan *et al.*, 2005; He *et al.*, 2005a; Iorio *et al.* 2005; Lu *et al.* 2005c; Takamizawa *et al.* 2004). Lu *et al.* suggested that the expression profiles of a few miRNAs (approximately 200 genes) are required to accurately classify human cancers (Lu *et al.*, 2005c). The alterations of miRNA expression may promote tumor formation by modulating the functional expression of critical genes involved in tumor development and progression (Lu *et al.*, 2005c).

Also some components of the machinery of miRNAs are involved in the process of tumorigenesis, such as Dicer (Karube *et al.*, 2005).

Since the first paper reported the link between the abnormal expression of miRNAs and cancer in 2002 (Calin *et al.*, 2002), more and more studies have shown that many miRNAs take part in the progression of various cancers, including tumor growth, differentiation, adhesion, apoptosis, invasion, and metastasis (Calin *et al.*, 2004b; Calin and Croce, 2006; Gaur *et al.*, 2007). miRNA profiling experiments have revealed that many miRNAs are abnormally expressed in clinical cancer samples, since cancer is ultimately a consequence of a disordered gene expression.

Liu *et al.* define miRNAs as “star molecules”, in their opinion miRNAs have become the focus in recent years and the studies of their roles in cancers have continued (Lu *et al.*, 2005c).

Generally, the mechanisms implicated in oncogenesis and tumor suppression related to miRNAs have been proposed (**Figure 8**). However, the exact mechanisms and entire networks of miRNAs in cancer progressions are still unclear and deserve deep investigation.

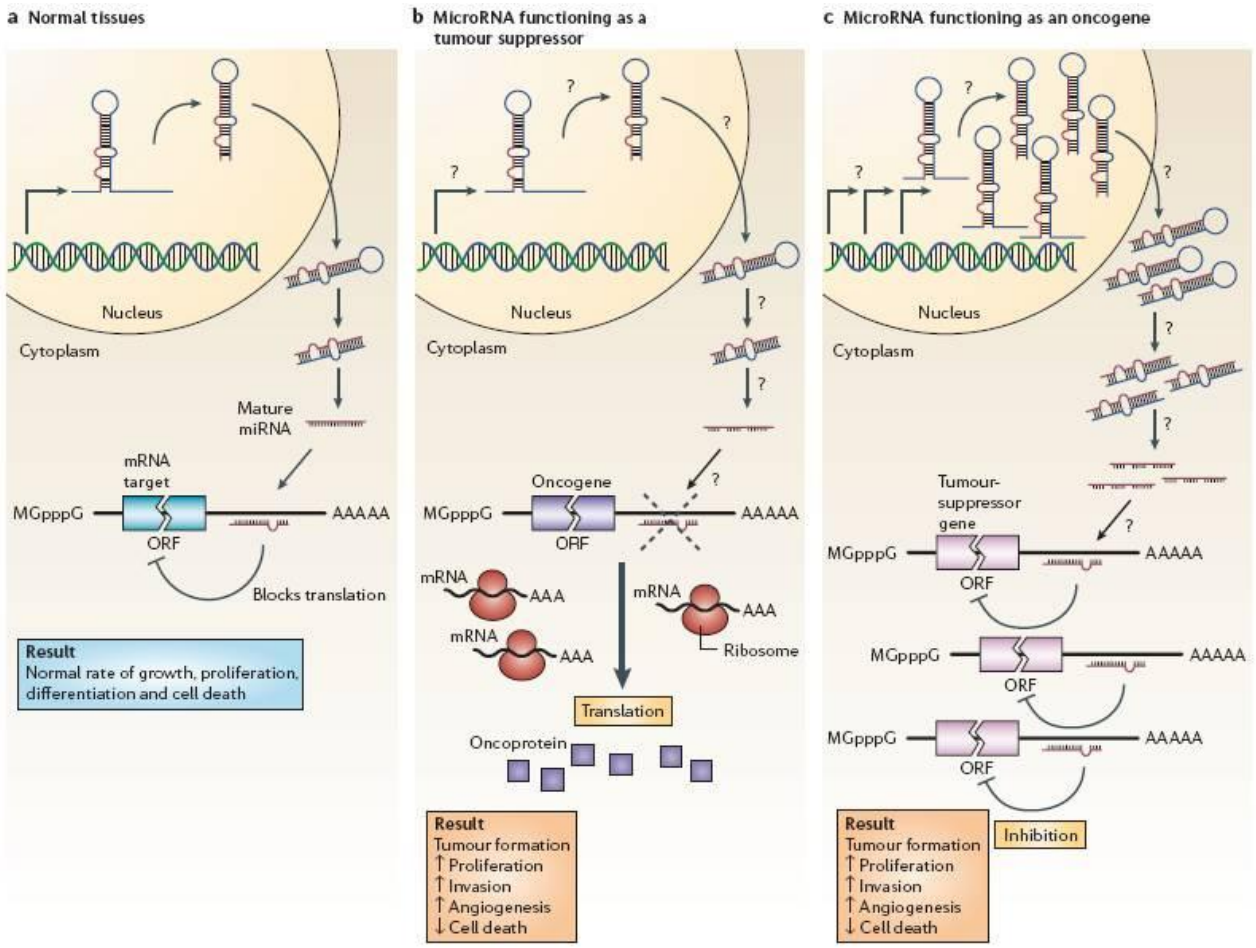

Figure 8. microRNAs can function as tumor suppressors and oncogenes. (a) In normal tissues, proper miRNA transcription, processing and binding to complementary sequences on the target mRNA results in the repression of target gene expression through a block in protein translation or altered mRNA stability (not shown). The overall result is normal rates of cellular growth, proliferation, differentiation and cell death. (b) The reduction or deletion of a miRNA that functions as a tumor suppressor leads to tumor formation. A reduction in or elimination of a mature miRNA may be due to defects at any stage of miRNA biogenesis (indicated by question marks) and ultimately leads to the inappropriate expression of the miRNA-target oncoprotein (violet squares). The overall outcome might involve increased proliferation, invasiveness or angiogenesis, decreased levels of apoptosis, or undifferentiated or de-differentiated tissue, ultimately leading to tumor formation. (c) The amplification or over-expression of a oncogenic miRNA would also result in tumor formation. In this situation, increased amounts of a miRNA, which might be produced at inappropriate times or in the wrong tissues, would eliminate the expression of a miRNA-target tumor suppressor gene, leading to cancer progression. Increased levels of a mature miRNA might occur because of amplification of the miRNA gene, a constitutively active promoter, increased efficiency in miRNA processing or increased stability of the miRNA (indicated by question marks). ORF, open reading frame. (Adapted from Esquela-Kerscher and Slack, Nat Rev Cancer, 2006).

1.2.6 Methods to detect miRNA expression

miRNA expression profiles are closely related to developmental stages and physiological states as well as disease processes; thus, miRNA expression assessment and analysis are basic and preliminary procedures in most miRNA studies. Moreover, the use of the expression profiles of miRNAs to distinguish different types of cancer might facilitate the diagnosis and treatment of many diseases. These studies have produced a large number of miRNA-disease associations and have shown that the mechanisms of miRNAs implicated in diseases are very complex. Therefore, a large-scale analysis and integrating of these miRNA-disease associations at a system level will offer a platform to dissect the mechanisms of miRNAs in disease, although the current miRNA-disease associations are far from complete. In fact, the Human MicroRNA & Disease Database (HMDD, http://202.38.126.151/hmdd/mirna/md/) has been developed to retrieve the associations of miRNA and disease from literature. HMDD contains miRNA names, disease names, dysfunction evidences, and literature PubMed ID (Lu *et al.*, 2008).

At present, methods widely used for miRNA expression detection mainly include miRNA cloning, northern blotting, quantitative PCR (qPCR), *in situ* hybridization (ISH), and miRNA arrays (Li and Ruan, 2009d). Each methodology has its own advantages and disadvantages. miRNA cloning is mainly used to discover new miRNAs, but it's not accurate in miRNA quantification. Northern blotting can reflect the miRNA expression profile more accurately than cloning, in fact, it's considered the "gold standard" of miRNA detection. On the other hand, northern blotting it's very time consuming, requires large amounts of RNA samples and radioactive probes. qPCR is another method widely used to quantify specific miRNAs in samples. It's a very high sensitive and specific method, but limited by high cost. ISH can provide information on the location of miRNA expressed in cells or tissues as well as the miRNA abundance. Unfortunately, ISH is not suitable for high-throughput profiling. Instead, miRNA arrays offer rapid and high-throughput analysis and are useful to study the expression levels of hundreds of miRNAs at the same time. At now, many different miRNA microarray platforms exist (Sato *et al.*, 2009). Nowadays, deep-sequencing expression analysis allows to accurately quantify miRNA and also mRNA expression levels on whole-genome scale and to discover novel miRNAs and mRNAs. Deep-sequencing provides a major advance in robustness, comparability and richness of expression profiling data respect to microarray and qPCR ('t Hoen *et al.*, 2008; Zhou *et al.*, 2010a).

1.2.7 miRNA and RCC

Differential levels of specific miRNAs have been observed in several tumor types when compared to normal tissues. In solid cancers, the spectrum of expressed miRNAs is very different from that of normal cells (Volinia *et al.*, 2006). In fact, global reduction in miRNA expression is a feature of many cancers, miRNA gene copy number variation appears common in cancer, and over-expression of miRNAs can contribute to oncogenesis. Epigenetic silencing is another regulatory mechanism that controls miRNA expression (Lu *et al.*, 2005c; Vogt *et al.*, 2011; Volinia *et al.*, 2006). Thus, the modulation of miRNA expression in cancer is well-established.

miRNA expression profiles have some potential advantages in respect to standard mRNA or other protein-based profiles: (1) miRNAs appear to be very stable in tissues and biological fluids, including serum and urine, even in degraded preparations (Jung *et al.*, 2010), and are protected from endogenous RNase since they have a small size and perhaps have packaged within exosomes; (2) their tissue-specific nature makes

miRNAs ideal candidates for biomarkers (Li *et al.*, 2010a). In recent years, many efforts have been made not only to obtain tissue-specific and tumor type-specific signatures, but also to identify new diagnostic biomarkers within miRNA class.

Since miRNAs are tissue-specific, it's possible to find miRNA specifically expressed in the kidney. In particular, I'll described below some differential expression studies on RCC and ccRCC subtype. The role of miRNAs in the regulation of renal development, physiology, and pathology has emerged as an important and potentially fruitful area of research. Multiple studies have shown that miRNA expression can be used as a useful diagnostic tool.

One of the first studies on the involvement of miRNAs in RCC dates back to 2007, in which Gottardo and colleagues reported, specifically, the up-regulation of four miRNAs (miR-7-2, miR-28, miR-185, and let-7f-2) in RCC tissues compared to normal kidney (Gottardo *et al.*, 2007).

In 2008, Nakada *et al.* investigated expression profiles of miRNAs in ccRCC (16 patients) and chRCC (4) and in normal kidneys (6). They found that the two histotypes were separable. In particular, 43 miRNAs were differentially expressed between ccRCC and normal kidney, whose 37 down- and 6 up-regulated genes; while 57 miRNAs were differentially expressed between chRCC and normal kidney, whose 51 down- and 6 up-regulated genes. These data indicated that miRNAs tend to be down-regulated in both ccRCC and chRCC compared with normal kidney. Moreover, they observed that the most down-regulated miRNAs in ccRCC were miR-141 and miR-200c, and that their putative target was *ZEB2*, gene involved in repression of *CDH1*/E-cadherin and in epithelial to mesenchymal transition. By functional validation, they suggested that the down-regulation of these two miRNAs could be involved in suppression of *CDH1* transcription via up-regulation of *ZEB2*. They also showed that genome copy number aberrations could affect the expression of miRNAs, in particular of those that are each cleaved from a single precursor. (Nakada *et al.*, 2008). Today, the involvement of miR-200 miRNA family in EMT is fully validated by other studies (Gregory *et al.*, 2008, 2008a; Kim *et al.*, 2011a; Tellez *et al.*, 2011). For example, Park *et al.* by evaluating the expression of 207 miRNAs in the 60 cell lines of the drug screening panel maintained by the Nation Cancer Institute (NCI-60), identified the miR-200 miRNA family as an extraordinary marker for cells that express *CDH1* but lack expression of Vimentin (*VIM*), that are epithelial and mesenchymal markers, respectively. miR-200 was found to directly target the mRNA of the *CDH1* transcriptional repressors *ZEB1* and *ZEB2.* The ectopic expression of miR-200 caused up-regulation of *CDH1* in cancer cell lines and reduced their motility. Conversely, inhibition of miR-200 reduced *CDH1* expression, increased expression of *VIM*, and induced EMT. The authors suggested miR-200 as a powerful marker and determining factor of the epithelial phenotype of cancer cells (Park *et al.*, 2008). It has been reported that also miR-205 is involved in EMT process by repressing *CDH1* (Gregory *et al.*, 2008, 2008a; Tellez *et al.*, 2011).

In another study, the miRNA expression levels were used to distinguish kidney cancer subtypes, using tumor tissues from 20 patients, four cases from each of the following histotypes: oncocytoma, chromophobe, papillary, poor-prognosis clear cell, and good-prognosis clear cell. The researchers found a unique miRNA signature for each subtype of renal tumor; in particular, they identified a genomic similarity between chromophobe and oncocytoma, and between papillary and clear cell RCC; and distinct miRNA patterns correlated to good and poor prognosis ccRCC subtypes (Petillo *et al.*, 2009).

A study by Huang *et al.* showed a total of 76 differentially expressed miRNAs comparing 11 pairs samples (ccRCC and normal matched), whose 50 up- and 26 down-regulated genes, among them miR-27a, miR-221, miR-34a, miR-103, miR-143 were specifically expressed in ccRCC samples. The highest expression level was detected in let-7-g and miR-21, while the lowest in miR-145, miR-320, miR-494 (Huang *et al.*, 2009j).

Chow *et al.* performed a comparison between 3 ccRCC tissues and their normal counterpart. They found a total of 33 dysregulated miRNAs, including 21 up-regulated miRNAs, and that many of these miRNAs have been reported to be dysregulated in other malignancies (Chow *et al.*, 2010).

Weng *et al.* performed whole-genome small RNA deep sequencing in paired frozen and formalin-fixed paraffin-embedded (FFPE) tissue specimens of benign kidney and ccRCC. They found 73 differentially expressed miRNAs in frozen and 133 in FFPE samples, respectively, with a high correlation not only among different types of samples but also between deep sequencing, microarray and qPCR technologies used on the same samples, highlighting that miRNAs are relatively stable also in FFPE samples (Weng *et al.*, 2010).

Another study reported a total of 35 miRNAs that can robustly distinguish ccRCC from their patient-matched normal kidney tissue samples (28 samples) with high confidence; among them 26 were down- and 9 up-regulated. Furthermore, miRNAs identified down-regulated in this study were correlated also to common deletions in ccRCC (Juan *et al.*, 2010).

Also Fridman and his collaborators used miRNA expression to accurate molecular classify renal tumors among 125 FFPE samples, including 38 oncocytomas, 27 chromophobe RCCs, 34 ccRCCs, and 26 pRCC. They identified 33 differentially expressed miRNAs through pairwise comparisons of each of the four histotypes and high degree of similarity between ccRCC and pRCC, and between chRCC and oncocytoma, thus they selected miRNAs in order to identify each pair of types, that were miR-31 and miR-126 for the first pair, and miR-221 and miR-210 for the pair composed by chRCC and oncocytoma, obtaining a clear separation between the four groups (Fridman *et al.*, 2010a).

A recent study of White *et al.* reported the analysis of 70 matched pairs of ccRCC and normal kidney tissues from the same patients by microarray, followed by validation in qPCR. They identified 166 dysregulated miRNAs (89 up- and 77 down-regulated genes), including miR-122, miR-155 and miR-210, which had the highest over-expression, and miR-200c, miR-335 and miR-218, which were most down-regulated. They conducted an extensive target prediction analysis showing that many predicted target genes are involved in RCC pathogenesis. They also demonstrated that miRNA dysregulation might be attributed in part to chromosomal aberrations, co-regulation of miRNA clusters and co-expression with host genes (White *et al.*, 2011b).

Youssef *et al.* developed a classification system that can distinguish the different RCC subtypes. Using miRNA microarray analysis, they identified 91 miRNAs as statistically differentially expressed among different subtypes, and that ccRCC is more closely related to pRCC and that both are distinct from oncocytoma and chRCC. Also in this study the correlation between cytogenetic changes and miRNA dysregulation was highlighted (Youssef *et al.*, 2011).

Whereas, Heinzelmann *et al.* detected a miRNA signature, composed by 33 miRNAs, that potentially distinguishes between metastatic and non-metastatic ccRCCs, including miR-451, miR-221, miR-30a, miR-

10b and miR-29a. They also identified a group of 12 miRNAs (e.g., let-7 family, miR-30c, miR-26a), which were decreased in highly aggressive primary metastatic tumors (Heinzelmann *et al.*, 2011).

Powers *et al.* defined distinct miRNA expression profiles in the 4 most common renal epithelial tumor subtypes and showed that, despite the common chromosomal gains and losses in RCC, very few of the significant miRNA gene expression differences can be explained solely by a gene dosage effect, except in the cases of miR-21 and miR-143 (Powers *et al.*, 2011).

Neal *et al.*, through a functional study, found high levels of HIF in a renal cell line (RCC4) lacking functional *VHL* according to the literature, they demonstrated that following treatment to suppress HIF expression, the levels of miR-155 and miR-210 were decreased in the treated lines, thus their expression level is HIF-dependent. A striking positive correlation was also found between *CAIX* and miR-210 expression, they were significantly increased in tumors with identifiable *VHL* mutations, or promoter methylation, compared to tumors that did not show mechanisms for suppression of *VHL* function (Neal *et al.*, 2010).

In 2007, Kulshreshtha *et al.* demonstrated for the first time a functional link between hypoxia and miRNA expression, showing a specific spectrum of miRNAs (including miR-23, miR-24, miR-26, miR-27, miR-103, miR-107, miR-181, miR-210, and miR-213) that is induced in response to low oxygen, at least some via a hypoxia-inducible-factor-dependent mechanism. Moreover, a small group, such as miR-26, miR-107 and miR-210, decreased pro-apoptotic signaling in a hypoxic environment by inhibiting caspase activation, suggesting an impact of these transcripts on tumor formation (Kulshreshtha *et al.*, 2007a).

Interestingly, miR-210 plays a crucial role in the cellular response to hypoxia, because it's regulated by both HIF-1α and HIF-2α. HIF-1α directly binds to a hypoxia responsive element (HRE) on the proximal miR-210 promoter, thus defining miR-210 as a direct transcriptional target of HIF-1α (Kulshreshtha *et al.*, 2007a; Huang *et al.*, 2010). miR-210 was found to be involved in angiogenesis, cell cycle regulation, stem cell differentiation, DNA damage repair, mitochondrial metabolism and cancer, since it has a high expression level in many cancers. Since the close correlation between miR-210 expression and tumor hypoxia, circulating miR-210 might be a prognostic marker in cancer patients (Huang *et al.*, 2010). Nakada *et al.* demonstrated that miR-210 over-expression may cause multipolar spindle via centrosome amplification and that this phenomenon, in turn, contributes to the abnormal cell division and aneuploidy. Therefore, miR-210 over-expression may contribute to the tumorigenesis and/or progression of ccRCC (Nakada *et al.*, 2011).

All these studies show that miRNA profiling could represent an invaluable tool to classify tumors that represent diagnostic challenges. The discovery of distinctive miRNA signatures will likely improve the molecular classification of cancer and specify distinct roles within biologic processes of each miRNA. miRNAs can act as oncogenes or tumor suppressors depending on the tissue and the expression of their targets. Because miRNAs can target many genes, modulating the level of a single miRNA could eventually affect many pathways at the same time. For example, deregulation of specific miRNAs, which control important angiogenic and proliferative processes, may have an important role in the biology of RCC.

1.3 Integrative analysis of miRNA and mRNA expression profiles

1.3.1 Integrative genomics approach

The molecular complexity of a tumor manifests itself at the genomic, epigenomic, transcriptomic and proteomic levels, thus an integrated analysis may have an important role in characterizing a tumor. miRNA and gene expression patterns are closely related, they work cooperatively to form gene regulatory networks, therefore, integrative genomics and genetics approaches might be a useful tool in elucidating the complex relationships often found in these networks. (Shen *et al.*, 2009). Anyway, the specific functional roles of most miRNAs and their combinatorial effects in biological processes are still unclear.

A number of studies have provided the necessary experimental evidence confirming the validity of the casual relationships inferred using such an approach. The regulatory mechanisms of miRNA-mediated regulation are very complex and difficult to elucidate. Each miRNA can directly regulate hundreds of messanger RNAs (mRNAs); conversely, most mRNAs have a length that contain many binding sites for miRNAs (Su *et al.*, 2011).

Zhang *et al.* have explained the reasons for which identifying functional miRNA-gene regulatory networks is important, as follows: (1) one gene can be regulated by multiple miRNAs and one miRNA can regulate a large number of genes, thus, the aim of the research is to find a set of miRNAs and their co-regulated genes; (2) the miRNA-mRNA target relationships differ among tissues and conditions; (3) although miRNAs physically interact with mRNAs, ultimately miRNA regulation affects the quantities of proteins in cells rather than the quantities of mRNAs, so, the expression levels of miRNAs are not always anti-correlated with those of their target genes; (4) the genomic data are generally noisy and incomplete (Zhang *et al.*, 2011). Therefore, the availability of miRNA and gene expression profiles from the same patient or cell line and miRNA-gene networks, provides an opportunity to discover and accurately characterize miRNA-gene regulatory relationships.

Much of the current effort in miRNA studies is focused on the elucidation of their function. Typically miRNAs have been studied by using the gene profiling approach. Each miRNA has been studied for its single contribution to differential expression or to a compact predictive signature. Since one miRNA can regulate translation of tens or even hundreds of different mRNAs and in different ways, and a single mRNA can be regulated by more than one miRNA, as mentioned above, the effect of miRNAs on cell pathology and physiology is likely to be complex (Volinia *et al.*, 2010).

It should be noted that miRNA target prediction algorithms are prone to high degree of false positives and completely ignore the tissue- or disease-specific nature of miRNA-target interactions (Mestdagh *et al.*, 2011), thus, miRNA-mRNAs paired expression profiles may improve the accuracy of sequence-based miRNA-target predictions.

1.3.2 miRNA-mRNA integrated studies

Several laboratories are now producing expression profiles of miRNA and mRNA on the same set of samples, providing a global view on the dynamics of miRNA-gene regulatory networks (Huang *et al.*, 2007; Nunez-Iglesias *et al.*, 2010; Su *et al.*, 2010; Zhang *et al.*, 2011).

Starting from genome-wide miRNA and gene expression data by microarray analysis and target prediction by many existing algorithms, it's possible to reconstruct functional post-transcriptional miRNA-gene networks, since miRNAs tend to down-regulate their target genes, the expression profile of miRNA-gene pairs are expected to be anti-correlated (Sales *et al.*, 2010; Su *et al.*, 2010; Su *et al.*, 2011).

A number of exploratory studies have attempted to decipher how miRNAs, genes and proteins interact on a system level. Zhang *et al.* applied an integrative approach of multiple types of genomic data (i.e., predicted miRNA-gene interactions, the miRNA and gene expression profiles, the gene-gene interaction networks) to identify miRNA-gene regulatory relationships in 368 human ovarian cancer samples (Zhang *et al.*, 2011). Using a different procedure, Metsdagh *et al.* performed an integrative approach of miRNA and gene expression profiles, transcription target prediction and mechanistic models of gene network regulation in a total of 244 human samples belonging to 4 different data sets (normal adult tissues, neuroblastoma tumors, myeloma tumors and NCI-60 cancer cell lines) (Mestdagh *et al.*, 2011). In another study, miRNA expression levels were integrated with aCGH (array-comparative genomic hybridization) and mRNA expression profiles in 26 tumor and corresponding normal lung tissue samples from highly asbestos-exposed and non-exposed patients, and on 8 control lung tissue samples (Nymark *et al.*, 2011). An integrated approach applied to breast cancer revealed roles for miRNAs in 101 human primary breast cancer samples, identifying statistically significant differential expression of miRNAs that distinguish the reciprocal basal-like and luminal-A breast cancer subtypes (Enerly *et al.*, 2011). Elkan-Miller *et al.* identified functionally important miRNA-target pairs in the mammalian inner ear through an *in silico* prediction model that integrates miRNA, mRNA and protein expression, since studying both the mRNA and protein levels provides the most informative view of miRNA regulation and their functional roles in particular tissues or organs (Elkan-Miller *et al.*, 2011). Havelange *et al.* integrated miRNA and mRNA expression profiles obtained from 48 newly diagnosed AML (acute myeloid leukemia) patients by using microarray platforms, and performed correlation, gene ontology, and network analysis, and finally an experimental validation (Havelange *et al.*, 2011a).

In RCC field, Zhou *et al.*, using massively parallel sequencing technology, analyzed the miRNA and gene expression profiles in tumor tissues and matched normal adjacent tissues obtained from 10 ccRCC patients without distant metastases. They found that a total of 404 miRNAs and 9,799 mRNAs were differentially expressed in tumors compared to normal tissues. They also identified 56 novel miRNA candidates in at least two samples. They confirmed that canonical cancer gene and miRNAs (e.g., *VEGFA*, miR-210) play pivotal roles in ccRCC development, and proposed novel candidates without previous annotation in ccRCC carcinogenesis (e.g. *PNCK* and miR-122). They also confirmed that pathways controlling cell fates (e.g., cell cycle, apoptosis) and cell communication (e.g., focal adhesion, ECM-receptor interaction) were disrupted in ccRCC. In addition, their results showed that the expression of a miRNA gene cluster located on Xq27.3 was consistently down-regulated in at least 76,7% of about 50 ccRCC patients (Zhou *et al.*, 2010a).

Taken together, these studies highlight the importance of using an integrative approach of multiple genomics data in different type of diseases, despite the fact that each study is conducted by a different method and different target prediction algorithms are used.

In particular, in our study we integrated miRNA and gene expression profiles using a web-based tool namely MiRNA and Genes Integrated Analysis, MAGIA (Sales *et al.*, 2010). MAGIA allows to perform an integrative

analysis of miRNA and gene expression data, and target predictions, facilitating the detection of functional miRNA-mRNA relationships. Target predictions are based on a number of different algorithms (miRanda, PITA, TargetScan), with the possibility of combining them with Boolean operators. Integrative analysis can be performed adopting different functional measures (i.e., parametric and non parametric correlation indexes, a variational Bayesian model, mutual information, and a meta-analysis approach based on p-value combination) of miRNA and mRNA expression data. Moreover, MAGIA constructs bipartite regulatory networks of the best miRNAs and mRNA putative interaction and retrieves data about genes, miRNAs and diseases available in public databases (Sales *et al.*, 2010). For example, this type of integrative analysis of miRNA-mRNA expression and genome-wide copy number (CN) profiles has been applied to reconstruct a network of functional interactions occurring in multiple myeloma (MM), allowing the definition of specific patterns of miRNA expression that distinguish distinct subtypes of MM associated with distinct and well-known genetic alterations, and the reconstruction of a general miRNA-mRNA regulatory network that represents the putative functional regulatory effects (as supported by expression data) of all of these miRNAs on their targets in MM (Lionetti *et al.*, 2009).

2 AIM OF THE STUDY

During my PhD fellowship work, I focused on ccRCC, which is the most common, invasive and metastatic subtype among kidney adult tumors.

The present study aimed to identify the functional relationships and regulatory networks connecting genes and microRNAs potentially important for ccRCC tumorigenesis. To do this, three RCC cell lines, Caki-1, Caki-2 and A498, which are commonly used in functional studies for ccRCC, were analyzed for their genome-wide gene and miRNA expression profiles, using Affymetrix microarray technology. Two of them, Caki-1 and A498, are also included into the NCI-60 cancer cell line panel. These three tumor cell lines were compared to a normal tubular epithelial renal cell line (HK-2). Then, using an innovative statistical and bionformatical procedure, we combined and integrated gene and miRNA expression data in order to reconstruct miRNA-target post-transcriptional regulatory networks involved in RCC biology.

This PhD thesis is structured in three major sections:

Part I: High-throughput gene expression profiling. Assessment of *VHL* and HIF-1α mutational status in all the cell lines here used. Genome-wide analysis of gene expression profiles of RCC cell lines as compared to HK-2, using Affymetrix GeneChip® Human Gene 1.0 ST Array. Statistical and bioinformatics procedures to calculate differentially expressed genes and to perform a pathway and functional enrichment analysis. An extensive literature mining search to find association between genes and RCC and cancer.

Part II: High-throughput miRNA expression profiling. Genome-wide analysis of miRNA expression profiles by comparing RCC cell lines to HK-2, using Affymetrix GeneChip® miRNA Array. Statistical and bioinformatics analysis to calculate differentially expressed miRNAs, followed by functional enrichment analysis. Selection of miRNAs resulting associated with RCC and cancer in previous published papers. Validation of miRNA expression levels by quantitative PCR (qPCR).

Part III: Integrated analysis of miRNA and gene expression data. Statistical and bioinformatics analysis to carry out miRNA and gene expression profiles integration. Reconstruction of miRNA-target gene post-transcriptional regulatory networks involved in RCC pathology. Selection of some miRNA-gene anti-correlated pairs for qPCR validation.

3 PART I: HIGH-THROUGHPUT GENE EXPRESSION PROFILING

3.1 Material and Methods

3.1.1 Cell Lines

Three established RCC cell lines were used as *in vitro* model for ccRCC pathology (**Table 1**). They all are of epithelial origin: Caki-1 was derived from the skin metastasis of a ccRCC; Caki-2 was established from the primary tumor that originated Caki-1; A498 was derived from a renal carcinoma. As normal control, we used HK-2 (CRL-2190) cell line, which is an immortalized proximal tubule epithelial cell line derived from a normal adult human kidney. Cell lines were purchased from American Type Culture Collection (ATCC, Manassas, VA, USA) and were cultured in our laboratory according to their corresponding ATCC datasheets. Two cell lines, Caki-1 and A498, are also included in the NCI-60 cell line collection (http://www.sanger.ac.uk/genetics/CGP/NCI60/).

Cell Line	ATCC No.	Disease	Gender	Age
Caki-1	HTB-46	Clear cell carcinoma (s)	Male	49
Caki-2	HTB-47	Clear cell carcinoma	Male	69
A498	HTB-44	Renal carcinoma	Female	52

Table 1. Description of the RCC cell lines used in these analyses. s, skin metastasis (site of origin for Caki-1).

3.1.2 Total RNA and DNA extraction

Total RNA was extracted from RCC and normal cell lines using the miRNeasy extraction kit (Qiagen, Hilden, Germany), according to the manufacturer's instructions. After elution in RNase free-water, RNA samples were quantified by ND-1000 spectrophotometer (NanoDrop Technologies, Wilmington, DE, USA). RNA quality was checked by microcapillary electrophoresis on 2100 BioAnalyzer (Agilent Technologies, Santa Clara, CA, USA), using a RNA 6000 Nano LabChip kit, following the manufacturer's instructions. Thus, total RNA integrity was assessed on the basis of the RIN (RNA Integrity Number) factor. The RIN is generated for each sample across a ten point scale: samples with a RIN ≥ 7 have a good quality, lower values indicate partial or complete RNA degradation. The 28S/18S rRNA ratio and an estimated concentration are also provided, and presence of low molecular weight RNA molecules (including 5S rRNA and small RNAs) was verified. RNA samples were stored at -80°C until use.

Genomic DNA was extracted from the RCC and normal cell lines using the standard phenol-chloroform procedure, eluted in TE buffer and quantified by ND-1000 spectrophotometer (NanoDrop Technologies). DNA samples were stored at -20°C until use.

3.1.3 Assessment of *VHL* and HIF status

In order to perform a *VHL* mutation screening by direct Sanger sequencing, the three exons of this gene were entirely amplified by PCR. Exon 2 was amplified according to Matsuda (Matsuda *et al.*, 2008), but adapting the procedure to Platinum *Pfx* DNA Polymerase and using 10 ng of genomic DNA per sample. Exon 1 and exon 3 were amplified by PCR in a total volume of 25 µl containing: 20 ng of genomic DNA, 1x

PCR buffer (Roche Diagnostics, Germany), 0.3 mM each dNTP (Roche), 1 mM $MgCl_2$ (Roche), 1U FastStart Taq DNA Polymerase (Roche), 0.3 µM Primer Forward, 0.3 µM Primer Reverse. Thermal program includes: 95°C for 4 min, followed by 35 cycles of 95°C for 30 sec, 63.5°C for 30 sec (56°C for exon 3), and 72°C for 45 sec, with a final extension of 72°C for 7 min. After PCR, amplification products were checked out by 2% agarose gel electrophoresis. Sequencing reactions were performed using the BigDye® Terminator v3.1 Cycle Sequencing Kit (Applied Biosystems, Life Technologies, Carlsbad, CA, USA), on a DNA Sequencer ABI 3130XL instrument (Applied Biosystems), following the manufacturer's instructions. Then, the electropherograms were visualized by use of Chromas free software v. 1.45 (http://www.technelysium.com.au/chromas.html), and nucleotide variations were sought out taking into reference the *VHL* sequence annotated in Ensembl database (http://www.ensembl.org/Homo_sapiens/Transcript/Exons?db=core;g=ENSG00000134086;r=3:10182692-10193904;t=ENST00000256474). The sequence of primers used in both PCR and sequencing reactions are reported in **Table 2**.

PRIMER	SEQUENCE
Ex_1F	5' AGCGCGTTCCATCCTCTAC 3'
Ex_1R	5' GTCACCCTGGATGTGTCCTG 3'
Ex_2F	5' CTTTAACAACCTTTGCTTGTCCCGATA 3'
Ex_2R	5' GTCTATCCTGTACTTACCACAACAACCT 3'
Ex_3F	5' GCAAAGCCTCTTGTTCGTTC 3'
Ex_3R	5' CCGCTACGGATGTAGAATGG 3'

Table 2. Primers used in PCR and sequencing reactions.

To assess HIF-1α protein expression, western blot analysis was carried out. For one-dimensional electrophoresis (1-DE) western blotting, 30 µg of protein lysates, obtained from renal cell lines, quantified with a Bio-Rad microassay (Hercules, CA), were separated on 10% SDS-PAGE and on NuPage 4 to 12% Bis-Tris pre-cast gels using MOPS SDS running buffer (Invitrogen), with described conditions (Perego *et al.*, 2005). 1-DE gel was blotted onto a nitrocellulose membrane that was stained with Ponceau S (Sigma-Aldrich) to check transferred proteins. The membrane was incubated for two hours with a mouse monoclonal antibody against HIF-1α (dilution 1:500, clone 54, BD Transduction Laboratories, Lexington, KY) and against α-actin (dilution 1:1000, Sigma-Aldrich). The detection was performed by one-hour incubation at room temperature with a secondary antibody coupled with horseradish peroxidase and SuperSignal West Dura Detection System (Pierce, Rockford, IL). Densitometric analysis was performed using a GS-710 imaging densitometer equipped with Quantity One Software (Bio-Rad).

3.1.4 High-throughput gene expression analysis

3.1.4.1 Target sample preparation for microarray gene expression analysis

In order to perform a differential gene expression analysis by comparing the three RCC cell lines to HK-2, we assessed gene expression levels in tumor and normal cell lines by use of Affymetrix microarray technology. For each sample, three technical replicates were prepared and hybridized onto the GeneChip® Human Gene 1.0 ST Array (Affymetrix, Santa Clara, CA, USA), which measures gene expression levels of 19,973 well-annotated genes, using a single probe set per gene comprised of multiple probes distributed along the entire

length of the genomic locus, thus offering a whole-transcript coverage. The array contains 764,885 distinct probes, with a mean of 28 probes per gene, and all probe sets are perfect match (PM) only. Gene 1.0 ST Array probe design is based on the March 2006 human genome sequence assembly (UCSC hg18, NCBI Build 36). This platform provides more than 99% coverage of sequences present in the RefSeq database (November, 2006; http://www.ncbi.nlm.nih.gov/RefSeq/). Starting from 100 ng of total RNA per sample, labelled targets were prepared using Ambion® Whole Transcript (WT) Expression Kit (Applied Biosystems, Life Technologies) and GeneChip® WT Terminal Labeling and Controls Kit (Affymetrix), following manufacturers' instructions.

Briefly, as illustrated in **Figure 9,** total RNA is primed with synthetic primers containing a T7 promoter sequence and reverse transcribed into first-strand cDNA. Afterwards, the single-stranded cDNA is converted into double-stranded cDNA, using DNA Polymerase and RNase H to simultaneously synthesize second-strand cDNA and degrade the original RNA. The *in vitro* transcription (IVT) reaction is then performed to synthesize and amplify the antisense cRNA. Next, the cRNA is purified and measured for yield and size distribution. 10 µg of cRNA are reverse transcribed using random primers, to synthesize second-cycle cDNA. The cRNA template is degradated by RNase H to leave a single-stranded cDNA, that is ,purified and assessed for size distribution. Lastly, 5.5 µg of cDNA is fragmented, biotin terminally labeled, and hybridized for 16 hours at 45°C onto Gene 1.0 ST Array. The array is then washed and stained using the Affymetrix Fluidics Station FS-450. Fluorescent images of each array are acquired using Affymetrix GeneChip® Scanner 3000 7G and analyzed using GeneChip® Operating Software (GCOS).

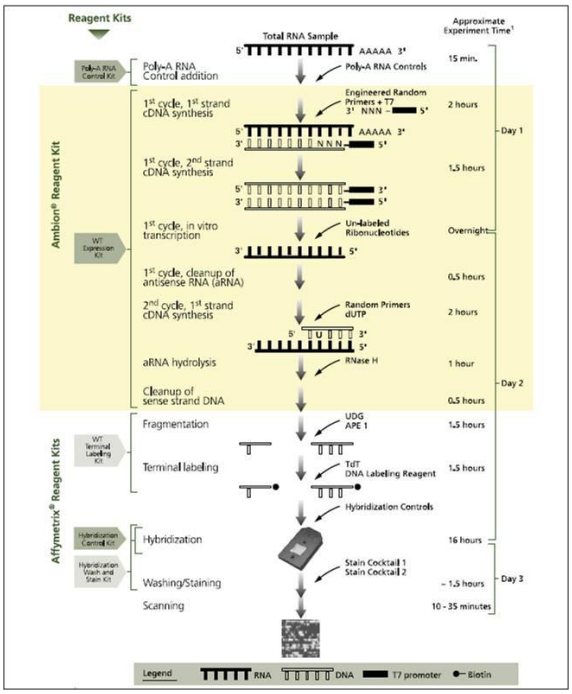

Figure 9. Affymetrix whole transcript target preparation for hybridization onto GeneChip® Human Gene 1.0 ST Array.

3.1.4.2 Differential gene expression analysis

Custom definition file (CDF) from M. Dai (v. 12.1.0, http://brainarray.mbni.med.umich.edu/Brainarray/Database/CustomCDF/genomic_curated_CDF.asp) was used to annotate the 19,973 genes interrogated by GeneChip® Gene 1.0 ST Array. RMA (Robust Multi-array Average, Irizarry *et al.*, 2003) procedure was used to quantify, normalize and summarize probe intensity levels, thus obtaining an expression raw data matrix. Array data quality control was conducted using Affymetrix Expression Console (V 1.2). Differential gene expression analysis was performed comparing each RCC cell line to normal HK-2 cell line and using the Rank Product (RP) statistical algorithm to identify differential expressed genes (DEGs) in each pairwise comparison, setting the p-value threshold at 0.1. RP was chosen since the groups to be compared have a small size (three replicates each). All calculations were performed in R environment using several Bioconductor packages (Gentleman *et al.*, 2004; R Development Core Team, 2009).

3.1.4.3 Bioinformatics and functional enrichment analysis

To investigate the biological role of DEGs found in each pairwise comparison, functional enrichment analysis was carried out using the Database for Annotation, Visualization and Integrated Discovery (DAVID, v 6.7, http://david.abcc.ncifcrf.gov/, Huang *et al.*, 2009), in order to identify functional pathways enriched in DEGs. DAVID was also used to perform enrichment analysis of Gene Ontology (GO) molecular function (MF) and biological processes (BP) terms, with a p-value ≤ 0.001. Furthermore, we intersected the DEGs found in each comparison with the gene lists of a series of interesting pathways retrieved by KEGG database (http://www.genome.jp/kegg/pathway.html), such as Apoptosis (KEGG code: hsa04210, including 86 genes), Cell Cycle (hsa04110, 128 genes), RCC (hsa05211, 70 genes), VEGF (hsa04370, 76 genes), mTOR (hsa04150, 52 genes), and Immune System (including 785 genes and manually composed by combining 13 lists of genes related to immune system, to avoid gene redundancy). Additionally, we intersected the DEGs with a list of angiogenesis-related genes, which we generated by selecting a total of 127 genes from the following BioCarta pathways: Akt, MAPKinase, Wnt, NF-kB Signaling Pathways and VEGF, Hypoxia and Angiogenesis Pathway (http://www.biocarta.com/genes/index.asp). In the same way, we also used a list of 154 genes associated to *VHL* and HIF pathways (by PID, Pathway Interaction Database, http://pid.nci.nih.gov/, **Table 1 Appendix**), which we obtained by combining 2 lists of genes related to *VHL* and HIF pathways, to avoid gene redundancy.

3.2 Results

3.2.1 Assessment of *VHL* and HIF status

By direct Sanger sequencing of the three *VHL* exons in RCC and HK-2 cell lines, we found that A498 harbours a frameshift mutation (p.G144fs*14) on exon 2, which creates a stop codon replacing the lysine at position 159. Caki-2 shows a transversion from A to T (p.R177*) on exon 3, which introduces a premature stop codon, resulting in absence of the last 36 aminoacids of the tumor suppression region of VHL protein. Caki-1 and HK-2 cell lines have a wild-type gene. Additionally, we found the hemizygous (one copy) loss of chromosomal arm 3p in all the three RCC cell lines by Affymetrix 250K SNP Array analysis (*data not shown*).

Western blot analysis showed a high abundance of HIF-1α protein in Caki-1 and Caki-2 compared to HK-2. Conversely, HIF-1α protein was expressed at low level in A498 cell line (**Figure 10**).

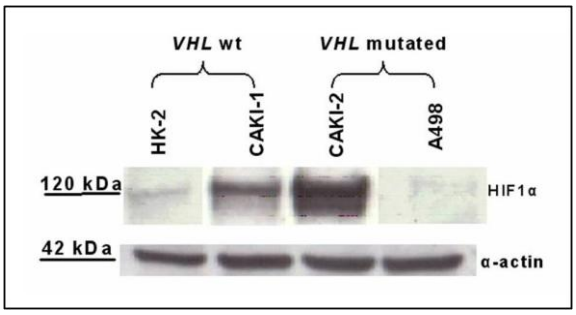

Figure 10. Western blot analysis of HIF-1α protein expression in HK-2, Caki-1, Caki-2 and A498 cell lines.

3.2.2 High-throughput gene expression analysis

We performed a differential gene expression profiling by comparing each RCC cell line to the normal HK-2 cells, using Affymetrix GeneChip® Human Gene 1.0 ST Array platform. Using RP algorithm, we identified the DEG lists for each pairwise comparison.

3.2.2.1 Differential gene profiling of Caki-1 vs HK-2

We found a total of 1,954 DEGs (1,003 up- and 951 down-regulated genes) in Caki-1 as compared to HK-2. DAVID functional enrichment analysis evidenced DEGs related to relevant pathways, such as p53 signaling pathway (15 genes, e.g. *BID*, *TP53*, *ATR*, *ATM*, *MDM2*, *FAS*), metabolic pathways (25 genes, e.g. *ARG2*, *ALDH2*, *GSTM1*) and ECM-receptor interaction pathway (17 genes, e.g. *ITGA1*, *ITGA6*, *THBS2*, *SDC2*).

Enrichment analysis on GO Molecular Function terms highlighted that binding and enzymatic activities involved many up-regulated (e.g. *ATM*, *ATR*, *RAP1B*, *CHUK*, *RAD50*, *RPS6KB1*, *ABCC2*, *KRAS*, *FER*, *HELZ*, *MYSM1*, *SMARCA1*, *APC*, *MET*) and down-regulated genes (e.g. *MT1F*, *MT1M*, *PIGU*, *PIGT*, *GPAA1*) (**Figure 11**). In particular, regarding enriched GO Biological Process terms, there was an overall up-regulation of genes involved in cell cycle process (e.g. *BRCA2*, *CDC27*, *ERCC5*, *STAG1*, *CASP3*, *SOD2*, *XRCC4*, *NUF2*, *CENPF*, *UGP2*, *SKA2*, *NT5E*), while many down-regulated genes were associated to the nucleosome assembly processes within the cell and response to different stimula (e.g. *H2AFX*, *ASF1B*, *GAL*, *TGFB1*, *CCND2*, *SERPINA1*, *ARSA*, *TP53*, *CD74*, *EGR2* and several members of the histone family) (**Figure 1 Appendix**).

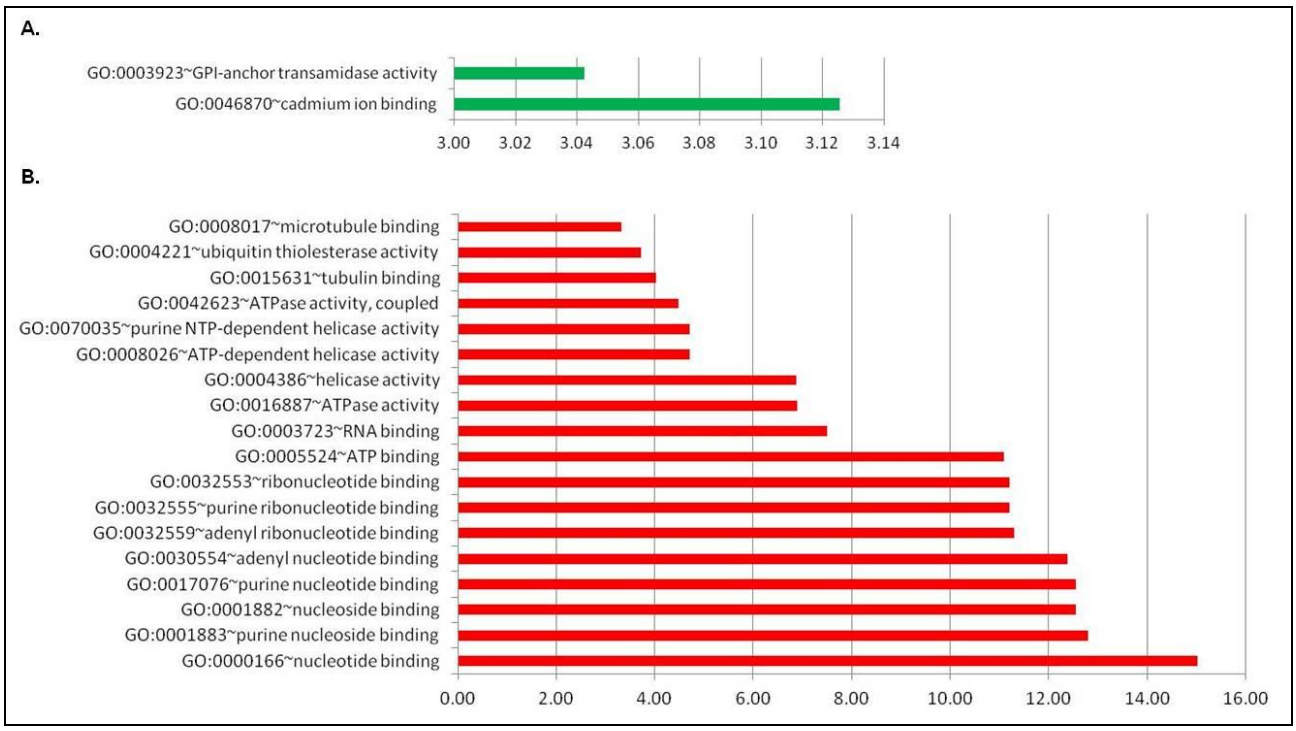

Figure 11. Caki-1 vs HK-2: DAVID enrichment analysis on GO Molecular Function terms for the 951 down-regulated genes (panel A) and the 1003 up-regulated genes (panel B). On the X-axis, the log(p-value) of DAVID enrichment test is reported.

3.2.2.2 Differential gene profiling of Caki-2 vs HK-2

We found 1,958 DEGs (1,007 up- and 951 down-regulated genes) in Caki-2 as compared to HK-2. By DAVID functional enrichment analysis, we observed the involvement of several DEGs in relevant pathways, such as p53 signaling pathway (16 genes, e.g. *CCND2*, *PERP*, *GADD45A*, *ATM*, *MDM2*, *FAS*), leucocyte transendothelial migration (22 genes, e.g. *ICAM-1*, *VCAM1*, *ROCK1*, *JAM3*, *ITGB1*) and glutathione metabolism (11 genes, e.g. *GSTM1*, *GSTM3*, *IDH2*, *GSTP1*). DAVID enrichment analysis on GO Molecular Function terms showed that many DEGs, both up-regulated (e.g. *IFIH1*, *HELB*, *ACSL3*, *UBE2Q2*, *RPS6KB1*, *RAB1A*, *ATR*, *ROCK2*, *LARS*, *UGDH*, *SUCLA2*, *MTIF2*, *RND3*, *MFN1*) and down-regulated (e.g. *MMP9*, *DCN*, *SPARC*, *THBS1*, *CYR61*, and several members of the metallothionein family), were involved in binding and enzymatic activities (**Figure 12**). By characterizing DEGs also in terms of GO Biological Processes, we noted that many up-regulated genes were related to centrosome organization and response to DNA damage (e.g. *BRCA1*, *GADD45A*, *CETN3*, *TUBE1*, *HAUS6*, *UGP2*, *XRCC4*, *APC*, *RIF1*, *SSB*, *CWC22*), while down-regulated genes were involved in growth regulation and cell assembly processes (e.g. *ENPP1*, *GREM1*, *TGFB2*, *CDKN2A*, *IDH3G*, *LUM*, *ERCC2*, and several members of the histone family) (**Figure 2 Appendix**).

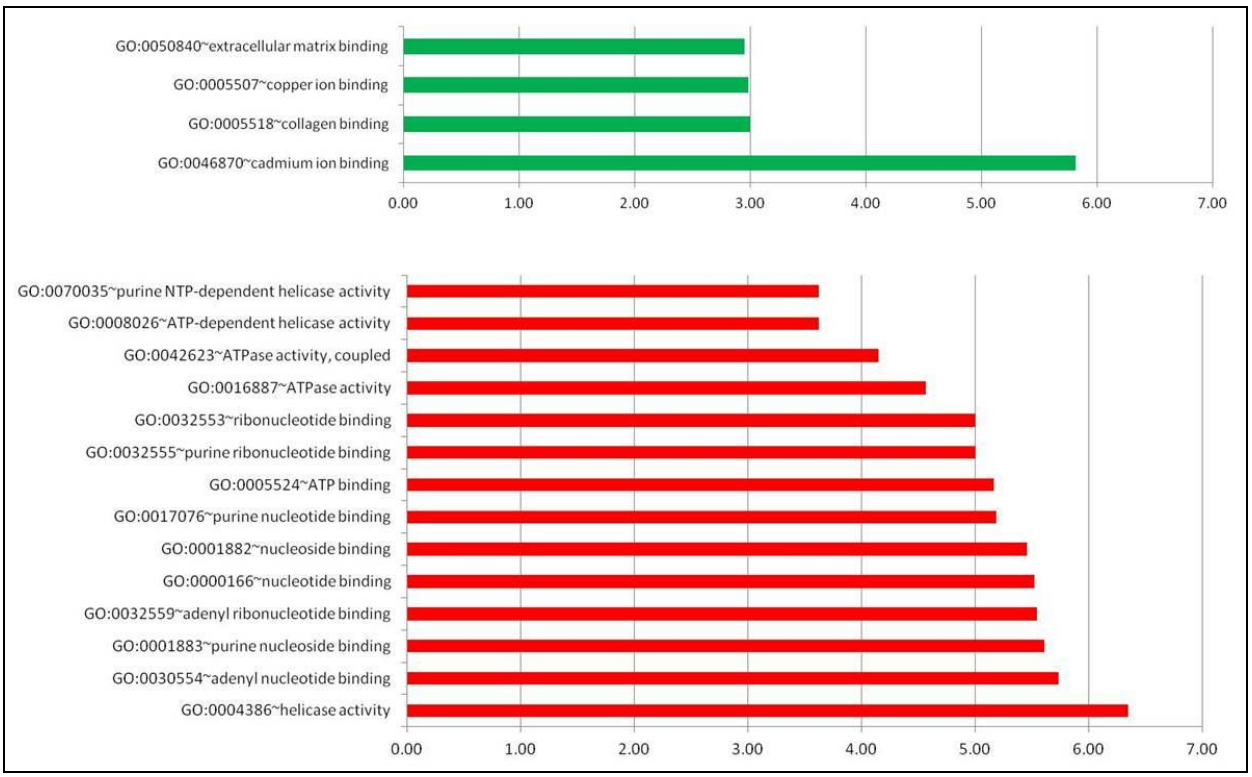

Figure 12. Caki-2 vs HK-2: DAVID enrichment analysis on GO Molecular Function terms for the 951 down-regulated genes (panel A) and the 1007 up-regulated genes (panel B). On the X-axis, the log(p-value) of DAVID enrichment test is reported.

3.2.2.3 Differential gene profiling of A498 vs HK-2

By comparing A498 cell line to HK-2, we obtained a total of 1,968 DEGs (997 up- and 971 down-regulated genes). DAVID functional enrichment analysis showed some enriched pathways, such as p53 signaling pathway (15 genes, e.g. *BID*, *ATR*, *CASP9*, *IGFB3*, *MDM2*, *APAF1*, *FAS*), ubiquitin mediated proteolysis (23 genes, e.g. *UBE2A*, *HERC4*, *CDC27*, *RBX1*, *CUL2*, *MDM2*), oxidative phosphorylation (22 genes, e.g. *NDUFA5*, *NDUFA2*, *NDUFB9*, *ATP6AP1*, *UQCRQ*, *COX5B*), leukocyte transendothelial migration (20 genes, e.g. *CLDN16*, *ICAM-1*, *GNAI1*, *PTPN11*, *PIK3R3*, *VCAM1*, *ITGB1*, *RAP1B*, *JAM2*). By enrichment analysis on GO Molecular Function terms, we observed that many up-regulated genes were associated to binding and enzymatic activities (e.g. *KRAS*, *EPHA7*, *AGPS*, *NPR2*, *MAPK6*, *FER*, *APAF1*, *CHUK*, *SMC2*, *SMC3*, *RPS6KB1*, *ATM*, *TRPM7*, *ZAK*, *GNAQ*, *IREB2*, *USP7*, *MYSM1*), while many down-regulated genes were involved in transport activities (e.g. *ATP1A3*, *SLC9A1*, *XRCC1*, *JUNB*, *TFDP2*, *E2F1*, *PPARD*, *SNAI1*, *GSTM1*, *FNTB*, *GSTT1*) (**Figure 13**). By characterizing DEGs also in terms of GO Biological Processes, we found that many up-regulated genes were involved in cell cycle and response to stress and DNA damage (e.g. *PHAX*, *FGF2*, *CAV2*, *MITD1*, *UPF2*, *CSTF3*, *CDC27*, *SKA2*, *DOCK2*, *RANBP2*, *MDM2*, *XRCC4*, *RRM2B*, *ERCC4*, *BRCA1*, *BRCA2*, *ATR*, *ATM*) and down-regulated genes were implicated in cell assembly processes, such as protein-DNA complex, chromatin and nucleosome assembly (e.g. *GTF2A2*, *ASF1B*, *CENPV*, *SUV39H1*, *HDAC8*, and several members of the histone family) (**Figure 3 Appendix**).

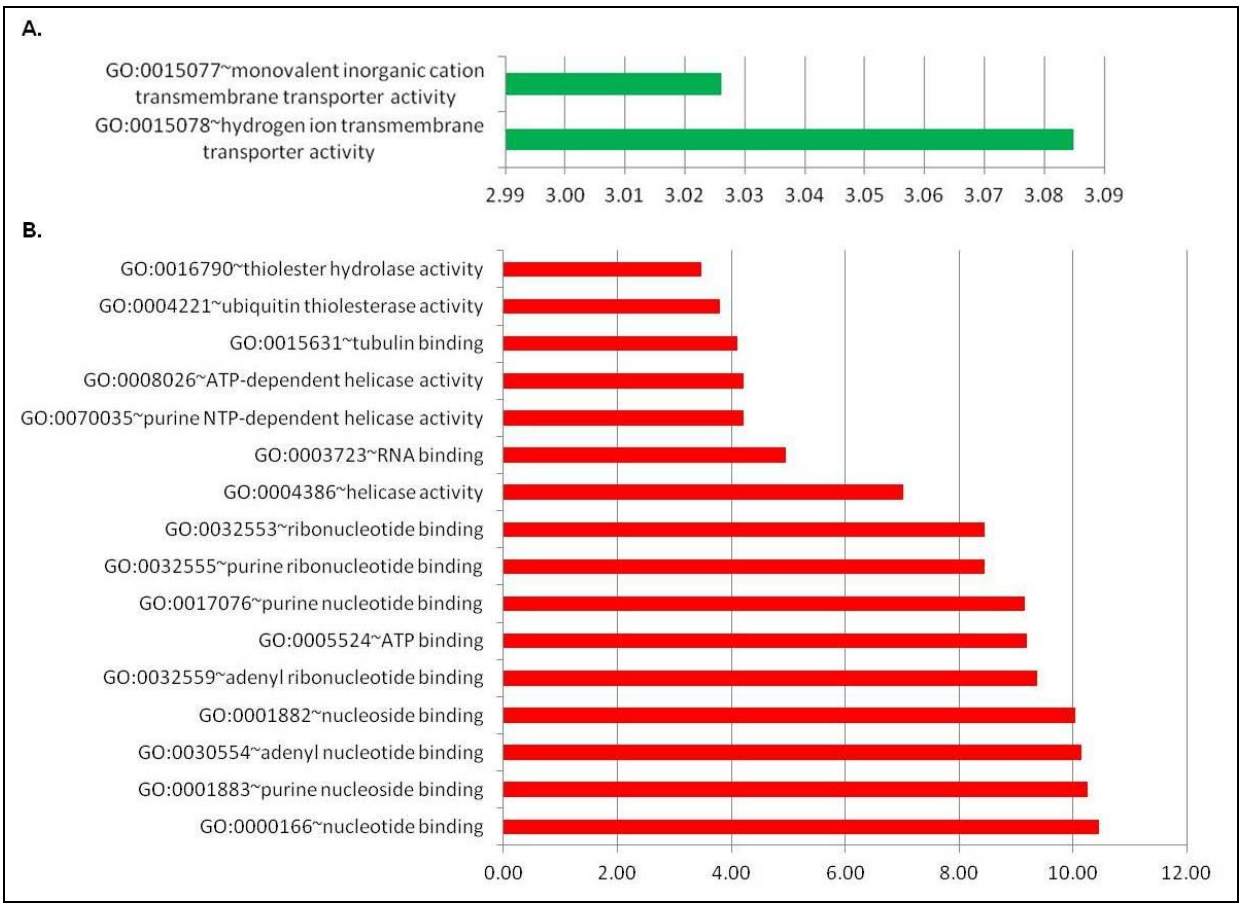

Figure 13. A498 vs HK-2: DAVID enrichment analysis on GO Molecular Function terms for the 971 down-regulated genes (panel A) and the 997 up-regulated genes (panel B). On the X-axis, the log(p-value) of DAVID enrichment test is reported.

Using different pathway databases, such as BioCarta, KEGG and PID, we observed that many DEGs found in these differential analyses were related to pathways tipically correlated to cancer and RCC pathology, and some were in common among the three comparisons, as reported in **Table 3**.

	Caki-1	Caki-2	A498
Angiogenesis	TGFB2, MAPK13, TGFB1, MKNK2, MAP3K9, CHUK, MAP2K6, MAPK6, PIK3CA, **RPS6KB1**	MAPK13, TGFB2, **RPS6KB1**, MAPK6, PIK3CA, MAP2K6	CASP9, CHUK, **RPS6KB1**, MAPK6
Apoptosis	PIK3R3, TNFSF10, BID, TP53, AKT2, CASP3, PRKAR1A, CHUK, FAS, PIK3CA, BIRC2, IL1A, **ATM**	TNFSF10, IRAK3, PIK3R3, BID, IL1R1, MYD88, BIRC2, PRKAR2B, TNFRSF10A, FAS, PIK3CA, **ATM**, BIRC3	IRAK3, TNFSF10, AKT2, BID, PIK3R3, CASP9, CASP3, CHUK, APAF1, FAS, **ATM**, BIRC3
Cell Cycle	CCND2, CDKN2A, TGFB2, SMC1B, TGFB1, RBX1, SFN, TP53, MAD2L2, CCND3, **CDC27**, MDM2, STAG2, SMC3, STAG1, ATR, **ATM**	CCND2, CDKN2A, TGFB2, GADD45B, **CDC27**, ATR, STAG2, SMC3, STAG1, GADD45A, MDM2, **ATM**	CDKN2A, SFN, CDKN2C, SMC1B, MAD2L2, RBX1, E2F1, CDC20, CDC25B, TFDP2, ORC4L, ATR, **CDC27**, SMC3, GADD45A, MDM2, **ATM**
RCC	TGFB2, PIK3R3, TGFB1, RBX1, AKT2, PDGFB, MET, KRAS, PTPN11, PIK3CA, RAP1B, CUL2	PAK3, EPAS1, PIK3R3, TGFB2, CUL2, PIK3CA, RAP1B	AKT2, RBX1, EGLN3, PIK3R3, CUL2, KRAS, PTPN11, RAP1B
VEGF	MAPK13, PIK3R3, HSPB1, AKT2, RAC2, KRAS, PIK3CA, PLA2G4A	RAC2, PIK3R3, MAPK13, HSPB1, SH2D2A, PIK3CA	AKT2, RAC2, PIK3R3, CASP9, PLA2G4A, KRAS
***VHL*-HIF**	CITED2, PDGFB, NPM1, ABCG2, MDM2, **GRB10**, SOD2, ROCK1, YES1, CP, TFRC, **ATM**, **FER**	HMOX1, CD2AP, ROCK1, GADD45A, **GRB10**, **FER**, MDM2, ABCG2, TFRC, **ATM**, CP	IGFBP3, YES1, GADD45A, ROCK1, **GRB10**, MDM2, **FER**, **ATM**
mTOR	PIK3R3, AKT2, PRKAA1, PIK3CA, **RPS6KB1**	PIK3R3, **RPS6KB1**, PIK3CA	AKT2, PIK3R3, PRKAA1, **RPS6KB1**
Immune System	IFITM1, SERPINA1, CLDN4, IFI30, JAM2, HLA-DMB, ICAM-1, LGMN, MAPK13, HSPA2, PRKCZ, F3, JAM3, PIK3R3, MYL9, CCL28, CD74, GNG5, TNFSF10, CBLB, TAPBP, BID, PROS1, ARRB2, GSK3A, PIN1, HLA-DMA, CXCL16, LAT, PRKCD, WASF2, GNG7, AKT2, PSME1, ULBP2, GNG11, RAC2, JAK3, CASP3, LYN, GNAI3, JAK2, CHUK, FGB, MAP2K6, GNAI1, ITGA6, SERPINE1, TLR1, FAS, IFNE, KRAS, CARD11, CXCL2, PTPN11, ROCK1, DNM1L, ITGB1, TLR3, PIK3CA, BIRC2, RAP1B, CTSS, TLR4, DOCK2, HSPA4, MYO10, ITGA1, ROCK2, PLA2G4A, TBK1, NFYB, TFRC, IL7R, TFPI, SUGT1, DDX3X, **RPS6KB1**, HLA-DPA1, ITGA4, IL1A, CASP1, TLR6, CD9, C1S, CXCL5, CXCL1, ANPEP, SCIN, BIRC3, VCAM1, CXCL6	C3, CLDN11, PAK3, F3, CXCL16, PIN1, CBLB, ARRB2, VCAM1, SHC3, GNG7, CXCL2, TNFSF10, IFITM1, SERPINA1, ICAM-1, CLDN2, MYL9, PLAU, GNG4, JAM2, IL8, RAC2, PIK3R3, JAM3, CD74, MAPK13, SERPINE1, BID, IL1R1, CFB, LGMN, HLA-DMB, ACTN1, GNG5, SIPA1, HLA-DMA, F11R, GNG10, CFH, PIP5K1C, GNG11, MMP9, PROS1, PRKCZ, MYD88, GNB2, DNM1L, IFNGR1, SUGT1, BIRC2, ROCK1, HSPA4, ITGB1, TIAM2, LY96, RAPGEF3, TNFRSF10A, ITGA1, KITLG, **RPS6KB1**, PLCB1, NFYB, FAS, IFIH1, PIK3CA, ROCK2, DDX3X, MYO10, GNAI1, MAP2K6, ITGA2, TFRC, TLR6, CCL5, ITGA6, TBK1, RAP1B, SYK, PREX1, PLA2G4A, TLR4, SCIN, BIRC3, CD9, CLDN16, DDX3Y	HSPA1A, IFITM1, ICAM-1, CLDN4, CLDN2, GNG4, IFI30, TNFSF10, SERPINA1, ARRB1, MYL9, HLA-A, F2R, HSPA2, GSK3A, HSPA1B, JAM2, PIN1, GNG5, F3, LGMN, AKT2, BID, WASF2, CX3CL1, CLDN11, RAC2, JAK3, PIK3R3, CFH, MICB, CASP3, NLRP3, ITGB1, SUGT1, PIKFYVE, IFIH1, HLA-DPB1, HSPA4, CHUK, PLCB4, CXCL1, CASP1, ITGA2, **RPS6KB1**, FAS, TFPI, PLA2G4A, RAPGEF3, DDX3X, DNM1L, KRAS, ROCK1, PTPN11, PIK3AP1, TLR3, CARD11, GNAI1, OCLN, TLR4, PLCB1, TBK1, ITGA6, DOCK2, ROCK2, ITGA1, VCAM1, NFYB, BIRC3, RAP1B, HLA-DPA1, ITGA4, THY1, CD9, SCIN, CLDN16

Table 3. DEGs related to typical cancer pathways found for each comparison (with respect to HK-2). Down-regulated genes are in green, up-regulated genes are in red, genes found in common in at least two analyses are underlined. Genes validated in qPCR are in bold.

By intersecting the three lists of DEGs obtained comparing each RCC cell line to HK-2, we found a total of 790 common DEGs. Among them, 779 were also concordant in their differential expression direction, including 413 up- and 366 down-regulated genes. In particular, as illustrated in the Venn diagram (**Figure 14**), Caki-1 has a total of 1,095 DEGs in common with Caki-2, whose 1,082 are concordant (551 up- and 531 down-regulated genes), and 1,148 DEGs in common with A498 (1,136 are concordant, 592 up- and 544 down-regulated genes); while Caki-2 and A498 have a total of 1,041 DEGs in common, whose 1,020 are concordant (532 up- and 488 down-regulated genes). More specifically, we found 501 genes that are modulated only in Caki-1, whose 265 are up- and 236 are down-regulated genes; while 305 genes are shared with Caki-2, whose 136 are up-, 161 are down-regulated and 8 modulated in different way in these two cell lines. Instead, Caki-1 and A498 shared 358 genes, whose 178 are up-, 177 are down-regulated and 3 modulated in different way. Finally, Caki-2 and A498 have 251 genes in common, whose 118 are up-, 120 down-regulated and 13 modulated in different way in these two cell lines. There were 612 genes modulated only in Caki-2 (322 up- and 290 down-regulated genes) and 569 genes modulated only in A498 (278 up- and 291 down-regulated genes). In particular, we carried out an extensive data mining focusing the investigation to those modulated genes associated to ccRCC pathology and to cancer.

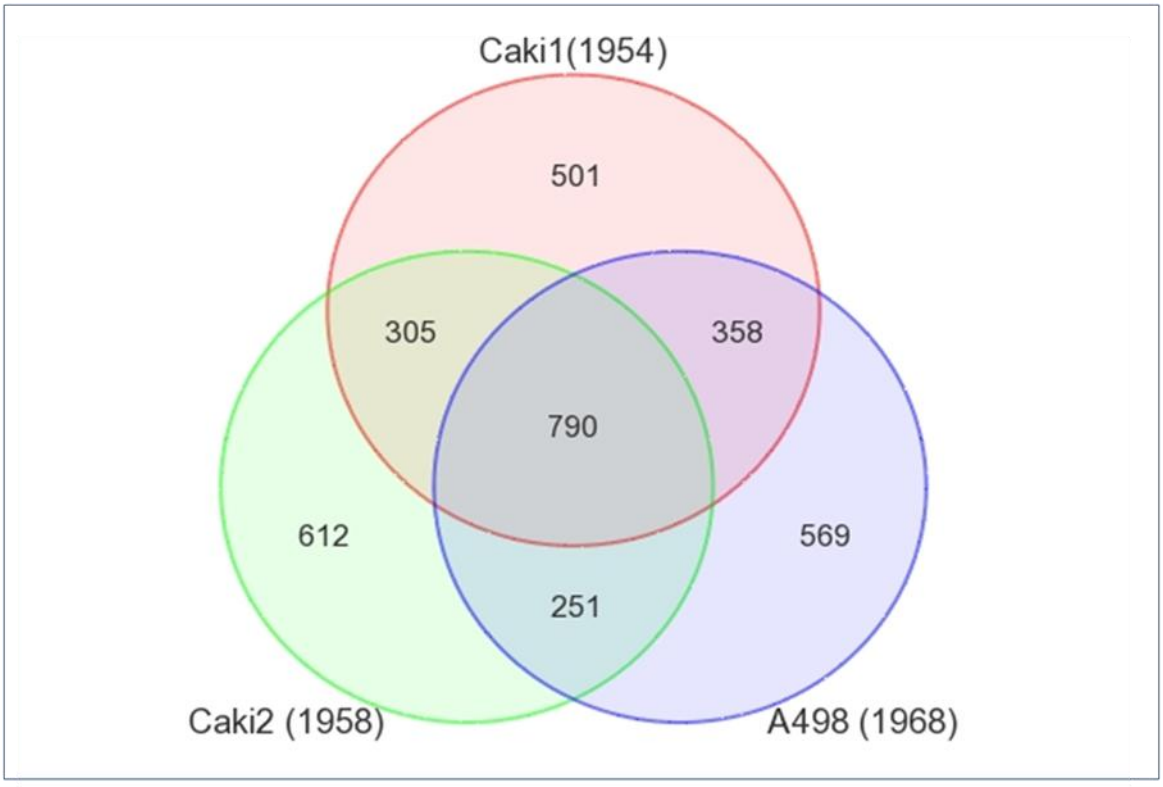

Figure 14. Venn diagram representing the intersection among the DEG lists obtained from the three comparisons.

3.3 Discussion

In this section, we performed a genome-wide differential gene expression analysis using Affymetrix microarray technology, which is able to simultaneously investigate about 19,973 well-known genes. To do this, we used three RCC cell lines as *in vitro* model of RCC pathology, i.e. Caki-1, Caki-2 and A498, and we compared the gene profiles of these cell lines to that of a normal one, HK-2 (human kidney 2), which was chosen since being a proximal tubular cell line derived from a normal adult kidney (Ryan *et al.*, 1994).

First of all, we characterized the *VHL* mutational status in all these cell lines by direct sequencing. We found that both Caki-2 and A498 cell lines had a *VHL*$^{-/-}$ status, while Caki-1 had a wild-type gene. Mutations found in Caki-2 and A498 affected the tumor suppression region of the VHL protein, and particularly in Caki-2 also the region necessary to bind Elongin C (Richards, 2001). In this way, we confirmed literature data about *VHL* mutations in A498 and Caki-2 cell lines (Whaley *et al.*, 1994); although most literature about Caki-2 reports a wild-type *VHL* status. We also assessed the HIF expression by western blot and we found a high level of HIF-1α protein in Caki-1 and Caki-2, and a low level in A498. Our results demonstrated the agreement between a mutated *VHL* status and the high HIF-1α protein expression level in Caki-2 cell line. Whereas, in A498 and Caki-1, which resulted *VHL*-/- and wild type cell lines, respectively, we found a high and a low expression level, respectively, of HIF-1α protein, which could be the result of an oxygen/pVHL-independent regulation (Baldewijns *et al.*, 2010). In fact, recent evidences suggested that HIF-1α degradation may also be regulated in an oxygen/prolyl hydroxylases/pVHL/independent manner by HSP90 (heat shock protein 90). The role of this protein is to protect proteins from misfolding and degradation through its ATPase activity. HSP90 binds and stabilizes HIF-1α by excluding *RACK1* (receptor for activated C-kinase 1), which can promote proteasome-dependent degradation of HIF-1α. Another possible way to degradate HIF-1α in an oxygen-independent manner can be through the hypoxia-associated factor (HAF), which is an E3 ubiquitin ligase for HIF-1α. In addition to being activated during hypoxia or in the absence of *VHL*, HIF-1α can be activated by interaction with reactive oxygen species (ROS), probably inhibiting prolyl hydroxylases (PHDs) hydroxylation. Possible mechanisms include direct inhibition of the PHDs or effects of ROS on the levels of ascorbate, iron, or Krebs cycle intermediates (Baldewijns *et al.*, 2010).
As reported in Catalogue Of Somatic Mutations In Cancer (COSMIC, http://www.sanger.ac.uk/genetics/CGP/CellLines/), which collects somatic mutation information and related details and contains information concerning human cancers, Caki-1 and A498 cell lines also carried mutations in *CDKN2A* (cyclin-dependent kinase inhibitor 2A) gene, and A498 also resulted mutated in *SETD2* (SET domain containing 2) gene, while Caki-2 cell line is not included in this database.

In our laboratory, we performed the genome-wide analysis of DNA copy number alterations (CNAs) of these RCC cell lines, using the Affymetrix GeneChip® Human Mapping 250K SNP Array platform (*data not shown*). We detected CNAs on all chromosomes, except the chr 2 and 12. Among them, five chromosomes showed regions of both DNA gain and loss (chr 1, 3, 11, 17 and 18), while the remaining chromosomes had regions of either CN gain (chr 4, 5, 7, 8, 10 and 16) or CN loss (chr 6, 9, 13, 14, 15, 19, 20, 21 and 22). The Caki-2 showed CNAs on all autosomes, covering either whole chromosomes (chr 17 and 20) or one chromosomal arm (chr 2p+, 3p-, 6p+, 7p+, 9p-, 10p+, 11q-, 13q-, 16p+, 18q-, 19q+, 21q+ and 22q+). Six chromosomes showed long regions of CNN-LOH (copy number neutral-loss of heterozygosity) (chr 4, 8, 9, 11 and 14),

while on chr 8 we found a LOH associated with a CN gain status, where the major allele was duplicated twice and the minor allele was lost. Finally, in the A498 cell line only two chromosomes (chr 4 and 10) showed no alterations in DNA copy number status, while the whole chr 12 showed only CNN-LOH. The other chromosomes had either deletions (chr 1p, 3p, 6 p, 6q, 8p, 11q, 14q, 18p, 18q and 20p) or amplifications (chr 1q, 2p, 2q, 5p, 7 p, 7q, 8q, 9p, 9q, 11p, 16p, 16q, 17p, 17q, 19q, 20p, 20q and 21q). Many of these alterations were in agreement with previously published SKY karyotype (Roschke *et al.*, 2003). Our results demonstrated that these cell lines had a very complex karyotype. Many studies focused on amplified and over-expressed genes and calculated that a fraction ranging from 44% to 62% of amplified genes showed concomitant up-regulated expression levels (Bicciato *et al.*, 2009; Hyman *et al.*, 2002). This suggests the presence of an aneuploidy-induced deregulation of the cancer transcriptome that occurs in addition to the transcriptional and post-transcriptional deregulation of oncogenes and tumor suppressor genes.

Gene expression profiling was performed by comparing the three RCC cell lines to HK-2. The list of the top 50 down- and up-regulated genes are reported in supplementary tables (**Tables 2-3-4 Appendix**).

DEG functional annotation analysis revealed a general activation of genes mostly belonging to p53 signaling pathway and extracellular matrix-interaction classes, and inactivation of genes principally involved in metabolic pathways. In particular, among down-regulated genes, we found genes involved in lipid pathways, carboxylic acid biosynthetic processes, macromolecular complex assembly and nucleosome assembly. As recently reported, the down-regulation of these pathways is symptom of the loss of a normal renal function (Tun *et al.*, 2010). Some up-regulated genes found in Caki-1 are involved in cell cycle and DNA repair processes. In particular, there are many genes known to be involved in p53 signaling and apoptosis pathways, such as *ATM*, *MDM2*, *FAS*, *ATR*, *SERPINE1*, *CASP3*, *BIRC2*.

An intriguing down-regulated gene, found in all three cell lines as compared to HK-2, is Gremlin1 (*GREM1*). According to literature (van Vlodrop *et al.*, 2010), it was already found down-regulated in several tumor cell lines (such as neuroblastoma, fibrosarcoma, colon adenocarcinoma, breast carcinoma), suggesting a tumor suppressor function. *GREM1*, a bone morphogenetic protein antagonist and putative angiogenesis-modulating gene, it's a secreted glycoprotein that binds and antagonizes bone morphogenetic proteins (BMPs) 2, 4, and 7, thereby preventing the ability of these ligands to interact with their receptors and resulting in inhibition of downstream TGF-signaling. BMPs have multiple functions in many cell and tissue types including angiogenesis, proliferation, apoptosis, differentiation, chemotaxis and extracellular matrix production during development as well as in adult life. Epigenetic silencing of *GREM1* by promoter CpG island methylation occurs in ccRCC cell lines, thus, during tumor progression, cumulative genetic/epigenetic events can activate additional angiogenic growth factors, resulting in an increased tumor driven angiogenesis. However, the role of *GREM1* in renal cancer pathogenesis and the mechanisms by which *GREM1* gene expression is regulated remain mostly unknown.

Another interesting gene is Arginase 2 (*ARG2*), which is down-regulated in our RCC cell lines compared to HK-2. Arginase, which catalyzes the conversion of arginine to urea and ornithine, exists in two distinct isoforms. Arginase I is expressed almost exclusively in the liver where it serves as an essential enzyme of the urea cycle. In contrast, arginase II is expressed in the kidney and many other extrahepatic tissues (Gotoh *et al.*, 1996; Miyanaka *et al.*, 1998). Although its functions have not been well documented, *ARG2* has been recognized to participate in the regulation of nitric oxide synthase (NOS) (Jansen *et al.*, 1992). In the kidney,

ARG2 is distributed in the proximal tubules (Miyanaka *et al.*, 1998), and metabolizes most of the arginine here present (Jansen *et al.*, 1992). Interestingly, current consensus is that *ARG2* plays also a role in blocking apoptosis as well (Esch *et al.*, 1998; Estévez *et al.*, 2006; Gotoh and Mori, 1999).

Moreover, we found that many dysregulated genes are involved in the protein ubiquitination pathway, which is very important for the hypoxia process. Among them, we highlighted the up-regulation of *CUL2* in RCC cell lines here analyzed, necessary to pVHL for HIF-1α proteasomal degradation (Cohen and McGovern, 2005), and many ubiquitin specific peptidases and heat shock proteins. Additionally, other genes are involved in NRF2-mediated oxidative stress response, such as members of aldo-keto reductase family, some glutathione S-transferases, phosphoinositide-3-kinases and superoxide dismutases. Oxidative stress is involved in many diseases and caused by an imbalance between the production of reactive oxygen species (ROS) and the detoxification of reactive intermediates. Oxidative stress has been hypothesized to play a role also in aging and age-related disorders, including essential hypertension. ROS intermediates such as peroxides and free radicals, can be very damaging for many cell components such as proteins, lipids and DNA. Severe oxidative stress can trigger apoptosis and necrosis. ROS can interfere with protein regulation, including the activity of renal transporters. The cellular defense response to oxidative stress includes induction of detoxifying enzymes and antioxidant enzymes. Nuclear factor-erythroid 2-related factor 2 (Nrf2) binds to the antioxidant response elements (ARE) within the promoter of these enzymes and activates their transcription. Inactive Nrf2 is retained in the cytoplasm by association with an actin-binding protein Keap1. Upon exposure of cells to oxidative stress, Nrf2 is phosphorylated in response to the protein kinase C, phosphatidylinositol 3-kinase and MAP kinase pathways. After phosphorylation, Nrf2 translocates to the nucleus, binds AREs and transactivates detoxifying enzymes and antioxidant enzymes, such as glutathione S-transferase, cytochrome P450, NAD(P)H quinone oxidoreductase, heme oxygenase and superoxide dismutase. The mitochondrial superoxide dismutase 2 (*SOD2*), that was found up-regulated in Caki-1 by our analysis, is a member of the iron/manganese superoxide dismutase family and binds to the superoxide byproducts of oxidative phosphorylation converting them to hydrogen peroxide (H_2O_2) and diatomic oxygen. H_2O_2 previously produced is converted to water and molecular oxygen by a catalase, which uses reduced glutathione as the hydrogen donor. Increased levels of ROS in cells and tissues may act as a signal to enhance the activity and expression of antioxidant enzymes. According to this hypothesis, an increase in antioxidant enzymes activity and/or expression with age would be expected, this being an adaptation to help cells and tissues to protect from oxidative stress (Silva and da Silva, 2007; Simao *et al.*, 2011).

Another interesting gene is *VCAM-1*, a member of the immunoglobulin (Ig) superfamily and a cell-surface glycoprotein expressed by cytokine-activated endothelium that interacts with the integrin, playing its role in cell-cell adhesion and in metastasis. This gene was identified as the single most predictive gene for survival in RCC patients in the study of Vasselli *et al.* This type I membrane protein mediates leukocyte-endothelial cell adhesion and signal transduction (Vasselli *et al.*, 2003). It is well known, that *VCAM1* is over-expressed in RCC and is involved in tumor immune escape and resistance induction (Lin *et al.*, 2007). In our case, *VCAM1* was found differently modulated among the three comparisons (up-regulated in Caki-1 and A498 and down-regulated in Caki-2). Moreover, we found another cell adhesion molecule *ICAM-1* (intercellular adhesion molecule-1), that normally is up-regulated in RCC (Tanabe *et al.*, 1997a). *ICAM-1* mediates two important functional aspects of tumor biology, namely enhancement of tumor metastasis and mediation of

host defense mechanisms such as lymphocyte-mediated tumor cytotoxicity (Juengel *et al.*, 2011). This gene encodes a cell surface glycoprotein which is typically expressed on endothelial cells and immune system cells and binds to integrins. *ICAM-1*, member of Ig superfamily, is mainly implicated in normal tissue epithelial architecture and/or immune responses. Generally, alternative expression of cell adhesion molecules is associated with pathogenesis and progression of benign and malignant neoplasms of various tissues (Albelda, 1993). Among the up-regulated genes, there were also integrins, such as *ITGA1*, *ITGA2*, *ITGA6* and *ITGAX*. Integrins are pivotal regulators of adhesion, migration, differentiation, proliferation and cell survival Tumor cells are known to modify their integrin expression to become highly motile and invasive. How and which integrin subtypes are involved in cancer progression has not been fully clarified.

The matrix metalloproteinases (MMPs) are the main proteases that are involved in remodelling of extracellular matrix (ECM). Many members of the MMP family were found to be down-regulated in all the three RCC cell lines, e.g. *MMP1*, *MMP9*, *MMP14*, *MMP16* and *MMP24*. A role played by pVHL is also to reduce MMP secretion (Baldewijns *et al.*, 2010).

An interesting gene is *ROCK1*, a member of Rho-kinases, that was found up-regulated together with *ROCK2* in all the three comparisons. Rho (Rho small GTP-binding protein) regulates formation of stress fibers, focal adhesions and cell migration through reorganization of the actin cytoskeleton (Abe *et al.*, 2008). *ROCK* is one of the major downstream effectors of Rho and induces stress-fiber formation and assembly. *ROCK* and Rho are involved in regulation of a variety of cellular processes such as cytoskeletal organization, cell cycle progression, malignant transformation and metastasis (Imamura *et al.*, 2000). *ROCK* has been reported to be involved in human tumor progression, while a *ROCK* inhibitor suppressed tumor growth and metastasis. According to the study by Abe *et al.*, *ROCK1* was found up-regulated in ccRCC, and its high expression level was shown to be associated with a shorter survival (Abe *et al.*, 2008).

Concordantly with the observation of an high HIF-1α protein expression level in Caki-2 cell line, two HIF targets were found up-regulated, i.e. the platelet-derived growth factor D (*PDGFD*) and the epidermal growth factor (*EGF*), involved in angiogenesis and cell proliferation and/or survival, respectively (Baldewijns *et al.*, 2010).

By Gene Ontology analysis we found many down-regulated genes involved in cadmium and copper ions binding, collagen binding and extracellular matrix binding. Also in this case this indicated a loss of the normal renal functions related to ion transport and binding, and maintenance of cell and tissue structure and function (Tun *et al.*, 2010). Among the up-regulated genes, many are involved in amino acids binding, ATP binding and enzymatic activities associated to ATP roles (energy metabolism), microtubules organization. These are some of the main processes implicated in RCC, even if some of these metabolic pathways were found down-regulated by Tun *et al.* (Tun *et al.*, 2010).

An important HIF target is the lysyl oxidase (*LOX*) gene, that was found up-regulated in A498, since this cell line is a *VHL-/-* cell line, even if HIF-1α is expressed at low concentration by our analysis of western blot, sign that other processes might be implicated in HIF degradation (Baldewijns *et al.*, 2010). *LOX* is involved in cell adhesion and motility processes. Lysyl oxidase has been reported to influence tumour cell motility and invasiveness by reshaping the collagen matrix (Kirschmann *et al.*, 2002; Stassar *et al.*, 2001). In the ECM, *LOX* initiates the covalent cross-linking of collagens and elastin, thereby increasing insoluble matrix deposition and tensile strength The increase of the ECM-protein *LOX* expression level has been correlated

with metastatic disease (e.g. in breast cancer) and is essential for hypoxia-induced metastasis (Erler and Giaccia, 2006). *LOX* elevation occurs in metastatic and/or invasive breast cancer cell lines and correlates with increased staging in RCC. Previous reports showed that genetic inhibition of *LOX* increased cell proliferation in renal cells (NRK-49F cells) (Giampuzzi *et al.*, 2005), again supporting the idea that *LOX* acts as a tumor suppressor. In fact, in the study by Erler and Giaccia, it was hypothesized that *LOX* might be a good therapeutic target for the prevention of metastasis in breast cancer and potentially other solid tumors, including RCC (Erler and Giaccia, 2006).

In A498, many down-regulated genes are involved in ion transport within the cell and in nucleosome organization, while up-regulated genes are involved in response to stress, DNA repair mechanisms, cell cycle process, and energy metabolism; therefore, similar processes already seen in the other two comparisons and that include the main renal functions.

Interestingly, among the 779 DEGs that we found concordantly modulated in the three comparisons, we observed that many genes are associated to cancer-related pathways and RCC pathology, such as apoptosis, angiogenesis, cell cycle, RCC, mTOR, VEGF, *VHL*-HIF and the immune system. In particular, many common up-regulated genes are implicated in the immune system, in agreement with Tun *et al.* (Tun *et al.*, 2010). The activation of the immune system is striking in ccRCC and may be linked to the responsiveness of ccRCC to immunotherapies, which makes ccRCC one of the few cancers that respond to immunomodulatory therapies.

Most our results are consistent with already published, thus confirming that RCC cell lines are an optimal *in vitro* model to carry out functional investigations on RCC-related pathways. Naturally, it should be noted that RCC cell lines have gene expression profiles significantly different from those in tumor tissues, however, the most important patterns are preserved. We found a much higher percentage of DEGs in RCC cell lines than in RCC tissue samples, as previously reported by others (Liou *et al.*, 2004). Three factors might contribute to these differences: (1) the RCC cell lines were derived from metastatic RCC, therefore, more gene mutations have been possibly accumulated and thus more genes were differentially expressed; (2) the RCC cell lines are a pure population of cancer cells in contrast to the RCC tissue samples that contain many other different cell types apart from cancer cells, thus the expression intensity of differentially expressed genes was magnified in the RCC cell lines; (3) the RCC cell line *in vitro* culturing may have introduced changes in the gene expression profile as compared with *in vivo* tissue cancer cells. On the other hand, many important genes were consistently expressed in both types of tumor samples, thus suggesting that the main gene expression patterns of RCC tissues can be investigated also through the gene profiling of RCC cell lines. As a matter of fact, immortalized tumor cell lines have been widely used in several cellular and molecular studies, including comprehensive screening of 60 National Cancer Institute (NCI) cell lines (NCI-60) for gene expression (Wang *et al.*, 2006b), proteomic (Nishizuka *et al.*, 2003) and miRNA profiles (Blower *et al.*, 2007).

4 PART II: HIGH-THROUGHPUT MIRNA EXPRESSION PROFILING

4.1 Material and Methods

4.1.1 High-throughput miRNA expression analysis

4.1.1.1 Target sample preparation for microarray miRNA expression analysis

To assess the genome-wide miRNA expression level in RCC cell lines, we performed a differential miRNA expression analysis comparing the three RCC cell lines to HK-2. Total RNA of cell lines, extracted as described above, was prepared using FlashTag™ Biotin RNA labeling kit (Genisphere Inc., Hatfield, PA); for each sample, three technical replicates were carried out. Then, we used Affymetrix GeneChip® miRNA Array (Affymetrix Santa Clara, CA, USA). Each single array includes 7,815 probe sets, representing over 6,703 miRNA sequences for a total of 71 organisms (847 are human miRNA sequences), from Sanger miRNA database (V.11) (http://www.mirbase.org/) and an additional 922 sequences of human snoRNAs and scaRNAs from Ensembl database (http://www.ensembl.org/index.html) and snoRNABase (http://www-snorna.biotoul.fr/). Each array contains 4 identical probes for each miRNA sequence, and 11 probes for each snoRNA and scaRNA. Moreover, all probe sets are perfect match only. The oligonucleotide probe length is 25-mer; less, if the miRNA is shorter than 25 bases.

Briefly, total RNA samples were prepared using FlashTag™ Biotin RNA labeling kit, following the manufacturer's instructions. This kit allows the use of total RNA samples containing LMW (low molecular weight) RNA. For each sample we used 1 µg of total RNA, as recommended. The labeling reaction is based on Genisphere's proprietary 3DNA dendrimer signal amplification technology, as illustrated in **Figure 15**. Prior to array hybridization, labeling reaction efficiency was checked using the Enzyme Linked Oligosorbent Quality Control Assay (ELOSA QC Assay), following the manufacturer's instructions. The blue substrate color indicates a positive result (a qualitative result). For instrument quantitation, a Stop Reagent is added to each well. This converts the blue substrate to a yellow color. A plate reader is then used to read the absorbance at 450 nm: readings of greater than 0.10 OD over a negative control should be considered positive. This assay generates positive results of at least 0.15-1.00 OD when working appropriately. After that, biotin-labelled samples were hybridized onto the arrays at 48°C and 60 rpm for 16 hours. The arrays were then washed and stained using the Affymetrix Fluidics Station FS-450. We used Affymetrix GeneChip® Scanner 3000 7G to acquire fluorescent images of each array (.CEL files) and Affymetrix GCOS software to analyze them.

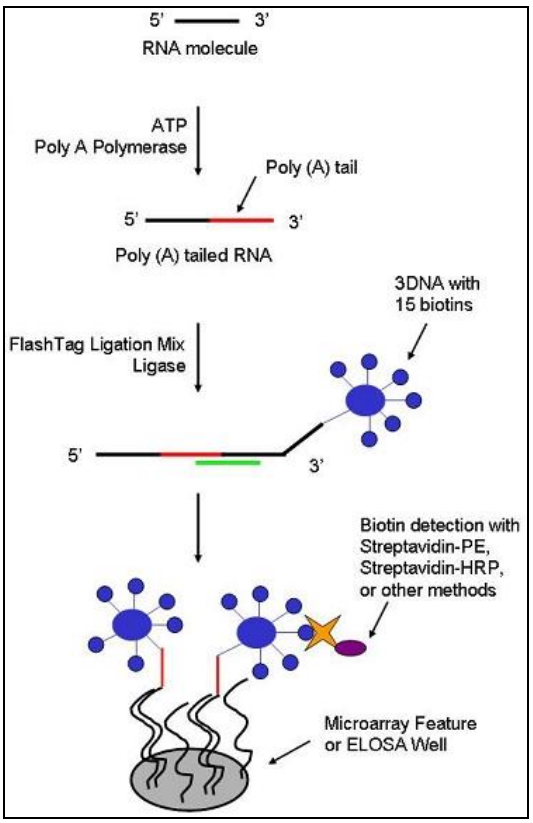

Figure 15. FlashTag Procedure Overview: 1µg of total RNA is used for a tailing reaction, followed by ligation of the biotinylated signal molecules to the target RNA sample (15 biotins to each sample). ELOSA QC Assay is then used to verify the labeling procedure prior to array hybridization, also using a positive (included in the kit) and a negative control (labeling reaction without any RNA Spike Control Oligos and no total RNA).

4.1.1.2 Differential miRNA expression analysis

Intensity .CEL files were imported into Affymetrix© miRNA QC Tool software (http://www.affymetrix.com/partners_programs/programs/developer/tools/devnettools.affx#miRNAQC, V.1.0.33.0) to perform data quality control and to convert intensities into expression values. Using the Affymetrix miRNA_1.0 Annotation file (http://www.affymetrix.com/support/technical/other/mirna-1_0_annotations_20090219.zip), we annotated 847 human miRNA probe sets (namely hsa-miRNAs) and 5,856 miRNA probe sets for the remaining 70 organisms and, finally, the control target content including background, control sequences, housekeeping (1 human 5.8s rRNA probe set) and oligo spike-in. According to Genisphere procedure (http://www.genisphere.com/pdf/FAQ_for_FlashTag_2.pdf), oligo spike-in 2, 23, 29, 31 and 36 probe sets should present a value of more than 1000 intensity units (signal-background) to accept array quality. These five oligos are spiked into the RNA samples prior to FlashTag labeling and contain controls for the GeneChip miRNA array and the ELOSA QC Assay, shown as follows:

- oligos 2, 23, and 29 are RNA, and confirm poly(A) tailing and ligation;
- oligo 31 is poly(A) RNA, and confirms ligation;
- oligo 36 is poly(dA) DNA, and confirms ligation and lack of RNAses in the RNA sample.

The differential miRNA expression analysis was performed by comparing the three RCC cell lines to HK-2. The statistical algorithm Rank Product (RP) was chosen to calculate the differentially expressed miRNAs

(DEMs) for each pairwise comparison, setting the p-value threshold at 0.1. RP was chosen since the groups to be compared have a small size (three replicates each). All calculations were performed in R environment, using several Bioconductor packages (Gentleman *et al.*, 2004; R Development Core Team, 2009).

4.1.1.3 Bioinformatics and functional enrichment analysis

Bioinformatics analysis and data mining of differentially expressed miRNAs were carried out using Human MiRNA & Disease Database (HMDD, http://202.38.126.151/hmdd/mirna/md/, last update Oct-3-2011, Lu *et al.*, 2008) to assess which DEMs are related to cancer and renal carcinoma. An extensive literature mining of the data has been performed using supplementary miRNA data released from recent published article on RCC.

4.1.1.4 Data validation by qPCR

To validate the microarray results, we performed a quantitative reverse-transcribed polymerase chain reaction (qPCR). Globally, we validated 11 miRNAs showing modulation in microarray experiments in at least one comparison and resulting related to cancer and renal carcinoma in HMDD database. Starting from 10 ng of total RNA for each assay, qPCR reactions were performed by use of TaqMan® MicroRNA Reverse Transcription (RT) kit (Applied Biosystems, Life Technologies, Inc. Carlsbad, CA, USA) and specific miRNA primers provided with TaqMan® microRNA Assays, according to the manufacturer's protocol. RT reactions were performed on the Applied Biosystems 7900 Thermocycler machine. To normalize RNA samples, we used RNU48 as endogenous control (provided as TaqMan® microRNA Assays-Control). Reactions were run, in triplicate, on the Applied Biosystems 7900HT Fast Real-Time PCR System machine. Ct values were calculated using the SDS software version 2.3 (Applied Biosystems), by applying automatic baseline and standard threshold settings. We applied the $2^{-\Delta\Delta Ct}$ method (Applied Biosystems User Bulletin No.2) to obtain a relative quantification of miRNA expression levels. The assay list is provided in supplementary table (**Table 5 Appendix**).

4.2 Results

4.2.1 High-throughput miRNA expression analysis

4.2.1.1 Comparison between RCC cell lines and HK-2

We assessed miRNA expression levels by comparing the three RCC cell lines to a normal one, HK-2, using Affymetrix technologies. Expression values were used to obtain lists of differentially expressed miRNAs for each pairwise comparison using Rank Product algorithm, with the p-value threshold set at 0.1. All the arrays passed the quality control performed on oligo spike-in probe sets. The entire lists of differentially expressed miRNAs found in each comparison are reported in supplementary tables (**Tables 6-7-8 Appendix**). As showed by cluster analysing, we found that the miRNA Affymetrix profiling of replicated samples were highly correlated (**Figures 16-17-18**).

Globally, we found 50 DEMs (26 up- and 24 down-regulated miRNAs) in Caki-1 as compared to HK-2, 62 DEMs (32 up- and 30 down-regulated miRNAs) in Caki-2 as compared to HK-2 and 54 DEMs (18 up- and 36 down-regulated miRNAs) in A498 as compared to HK-2. The data showed that peculiar miRNA profiling is present for each comparison however some miRNA are concordantly modulated (**Table 4**).

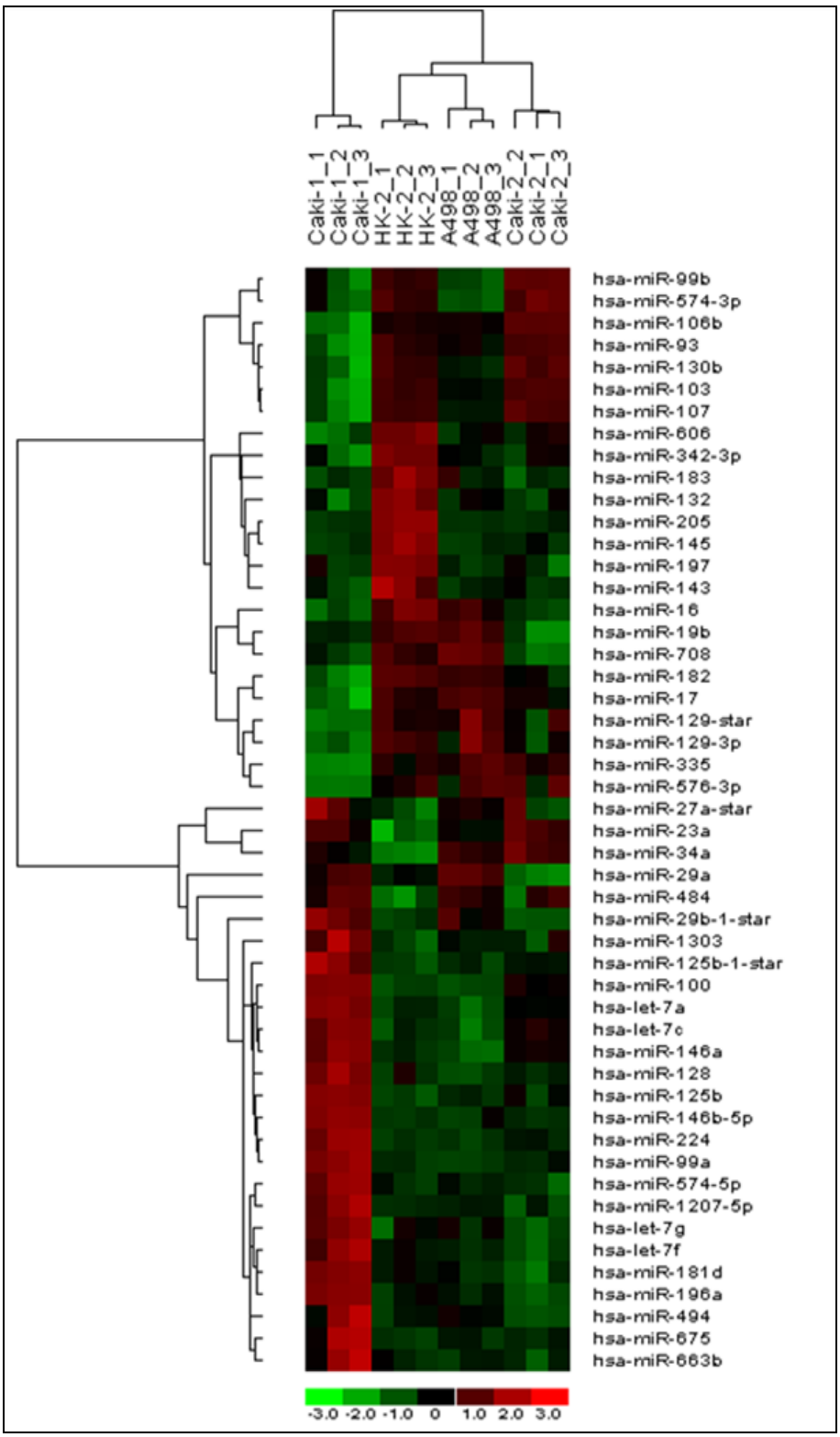

Figure 16. Caki-1 vs HK-2. Clustering heatmap of RCC cell lines and HK-2 based on the 50 DEMs found in the comparison Caki-1 vs HK-2. The heatmap was obtained by use of dChip (Li and Wong, 2001). Each row represents a single miRNA and each column an experimental sample. The color gradient is from green (down-regulated miRNA) to red (up-regulated miRNA).

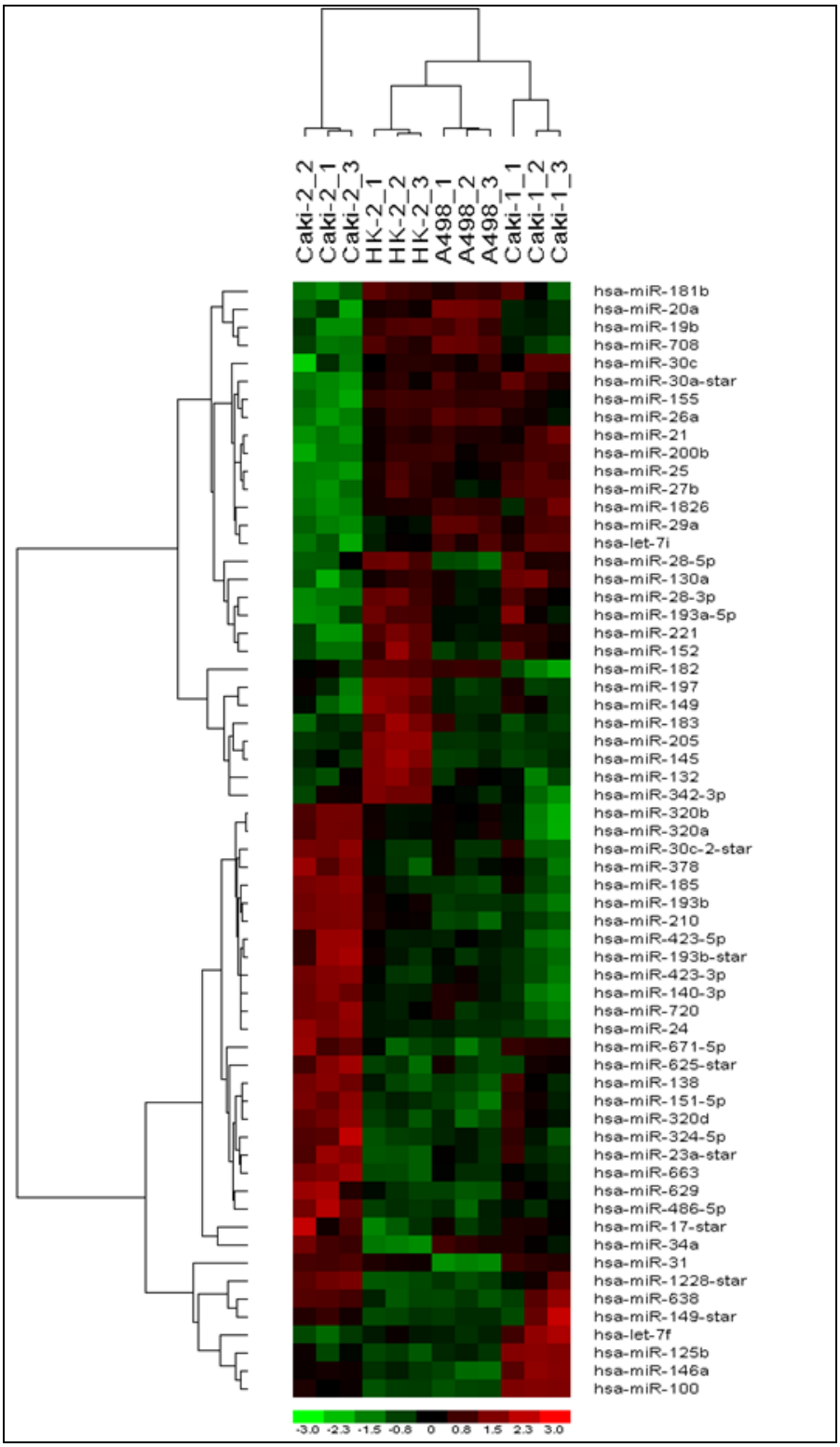

Figure 17. Caki-2 vs HK-2. Clustering heatmap of RCC cell lines and HK-2 based on the 62 DEMs found in the comparison Caki-2 vs HK-2. The heatmap was obtained by use of dChip (Li and Wong, 2001). Each row represents a single miRNA and each column an experimental sample. The color gradient is from green (down-regulated miRNA) to red (up-regulated miRNA).

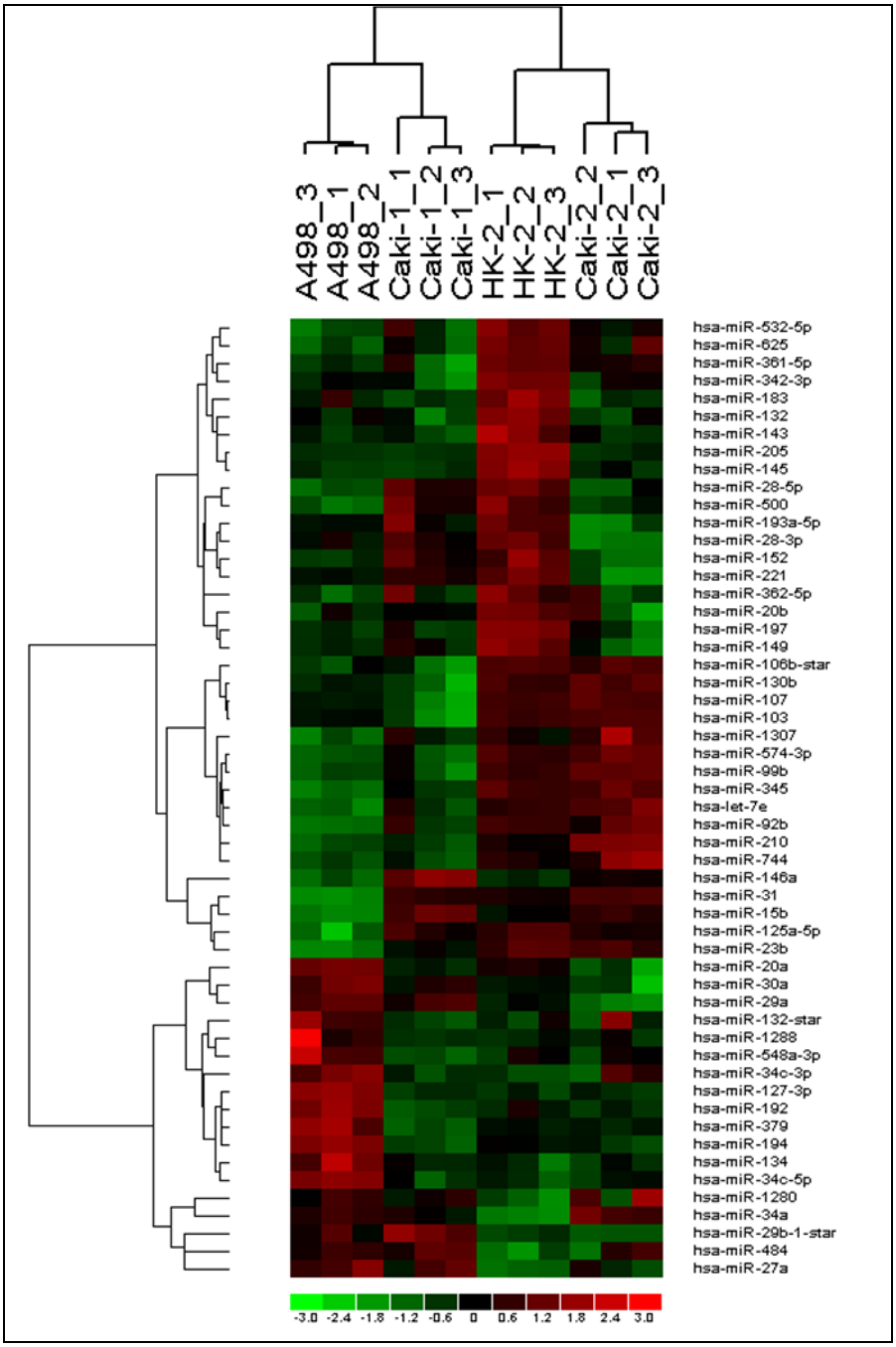

Figure 18. A498 vs HK-2. Clustering heatmap of RCC cell lines and HK-2 based on the 54 DEMs in the comparison A498 vs HK-2. The heatmap was obtained by use of dChip (Li and Wong, 2001). Each row represents a single miRNA and each column an experimental sample. The color gradient is from green (down-regulated miRNA) to red (up-regulated miRNA).

	MIRNAs	
COMPARISON	**DOWN-REGULATED**	**UP-REGULATED**
Caki-1 vs HK-2	hsa-miR-205, hsa-miR-182, hsa-miR-335, hsa-miR-129-star, hsa-miR-103, hsa-miR-130b, hsa-miR-129-3p, hsa-miR-107, hsa-miR-145, hsa-miR-576-3p, hsa-miR-93, hsa-miR-342-3p, hsa-miR-183, hsa-miR-19b, hsa-miR-132, hsa-miR-708, hsa-miR-106b, hsa-miR-197, hsa-miR-16, hsa-miR-99b, hsa-miR-574-3p, hsa-miR-17, hsa-miR-606, hsa-miR-143	hsa-miR-23a, hsa-miR-484, hsa-miR-181d, hsa-miR-1303, hsa-miR-128, hsa-miR-29a, hsa-miR-27a-star, hsa-miR-196a, hsa-miR-675, hsa-miR-34a, hsa-let-7c, hsa-miR-574-5p, hsa-let-7g, hsa-miR-663b, hsa-miR-1207-5p, hsa-miR-29b-1-star, hsa-let-7f, hsa-miR-125b-1-star, hsa-miR-224, hsa-miR-99a, hsa-miR-146b-5p, hsa-let-7a, hsa-miR-494, hsa-miR-146a, hsa-miR-125b, hsa-miR-100
Caki-2 vs HK-2	hsa-miR-205, hsa-miR-155, hsa-miR-21, hsa-miR-25, hsa-miR-28-3p, hsa-miR-19b, hsa-miR-1826, hsa-miR-193a-5p, hsa-miR-708, hsa-miR-30a-star, hsa-miR-27b, hsa-miR-29a, hsa-miR-221, hsa-miR-26a, hsa-miR-145, hsa-miR-183, hsa-miR-197, hsa-miR-152, hsa-miR-149, hsa-miR-182, hsa-miR-200b, hsa-miR-30c, hsa-miR-20a, hsa-miR-132, hsa-let-7i, hsa-miR-28-5p, hsa-miR-130a, hsa-miR-181b, hsa-let-7f, hsa-miR-342-3p	hsa-miR-720, hsa-miR-151-5p, hsa-miR-17-star, hsa-miR-625-star, hsa-miR-671-5p, hsa-miR-320b, hsa-miR-320a, hsa-miR-146a, hsa-miR-125b, hsa-miR-629, hsa-miR-638, hsa-miR-149-star, hsa-miR-1228-star, hsa-miR-193b, hsa-miR-24, hsa-miR-31, hsa-miR-423-3p, hsa-miR-324-5p, hsa-miR-423-5p, hsa-miR-30c-2-star, hsa-miR-140-3p, hsa-miR-320d, hsa-miR-378, hsa-miR-193b-star, hsa-miR-486-5p, hsa-miR-138, hsa-miR-23a-star, hsa-miR-663, hsa-miR-185, hsa-miR-210, hsa-miR-34a, hsa-miR-100
A498 vs HK-2	hsa-miR-31, hsa-miR-205, hsa-miR-345, hsa-miR-125a-5p, hsa-miR-145, hsa-miR-574-3p, hsa-miR-210, hsa-miR-99b, hsa-miR-197, hsa-miR-28-5p, hsa-let-7e, hsa-miR-149, hsa-miR-361-5p, hsa-miR-130b, hsa-miR-532-5p, hsa-miR-152, hsa-miR-15b, hsa-miR-193a-5p, hsa-miR-362-5p, hsa-miR-132, hsa-miR-28-3p, hsa-miR-342-3p, hsa-miR-183, hsa-miR-92b, hsa-miR-23b, hsa-miR-500, hsa-miR-143, hsa-miR-1307, hsa-miR-146a, hsa-miR-107, hsa-miR-625, hsa-miR-20b, hsa-miR-221, hsa-miR-103, hsa-miR-744, hsa-miR-106b-star	hsa-miR-484, hsa-miR-1280, hsa-miR-30a, hsa-miR-1288, hsa-miR-132-star, hsa-miR-379, hsa-miR-20a, hsa-miR-548a-3p, hsa-miR-27a, hsa-miR-34c-3p, hsa-miR-29b-1-star, hsa-miR-134, hsa-miR-34c-5p, hsa-miR-34a, hsa-miR-192, hsa-miR-29a, hsa-miR-194, hsa-miR-127-3p

Table 4. List of differentially expressed miRNAs found in each comparison between RCC cell lines and HK-2. miRNAs are ordered according to their expression values, from the most down-regulated miRNA to the most up-regulated miRNA. Down-regulated miRNAs are in green, up-regulated miRNAs are in red, and common DEMs are underlined.

Moreover, we found 9 DEMs in common among the three comparisons, in particular 7 were also concordant, as follows: hsa-miR-34a is up-regulated, while hsa-miR-205, hsa-miR-145, hsa-miR-183, hsa-miR-197, hsa-miR-132 and hsa-miR-342-3p are down-regulated in all the RCC lines vs HK-2 (**Figure 19**). Whereas, hsa-miR-146a was found up-regulated in Caki-1 and Caki-2 cell lines vs HK-2 and down-regulated in A498 vs HK-2; while hsa-miR-29a was found up-regulated in Caki-1 and A498 vs HK-2, and down-regulated in Caki-2 vs HK-2.

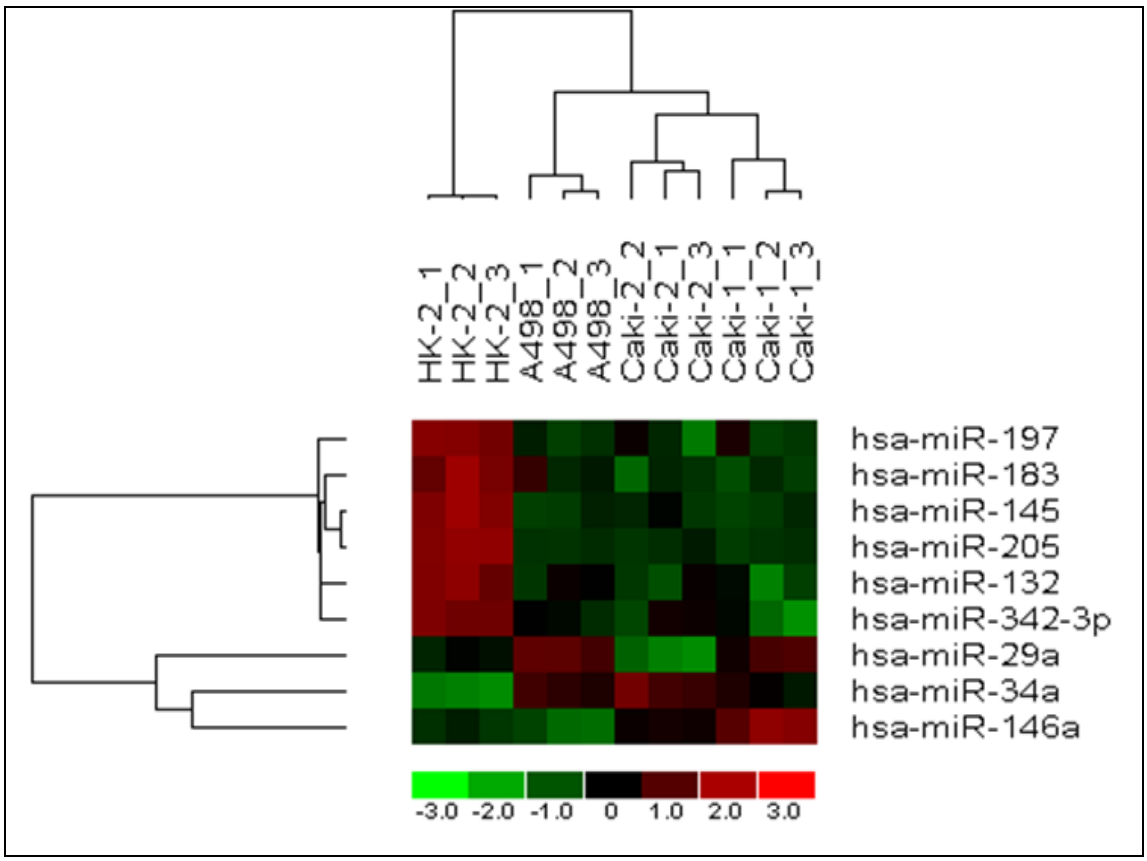

Figure 19. Common and concordant DEMs. Clustering heatmap of RCC cell lines and HK-2 based on the 7 common and concordant DEMs found in all the three comparisons. The heatmap was obtained by use of dChip (Li and Wong, 2001). Each row represents a single miRNA and each column an experimental sample. The color gradient is from green (down-regulated miRNA) to red (up-regulated miRNA).

In each comparison, by clustering heatmaps, we observed that some miRNAs are characteristically up- or down-regulated, at a statistically significant level, only in one RCC cell line compared to HK-2. For example, we found that miR-335 and miR-576-3p are down-regulated, while 14 miRNAs (e.g., miR-128, miR-125, miR-224, let-7g, let-7f, miR-494) are up-regulated only in Caki-1 vs HK-2. The down-regulation of 8 miRNAs (i.e., miR-30c, miR-30a*, miR-155, miR-26a, miR-21, miR-200b, miR-25, miR-27b) and the up-regulation of 13 miRNAs (e.g., miR-320b, miR-320a, miR-30c-2*, miR-378, miR-185, miR-193b, miR-210, miR-720) were found only in Caki-2 vs HK-2. Finally, miR-31 and miR-15b were down-regulated and 6 miRNAs (i.e., miR-127-3p, miR-192, miR-379, miR-194, miR-134, miR-34c-5p) were up-regulated only in A498 vs HK-2. These results demonstrate that each RCC cell line has a own miRNA signature, even if these miRNAs showed modulation also in the other RCC cell lines but not at statistically significant level. Despite a peculiar miRNA expression in each RCC cell line, we found 9 dysregulated miRNAs in common, whose 7 were also concordant.

Currently, Sanger miRNA database is at version 17 (April, 2011), so there are some differences with the version 11, on which the GeneChip miRNA array was designed. So, when comparing the two miRNA database versions (freely available for download in miRBase FTP site), we noted that 4 DEMs were no longer considered belonging to miRNA class in the latest version (hsa-miR-768-3p, hsa-miR-886-3p, hsa-miR-886-5p and hsa-miR-1308). Thus, these 4 miRNAs were not included in our DEM lists or used for further analyses.

4.2.1.2 Functional enrichment analysis and validation by qPCR

Bioinformatics analysis and data mining using HMDD (Human MicroRNA & Disease Database) highlighted 11 DEMs already associated to cancer and renal cell carcinoma in different studies (**Table 5**).

MIRNA	Caki-1	Caki-2	A498	REFERENCES
hsa-miR-21		down		Huang *et al.*, 2009; Juan *et al.*, 2010; Zhang *et al.*, 2011
hsa-miR-34a	up	up	up	Dutta *et al.*, 2007; Liu *et al.*, 2010; Juan *et al.*, 2010; Vogt *et al.*, 2011; White *et al.*, 2011
hsa-miR-143	down		down	Huang *et al.*, 2009; White *et al.*, 2011
hsa-miR-145	down	down	down	Huang *et al.*, 2009; Gan *et al.*, 2010; Jung *et al.*, 2009; Sachdeva *et al.*, 2010
hsa-miR-146a	up	up	down	Ha *et al.*, 2010; Perske *et al.*, 2010
hsa-miR-149		down	down	Juan *et al.*, 2010; Liu *et al.*, 2010
hsa-miR-152		down	down	Wang *et al.*, 2010
hsa-miR-183	down	down	down	Jung *et al.*, 2009; Nakada *et al.*, 2011; White *et al.*, 2011
hsa-miR-205	down	down	down	Gregory *et al.*, 2008; Majid *et al.*, 2011; Tellez *et al.*, 2011
hsa-miR-210		up	down	Jung *et al.*, 2009; Zhou *et al.*, 2010; Nakada *et al.*, 2011; White *et al.*, 2011
hsa-miR-221		down	down	Heinzelmann *et al.*, 2011; Huang *et al.*, 2009; White *et al.*, 2011

Table 5. List of DEMs already reported to be associated to cancer and renal carcinoma in the HMDD database. Corresponding publications are indicated.

To verify miRNA expression levels of miRNAs, we used miRNA specific TaqMan probes for qPCR validation. In total, we validated 11 miRNAs that we found modulated in at least one RCC cell line compared to HK-2. Moreover, these 11 miRNAs were already found associated to cancer and renal carcinoma in the HMDD database. Thus, by qPCR, we confirmed previously observed microarray expression values (**Table 6**). In details, we noted in all the three comparisons the down-regulation of hsa-miR-145, hsa-miR-183 and hsa-miR-205 and the up-regulation of hsa-miR-34a. Instead, in Caki-1 we confirmed the down-regulation of hsa-miR-143 and the up-regulation of hsa-miR-146a; in Caki-2 the down-regulation of hsa-miR-21, hsa-miR-149, hsa-miR-152 and hsa-miR-221, and the up-regulation of hsa-miR-146a and hsa-miR-210; and, finally, in A498 the down-regulation of hsa-miR-143, hsa-miR-146a, hsa-miR-149, hsa-miR-152, hsa-miR-210, hsa-miR-221. Moreover, we observed the down-regulation of hsa-miR-21, hsa-miR-149 and hsa-miR-152 and a tendency to the up-regulation of hsa-miR-210 and hsa-miR-221 in Caki-1, the down-regulation of hsa-miR-143 in Caki-2, and the down-regulation of hsa-miR-21 in A498, although these miRNAs were not found differentially expressed by microarray analysis.

MIRNA	Caki-1		Caki-2		A498	
	qPCR	*array*	*qPCR*	*array*	*qPCR*	*array*
hsa-miR-21	-10,33	n.s.	-10,87	-3,40	-1,89	n.s.
hsa-miR-34a	0,23	1,58	0,57	2,30	0,47	1,92
hsa-miR-143	-24,90	-1,31	-74,60	n.s.	-32,80	-1,15
hsa-miR-145	0,00	-2,09	0,00	-1,90	0,00	-2,11
hsa-miR-146a	43,85	3,57	30,03	1,34	-8,43	-1,13
hsa-miR-149	-2,69	n.s.	-1,34	-1,82	-2,64	-1,45
hsa-miR-152	-1,56	n.s.	-7,88	-1,83	-4,20	-1,41
hsa-miR-183	-61,87	-1,70	-1,46	-1,84	-3,54	-1,26
hsa-miR-205	0,00	-4,68	0,00	-4,57	0,00	-4,72
hsa-miR-210	0,27	n.s.	4,83	2,19	-5,88	-1,87
hsa-miR-221	1,30	n.s.	-1,66	-2,04	-3,19	-1,08

Table 6. Quantitative real-time PCR validation of miRNA microarray analysis in RCC cell lines compared to HK-2. Expression values are expressed in fold change both for qPCR and array results for each comparison (n.s.: not statistically significant).

4.3 Discussion

In this second section, we performed a genome-wide differential miRNA expression analysis using Affymetrix GeneChip® miRNA array, which allows the detection of a total of 6,703 miRNAs in 71 organisms, whose 847 are human miRNAs, based on the Sanger miRNA database (V.11). To do this, we used three RCC cell lines as *in vitro* model of renal cell carcinoma pathology, i.e. Caki-1, Caki-2 and A498, and we compared their miRNA profiles to that of HK-2, a proximal tubular cell line derived from normal adult kidney (Ryan *et al.*, 1994).

We found a total of 50 DEMs (26 up- and 24 down-regulated miRNAs) in Caki-1, 62 DEMs (32 up- and 30 down-regulated miRNAs) in Caki-2 and 54 DEMs (18 up- and 36 down-regulated miRNAs) in A498 as compared to HK-2.

By functional annotation analysis according to HMDD database and literature mining search, we observed that all DEMs found in the three comparisons were already known to be associated to at least one cancer and/or one disease, except five miRNAs, i.e. miR-576 and miR-606 (down-regulated in Caki-1 vs HK-2), miR-1303 (up-regulated in Caki-1), miR-1307 (down-regulated in A498) and miR-1288 (up-regulated gene in A498). Therefore, we could speculate that these miRNAs might have an important role in renal cancer cells, however further investigations are certainly needed.

Furthermore, functional annotation analysis showed that almost all miRNAs found in common in the three comparisons were already reported widely associated with RCC, as described below.

According to recent literature (Juan *et al.*, 2010; White *et al.*, 2011b), we found the common up-regulation of miR-34a in all the three RCC cell lines. This is a very interesting miRNA, since it is a potential tumor suppressor involved in many types of cancer, and found either up-regulated (e.g., in RCC, hematopoietic and head and neck tumors) or down-regulated (e.g., in neuroblastoma), working in a cell type-specific manner. A study conducted by Dutta and his colleagues suggested that miR-34a over-expression, an acquired trait during carcinogenesis, supports cell proliferation in the majority of cancers (Dutta *et al.*, 2007). When over-expressed, miR-34a leads to apoptosis or cellular senescence, whereas reduction of miR-34a function attenuates p53-mediated cell death. Moreover, miR-34a is a direct p53 target gene, since it has several candidate p53 binding sites in the promoter region and the intron. In fact, p53 transcriptionally activates miR-34a, and other members of the same family (such as miR-34b and miR-34c), in response to multiple cellular stresses. Then, miR-34a, in turn, induces apoptosis or growth arrest by post-transcriptional repression of its target genes (i.e. *E2F3* and *NOTCH1*) in a context-dependent manner (He *et al.*, 2007a). Furthermore, Vogt *et al.* reported that many tumors, including renal cancer, display CpG methylation of miR-34a and miR-34b/c at a relatively high frequency (Vogt *et al.*, 2011). Probably, it could be due to a tendency of cell lines to harbour p53 mutations, which may alleviate a requirement for miR-34a methylation, or alternatively, loss of CpG-methylation during *in vitro* passaging. The authors hypothesized that since ectopic expression of miR-34a has been shown to induce senescence, it is possible that miR-34a inactivation by CpG methylation contributes to the escape from oncogene-induced senescence in the early phases of tumor development, thus facilitating the emergence of tumor-initiating cells, since processes as cell cycle arrest,

senescence or apoptosis will presumably be attenuated in cells with loss of miR-34a function (Vogt *et al.*, 2011).

Some studies revealed the involvement of miR-205 in EMT (epithelial to mesenchymal transition) (Gregory *et al.*, 2008a; Tellez *et al.*, 2011). Recently, the down-regulation of miR-205 in RCC has been reported for the first time (Majid *et al.*, 2011). The authors demonstrated the role of this miRNA in inhibiting Src-mediated oncogenic pathways in renal cancer, using cell lines and tissues. The Src family of protein kinases (SFK) plays key roles in regulating fundamental cellular processes, including cell growth, differentiation, cell shape, migration and survival. They showed that miR-205 expression is inversely correlated with the expression of SFKs, and transient and stable over-expression of miR-205 caused induction of G_0/G_1 cell cycle arrest, and apoptosis, and suppressed cell proliferation, colony formation, migration and invasion in renal cancer cells. These results indicated that miR-205 is an important tumor suppressor miRNA in RCC, suggesting also its therapeutic potential.

According to literature (Huang *et al.*, 2009j; Jung *et al.*, 2009, White *et al.*, 2011b; Yi *et al.*, 2010), we found a down-regulation of miR-145 in all the three RCC cell lines. This miRNA locus is located on chromosome 5 (on 5q32-33), which is a well-known fragile site in human genome, this probably explaining the decreased expression of miR-145 observed in many tumors (e.g. breast, colon, prostate, lung, bladder). Thus, its role in controlling cell proliferation has been suggested, probably due to direct targeting of *c-Myc* oncogene by directly binding to its 3'UTR. Over-expression of miR-145 is able to down-regulate some of the *c-Myc* target genes such as cyclin D1 and elF4E which are involved in cell cycle regulation. Moreover, this miRNA also has a role in cell invasion and metastasis, the suppression of cell invasion is in part due to the silencing of the metastasis gene mucin 1, that causes a reduction of β-catenin as well as of the oncogenic cadherin-11. Given its involvement in cell growth and invasion, miR-145 has been proposed as tumor suppressor. This feature may be also related to the fact that miR-145 is regulated by p53, and that suppression of miR-145 alters the p53-mediated cell cycle arrest, which is likely in part by silencing of c-Myc. Surely, further studies will be required to evaluate the potential utility of miR-145 as novel biomarker or novel therapeutic target for cancer therapy (Sachdeva and Mo, 2010). Gan *et al.* confirmed, by qPCR, the down-regulation of miR-145 and the up-regulation of some of its targets such as c-Myc, in ccRCC compared with matched normal kidney samples, thus suggesting a role for miR-145 also in renal tumorigenesis (Gan *et al.*, 2010).

miR-183 was found down-regulated in all the three comparisons we analyzed, accordingly with many previous studies on ccRCC samples (Jung *et al.*, 2009; Nakada *et al.*, 2008; White *et al.*, 2011b). miR-183 locus is located on chromosome 7 and has been implicated in key cellular functions, such as neurosensory development (Sarver *et al.*, 2010). Recently, it has been reported that miR-183 functions as a potential oncogene in specific sarcoma types and in colon cancer by directly or indirectly regulating *EGR1* and *PTEN* expression levels, respectively. In addition, the authors showed that miR-183 knockdown in the corresponding tumor cell lines affect cellular migration (Sarver *et al.*, 2010).

Despite the fact that in some recent studies (Chow *et al.*, 2010; White *et al.*, 2011b) miR-342-3p was reported as up-regulated in RCC samples, we found that this miRNA was modulated in all the three comparisons but in the opposite direction. In the same way, we reported the down-regulation of miR-197 in all the three RCC cell lines, although White *et al.* detected the involvement of this miRNA in their ccRCC

samples but in the opposite direction (White *et al.*, 2011b). miR-197 has been reported to translationally repress Fus1 expression by targeting specific sequences in the 3′UTR of *FUS1*, which is a tumor suppressor gene located on human chromosome 3p21, and expression of Fus1 protein is highly regulated at various levels, leading to lost or greatly diminished tumor suppressor function in many lung cancers (Du *et al.*, 2009).

Recently, Anand *et al.* described how miR-132, an angiogenic growth factor-inducible miRNA expressed in the normal endothelium, facilitates pathological angiogenesis by down-regulating p120RasGAP, a molecular brake for Ras (Anand and Cheresh, 2011). Importantly, targeting miR-132 with a complementary, synthetic anti-miRNA restored the brake and decreased angiogenesis and tumor burden in multiple tumor models. They also showed that ectopic expression of miR-132 was sufficient to increase *in vitro* endothelial proliferation and tube formation. Conversely, the complementary anti-miR-132 decreased *in vitro* endothelial proliferation and tube formation, and both developmental and pathological angiogenesis *in vivo*. These observations highlighted that miR-132 is not only among the early response genes in endothelial activation but also a critical regulator of the downstream events controlling endothelial proliferation, tube formation and angiogenesis *in vivo*. Taken together, emerging evidences suggest a central role for microRNAs downstream of multiple growth factors in regulating endothelial proliferation, migration and vascular patterning (Anand and Cheresh, 2011). In our analyses, miR-132 was found down-regulated in RCC cell lines, so its relation with angiogenesis in renal cancer needs other studies.

Generally, the up-regulation of miR-146a in RCC samples has been reported (Ha *et al.*, 2010; Perske *et al.*, 2010; White *et al.*, 2011b). Accordingly, we found the up-regulation of this miRNA in Caki-1 and Caki-2 cell lines, but not in A498. Perske *et al.* demonstrated that miR-146a partially reduces or completely abolishes endogenous nitric oxide (NO) production to escape macrophage-mediated cell death, since it translationally inhibits the iNOS (Inducible Nitric Oxide Synthase) protein expression. It has been suggested that inhibition of miR-146a may render these tumor cells susceptible to therapeutic strategies (Perske *et al.*, 2010). In another study, miR-146a resulted up-regulated in renal cancer, and, its over-expression increased after stimulation by carbamylated albumin (cAlb), since carbamylation is a post-transcriptional modification; anyway, its pathophysiological consequences remain poorly understood (Ha *et al.*, 2010).

We detected that miR-29a is up-regulated in Caki-1 and A498, according to Chow et al. (Chow *et al.*, 2010), while it's down-regulated in Caki-2. Heinzelmann *et al.* reported miR-29a as one of the most down-regulated miRNAs in metastatic compared to non-metastatic ccRCC tumors (Heinzelmann *et al.*, 2011). Thus, this miRNA needs further investigations.

Another intriguing miRNA is miR-21, which was found down-regulated in Caki-2 vs HK-2, and reported up- or down-regulated in many tumors (White *et al.*, 2011b). Among oncogenic miRNAs, miR-21 is over-expressed in several different human cancer types, such as glioma, breast cancer, colon cancer, lung cancer, head and neck cancer, and plays critical roles in regulating the cancer malignant phenotype (Zhang *et al.*, 2011b). Recent studies have reported that miR-21 is up-regulated in RCC tissues compared with normal tissues (Juan *et al.*, 2010; Liu *et al.*, 2010a). However, few direct evidences exist to explain how this miRNA is involved in the RCC development. Zhang *et al.* showed that miR-21 knockdown by antisense oligonucleotides inhibited cell proliferation and induced cell apoptosis in RCC cells, indicating that miR-21 is a critical oncogenic miRNA that inhibits cell apoptosis in RCC (Zhang *et al.*, 2011b). The results of this study

suggested that the down-regulation of miR-21 expression promoted RCC cell apoptosis by way of the caspase pathway. In fact, knockdown of miR-21 could activate the caspase pathway, mediated by multiple potential target genes, such as *FASL* (Fas ligand) and *TIMP3* (metalloproteinase inhibitor 3), and subsequently induce cell apoptosis in RCC (Zhang *et al.*, 2011b). In our study, we confirmed the down-regulation of miR-21 by qPCR in all the three RCC cell lines, despite microarray results were not statistically significant in Caki-1 and A498 comparisons.

On the other hand, miR-210 was detected to be up-regulated in Caki-2 and down-regulated in A498, probably due to the different HIF-1α expression level, since miR-210 is a direct transcriptional target of HIF-1α (Kulshreshtha *et al.*, 2007a; Huang *et al.*, 2010). In fact, Caki-2 had a high HIF-1α protein level, while A498 showed a low protein level by our western blot analysis. qPCR results confirmed microarray data for Caki-2 and A498 cell lines, and showed a tendency of down-regulation in Caki-1.

Although the pri-miRNA structure has not been identified yet, it has been suggested that miR-145 could be co-transcribed with miR-143 (Cordes *et al.*, 2009). miR-145 and miR-143 are localized close to each other at chromosome 5q32, which is a locus often deleted (e.g., in myelodysplastic syndromes) (Le Beau *et al.*, 1989). By qPCR we confirmed the down-regulation of both miRNAs in our RCC cell lines.

We reported that miR-221 is down-regulated in Caki-2 and A498 cell lines, and confirmed our data by qPCR, showing a tendency of up-regulation in Caki-1. Interestingly, this miRNA was recently reported down-regulated (White *et al.*, 2011b) and up-regulated (Huang *et al.*, 2009j) in RCC. Moreover, Heinzelmann *et al.* reported that this miRNA is one of the most down-regulated genes that can distinguish metastatic from non-metastatic tumors (Heinzelmann *et al.*, 2011). In haematopoietic progenitor cells, it has been reported that miR-221 together with miR-222 inhibit endothelial cell migration, proliferation, and angiogenesis *in vitro* by targeting the stem cell factor receptor c-kit and by indirectly regulating endothelial nitric oxide synthase expression (Urbich *et al.*, 2008). The miR-221/222 family also reduces c-kit expression and consequently cell proliferation, and their depletion also changed the miRNA signature of HUVEC51 (human umbilical vein endothelial cells) indicating that miRNAs control the expression of other miRNAs. In fact, 9 miRNAs were found up-regulated and 23 miRNAs down-regulated in response to miR-221/ 222 depletion (Urbich *et al.*, 2008).

By qPCR we also confirmed the down-regulation of miR-152, which is a tumor suppressor silenced by aberrant DNA hypermethylation in endometrial cancer. miR-152 epigenetic silencing was consistent with its location at 17q21.32 in *COPZ2* (coatomer protein complex, subunit zeta 2) intron 1, which is often silenced in endometrial cancer by DNA hypermethylation, and also with evidences that miR-152 targets the DNA methyltransferase *DNMT1* (Tsuruta *et al.*, 2011). The CpG island methylation of miR-152 was also observed in non-small-cell lung cancer (NSCLC) clinical specimens (Kitano *et al.*, 2011).

According to literature, we assessed by microarray and qPCR the down-regulation of miR-149, which is reported under-expressed also in other studies and which targets lysyl oxidase (*LOX*), an important HIF target involved in extracellular matrix formation and turnover (Baldewjins *et al.*, 2011; Juan *et al.*, 2010; Jung *et al.*, 2010; Liu *et al.*, 2010a).

Many studies also demonstrated that the copy number alterations may affect miRNA expression levels in RCC samples (Powers *et al.*, 2011; White *et al.*, 2011b, Youssef *et al.*, 2011). In our study, we have not performed the integration between copy number and miRNA expression levels since, as described above, the RCC cell lines we used carried a very aberrant karyotype, with many CNAs on several chromosomes, and this would have make this analysis very difficult and unreliable.

Using the recent literature about ccRCC miRNA gene expression profiling, we compared our list of 125 differentially expressed miRNAs (the total number of DEMs found through the three comparisons) with the datasets of modulated miRNAs reported by other authors. Through this comparison, we observed that among 125 miRNAs, 64 were not found in any other paper, 36 were reported in at least one paper, and, thus, the remaining 25 miRNAs were cited in two or more papers (**Table 7**). Noticebly, we found 10 miRNAs (miR-149, miR-182, miR-183, miR-185, miR-200b, miR-224, miR-34a, miR-362-5p, miR-532-5p, miR-629) depicting concordant modulation between the present investigation performed on ccRCC cell lines and those reported by other authors on RCC tissues.

MIRNA	Caki-1	Caki-2	A498	Nakada *et al.*, 2008	Chow *et al.*, 2010	Juan *et al.*, 2010	Liu *et al.*, 2010	Zhou *et al.*, 2010	Yi *et al.*, 2010	White *et al.*, 2011
hsa-miR-125b	Up	Up				Down	Down			
hsa-miR-130b	Down		Down		Up					Up
hsa-miR-138		Up		Down	Down					
hsa-miR-149		Down	Down			Down	Down			
hsa-miR-155		Down		Up		Up	Up	Up		Up
hsa-miR-15b			Down						Up	Up
hsa-miR-16	Down								Up	Up
hsa-miR-17	Down				Up				Up	
hsa-miR-182	Down	Down		Down	Down					
hsa-miR-183	Down	Down	Down	Down	Down					
hsa-miR-185		Up				Up	Up			Up
hsa-miR-200b		Down			Down	Down	Down			
hsa-miR-20a		Down	Up		Up					Up
hsa-miR-20b			Down		Up			Down		
hsa-miR-21		Down			Up	Up	Up	Up	Down	Up
hsa-miR-210		Up	Down	Up	Up	Up	Up	Up		Up
hsa-miR-224	Up			Up	Up	Up	Up	Up		Up
hsa-miR-342-3p	Down	Down	Down		Up					Up
hsa-miR-34a	Up	Up	Up			Up	Up	Up		Up
hsa-miR-362-5p			Down		Down				Down	
hsa-miR-378		Up			Down				Up	
hsa-miR-379			Up	Down	Down					
hsa-miR-532-5p			Down		Down					Down
hsa-miR-629		Up			Up			Up		Up
hsa-miR-720		Up			Down				Up	Down

Table 7. List of 25 miRNAs cited as differentially expressed in two or more other papers.

The differences between miRNAs identified by each study could be due to the experimental methodology, including the platform used, cell lines or kidney cancer subtypes analyzed, experimental conditions, sample size or statistical analysis applied.

Overall, by literature mining, we observed that in many studies (Ha *et al.*, 2010; Majid *et al.*, 2011; Nakada *et al.*, 2008, 2011; Zhang *et al.*, 2009, 2011) RCC cell lines have been widely used as *in vitro* model of renal cell carcinoma in order to identify miRNAs that target relevant genes involved in pathways, like apoptosis, angiogenesis, epithelial to mesenchymal transition and so on, which are often altered in this cancer, so allowing sometimes to identify miRNAs potentially useful as novel biomarkers or therapeutic targets for RCC. Thus, we suggest that it is possible to extensively study the role of specific and novel miRNAs associated to renal cell carcinoma using immortalized RCC cell lines in combination with functional approaches.

5 PART III: INTEGRATED ANALYSIS OF MICRORNA AND GENE EXPRESSION DATA

5.1 Material and Methods

5.1.1 miRNA-gene integrated analysis

In order to study the miRNA-target gene relationships and their regulatory networks in RCC cell lines, we performed an integrated analysis, by combining miRNA and gene expression profiles using MAGIA (MiRNA And Genes Integrated Analysis) tool, based on the assumption that true target expression level is expected to be anti-correlated with that of its miRNA (Sales *et al.*, 2010). First of all, an adjacency matrix was reconstructed by target predictions, applying MiRanda (Enright *et al.*, 2003; John *et al.*, 2004) and PITA (Kertesz *et al.*, 2007) algorithms to the analysis of miRNA sequences and transcripts 3'UTR sequences. Thus, obtaining a list of miRNA-transcript predicted relationships, each associated to a score. For each algorithm, we chose the top 20% of all predictions, in order of score values, and combined the selected predictions to obtain their union. To reconstruct the adjacency matrix, we considered only 19,793 genes represented in the Affymetrix Gene 1.0ST Array and 125 DEMs (the total number of DEMs found through the three comparisons) in at least one comparison. The second step was the selection of target relationships significantly supported by expression data. For each pair of DEM and target gene, we computed the Pearson's correlation between the corresponding expression profiles and associated to a p-value. We selected as potentially functional relations, only those between miRNA-gene pairs associated to negative coefficients. In this way, we obtained the adjacency matrix of supported regulatory interactions. For each comparison, post-transcriptional regulatory networks, comprising only DEMs in the comparison and all predicted and supported target genes represented on the array, were reconstructed by Cytoscape software (V. 2.6.3). This analysis was carried out thanks to our collaboration with the group of Dr. Stefania Bortoluzzi of University of Padua.

5.1.2 Selection of relevant miRNA-gene anti-correlated pairs

Starting from the results of the integrated analysis of miRNA and gene expression data, we selected some relevant miRNA-gene anti-correlated pairs for further investigations. In order to do this, we focused our attention on common and concordant DEMs found in all three comparisons. Using the adjacency matrix of supported regulatory interactions previously obtained and DAVID functional enrichment analysis on DEGs previously described, we verified which and how many were the targets of each common and concordant DEM and, thus, we selected some genes that were already associated with pathways associated to RCC and cancer in general.

5.1.3 qPCR validation of selected target genes

Concerning the selected most relevant miRNA-gene pairs, we assessed their anti-correlated expression measuring the expression levels of the 3 DEMs and 8 DEGs by qPCR. For miRNAs, we conducted qPCR reactions as previously described. For target genes, we performed qPCR starting from 1 µg of total RNA using the High Capacity cDNA Reverse Transcription kit (Applied Biosystems, Life Technologies, Inc. Carlsbad, CA, USA) and gene-specific primers provided with TaqMan® Gene Expression Assays. To

normalize RNA samples, we used *ACTB* as endogenous control. Reactions were run in triplicate on the Applied Biosystems 7900HT Fast Real-Time PCR System machine. Threshold (Ct) values were calculated using the SDS software version 2.3, as described above, and the $2^{-\Delta\Delta Ct}$ method was applied to obtain a relative quantification of gene expression levels. The assay list is provided in supplementary table (**Table 9 Appendix**).

5.2 Results

5.2.1 miRNA-gene integrated analysis

Integrated analysis was performed by combining miRNA and gene expression data by using MAGIA tool. Through this analysis we found a total of 575,773 predicted relationships between 125 DEMs and 17,313 target genes (represented on the array and having at least one target site for at least one DEM). Among these predicted relationships, only 2,236 resulted really supported by gene expression data based on applied criteria, involving 88 DEMs out of 125 (~70%), and 1,695 target genes out of 17,313 (~10%).

Using Cytoscape, we reconstructed miRNA-gene networks, as previously reported (21), through the adjacency matrix of supported regulatory interactions, each comprising only DEMs in the comparison and all predicted and supported target genes. In each network we distinguished two types of nodes, miRNA and target gene, connected by directed edges, that represent probable relationships between miRNA and target genes.

For each comparison we found both wide networks, in which one DEM could regulate more than 100 target genes, and small networks, in which one DEM could affect only one single gene. Specifically, according to the stringency criteria applied, we found networks that involve a total of 40 DEMs (21 up- and 19 down-regulated miRNAs) and 968 target genes (whose 263 up- and 100 down-regulated genes) in Caki-1 compared to HK-2; 48 DEMs (21 up- and 27 down-regulated miRNAs) and 1,283 genes (whose 244 up- and 199 down-regulated genes) in Caki-2 compared to HK-2; 39 DEMs (11 up- and 28 down-regulated miRNAs) and 1,056 genes (whose 278 up- and 78 down-regulated genes) in A498 compared to HK-2.

Firstly, we focused our attention on common and concordant DEMs found in all the three comparisons and, thus, we investigated how many predicted targets were also differentially expressed genes in each comparison and how many were also common and concordant supported target genes. The counts of predicted and supported target genes for the three common and concordant miRNAs belonging to major networks is illustrated in **Table 8**. The distribution of target genes for each DEM is given in supplementary table (**Table 10 Appendix**).

MIRNA	PREDICTED TARGET GENES	Caki-1	Caki-2	A498	COMMON & CONCORDANT SUPPORTED TARGET GENES
hsa-miR-34a	217	53	87	62	50
hsa-miR-205	237	108	89	107	76
hsa-miR-145	280	137	95	135	84

Table 8. Counts of predicted target genes for three DEMs. Predicted target genes that are also differentially expressed in each comparison, and in common in the three comparisons are here reported. The up-regulation is highlighted in red, the down-regulation in green.

Afterwards, we focused our interest on wide networks that involved DEMs and more than 100 predicted target genes. Three networks were very interesting, because they were very big common miRNA-gene networks; moreover, they had many predicted target genes that were found differentially expressed in each comparison. An example of each miRNA-gene regulatory network is shown only for Caki-1 as compared to HK-2, since these are big common networks in all three comparisons (**Figures 20-21**). These networks were

composed by hsa-miR-34a which was up-regulated in the three comparisons, and hsa-miR-145 and hsa-miR-205. These two latter miRNAs were both down-regulated in all the three comparisons, and they also had a total of 94 predicted target genes in common, whose 31 were up-regulated in RCC cell lines compared to HK-2.

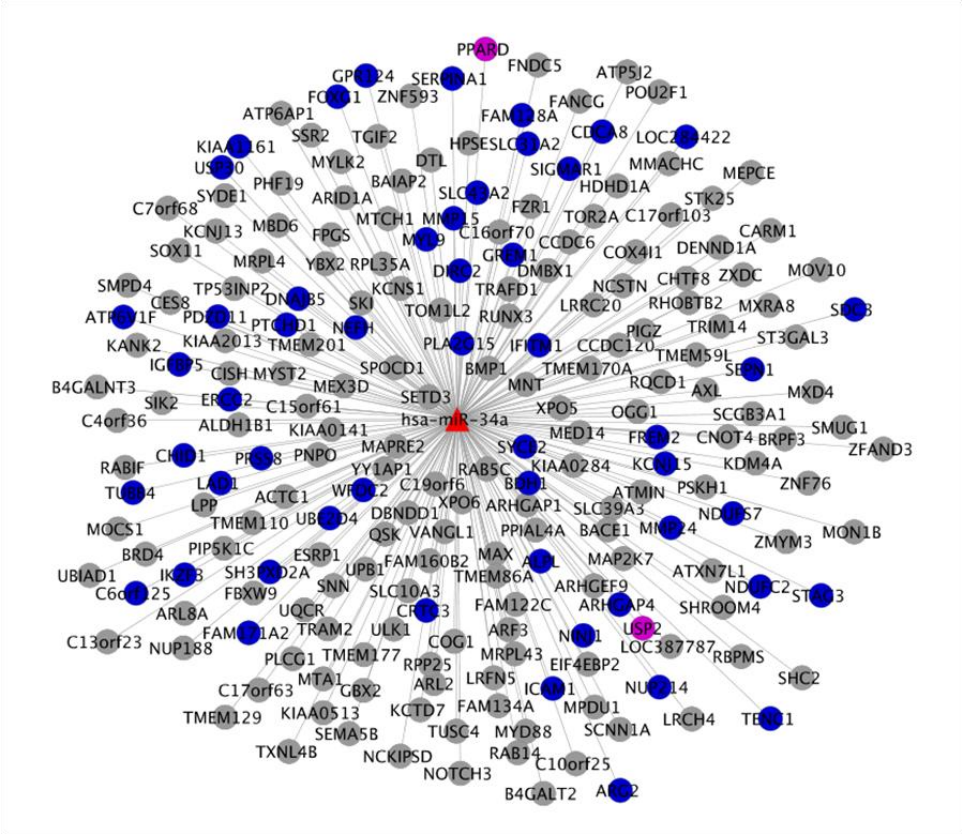

Figure 20. Example of a miRNA-gene regulatory network in Caki-1 vs HK-2 comparison (visualization by Cytoscape). hsa-miR-34a, that is up-regulated (red triangle), and its supported target genes (down-regulated genes in blue and other non differentially expressed targets in grey) are reported. DEGs validated by qPCR are in violet (USP2 and PPARD).

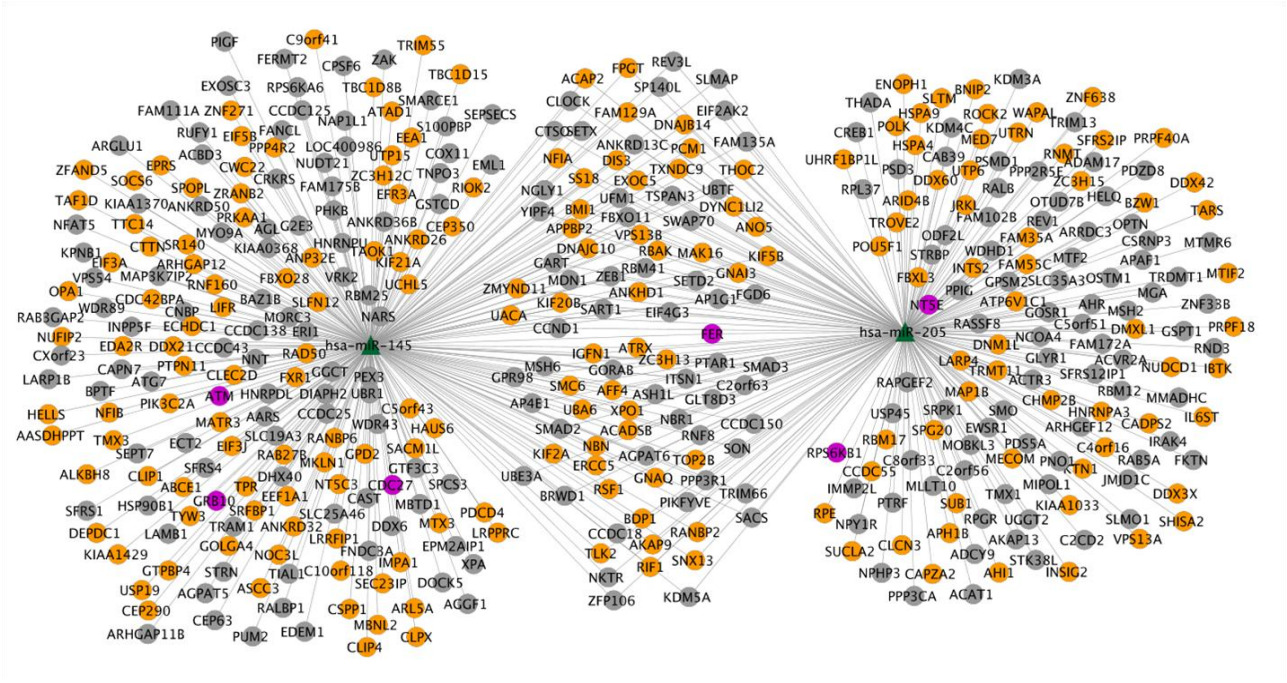

Figure 21. A miRNA-gene regulatory network in Caki-1 vs HK-2 comparison (visualization by Cytoscape). hsa-miR-145 and hsa-miR-205, that are down-regulated (green triangles), and their supported target genes (up-regulated genes in orange and other non differentially expressed targets in grey) are reported. DEGs validated by qPCR are in violet (ATM, CDC27, FER, GRB10, NT5E and RPS6KB1).

5.2.2 qPCR validation of selected target genes

To verify the anti-correlation among miRNAs and their target genes, we selected 8 genes that were predicted targets of the 3 DEMs, belonging to big common networks, and that were already associated to cancer-related pathways. Using bionformatics analysis we selected target genes involved in the following pathways: cell cycle (*CDC27*), leukocyte extravasation signaling *(FER*), *VHL*-HIF pathway *(GRB10*), metabolic pathways (*NT5E*), pathways in cancer (*ATM*, *PPARD*), mTOR, angiogenesis *(RPS6KB1*) and protein ubiquitination pathway (*USP2*). The following genes: *ATM*, *CDC27*, *FER* and *GRB10* were predicted targets of hsa-miR-145; *FER*, *NT5E* and *RPS6KB1* were predicted targets of hsa-miR-205 (*FER* was found in common with hsa-miR-145); and, finally, *PPARD* and *USP2* were predicted targets of hsa-miR-34a. By our results obtained by qPCR (**Table 6**), we confirmed that hsa-miR-34a was up-regulated, while hsa-miR-145 and hsa-miR-205 were down-regulated in the three comparisons. In regards to target genes, we confirmed by qPCR the up-regulation of *ATM*, *CDC27*, *FER*, *GRB10*, *NT5E* and *RPS6KB1*, and the down-regulation of *PPARD* and *USP2* in all the three comparisons (**Table 9**). In Caki-1 vs HK-2 comparison, we observed a significative down-regulation of *PPARD* gene by qPCR, while microarray analysis did not return a significant differential expression.

GENE	Caki-1		Caki-2		A498	
	qPCR	*array*	*qPCR*	*array*	*qPCR*	*array*
ATM	285,32	3,05	353,76	3,42	761,80	3,23
CDC27	140,43	1,90	120,66	1,98	365,07	2,05
FER	71,44	3,08	37,21	2,45	223,07	2,84
GRB10	12,13	2,17	14,91	2,41	45,27	2,56
NT5E	30,00	3,20	30,59	2,85	81,42	2,81
RPS6KB1	126,63	2,97	59,62	2,36	31,45	2,23
PPARD	-3,23	n.s.	-4,95	-1,74	-4,87	-1,89
USP2	-8,50	-2,07	-10,18	-2,54	-7,25	-2,29

Table 9. Quantitative real-time PCR validation of gene microarray analysis in RCC cell lines compared to HK-2. Expression values are expressed in fold change both for qPCR and array results for each comparison. Down-regulated genes are in green and up-regulated genes in red.

5.3 Discussion

Elucidating tissue-specific miRNA functions, going beyond miRNA target prediction and expression correlation, has become one of the major challenges in miRNA research. miRNAs contribute to the RCC development at different levels and it's evident that miRNAs can target various altered signaling pathways related to RCC pathogenesis (Redova *et al.*, 2011). Integrated analysis may have an important role in characterizing a tumor caused by its molecular complexity, that manifests itself at multiple levels (i.e. genomic, transcriptomic and proteomic) (Shen *et al.*, 2009). Presently, the number of studies that combine gene and miRNA expression profiles has been constantly increasing, thanks to the development of high-throughput technologies, next-generation sequencing and several bioinformatics tools.

In this study we performed an integrated analysis in order to combine gene and miRNA expression profiles using MAGIA (Sales *et al.*, 2010) and to reconstruct miRNA-gene post-transcriptional regulatory networks, under the assumption that, since miRNAs tend to down-regulate their targets, expression profiles of miRNAs and real targets are expected to be anti-correlated (Sales *et al.*, 2010). In particular, we focused our attention on three wide common networks, involving DEMs and more than 100 predicted target genes. These networks were composed by modulated miRNAs found in common in the three comparisons, i.e. miR-34, miR-145 and miR-205. These miRNAs have many predicted target genes that were also found differentially expressed in each comparison. For each network, our interest was focused on some supported target genes, their expression levels were also detected by qPCR to validate the anti-correlation between miRNA and gene.

As described above, miR-34a was detected up-regulated in the three comparisons. miR-34a is a potential tumor suppressor involved in many types of cancer, working in a cell type-specific manner. Over-expression of miR-34a leads to apoptosis or cellular senescence, while its reduction attenuates p53-mediated cell death (Dutta *et al.*, 2007). This miRNA is a direct p53 target gene, involved in apoptosis and growth arrest (He *et al.*, 2007a), and recently it has been shown that many tumors, including renal cancer, display CpG methylation of miR-34a (Vogt *et al.*, 2011).

In particular, among supported target genes of miR-34, we emphasize the down-regulation of of *PPARD* and *USP2.*

Peroxisomal proliferators-activated receptor-delta (*PPARD*) has been shown to play a key role in fatty acid utilization and oxidation in both skeletal muscle and adipose tissue (Barish *et al.*, 2006; Muoio *et al.*, 2002). It belongs to a family of nuclear hormone receptors that are bound and activated by fatty acids and/or their derivatives, and they regulate genes that are involved in lipid metabolism, storage, and transport (Muoio *et al.*, 2002). Additionally, PPARs may suppress inflammation through mechanisms involving the release of anti-inflammatory factors or the stabilization of repressive complexes at inflammatory gene promoters. *PPARD* has emerged as a powerful metabolic regulator in diverse tissues including fat, skeletal muscle, kidney, liver and the heart (Barish *et al.*, 2006). In addition, *in vitro* studies showed the involvement of *PPARD* in angiogenesis, proliferation of endothelial and smooth muscle cells (Piqueras *et al.*, 2007; Zhang *et al.*, 2002b). The evidence for a significant role of *PPARD* in humans is less clear. Therefore, since *PPARD* has been associated to lipid metabolism and angiogenesis, it might play an important role in renal

tumorigenesis and in loss of normal renal function, such as lipid metabolism, that exist in cancer (Tun *et al.*, 2010).

USP2 is an ubiquitin-specific protease, that belongs to deubiquitinating enzymes class. Ubiquitylation is a reversible post-translational modification with key roles in various signal transduction cascades and in determining protein stability. *USP2* has been shown to associate with and stabilize fatty acid synthase (FAS), a protein which is often over-expressed in biologically aggressive prostate cancer cells. siRNA knockdown of *USP2* induced apoptosis, which could be reversed by over-expression of FAS (Graner *et al.*, 2004). *USP2* expression has been correlated with tumor progression and worse prognosis in oral squamous cell carcinoma (da Silva *et al.*, 2009). In RCC cell lines used in our study *USP2* was detected down-regulated, thus this gene might induce apoptosis also in renal cancer cells, but further investigations are needed. Recently, it has been reported that *USP2* down-regulation inhibits *TNF-α*-induced *NF-kB* activity and nuclear translocation in different cell lines. Its depletion reduced *NF-kB*-dependent target gene expression and cytokine secretion. Deregulation of *TNF-α* (tumor necrosis factor-α) expression signaling and *NF-kB* (nuclear factor-kappa B) activity are involved in the pathology of many diseases, including cancer, since *TNF-α* is produced in response to inflammation, injury and other environmental changes, while *NF-kB* is a family of central transcription factors that regulate crucial cellular processes (e.g., cell proliferation, apoptosis, immune responses). Thus, the authors suggested *USP2* as a novel regulator of *TNF-α/NF-kB* signaling and tissue homeostasis, with a possible relevance for cancer therapy (Metzig *et al.*, 2011). The role of *USP2* in carcinogenesis remains to be elucitated.

miR-145 was down-regulated in the three RCC cell lines compared to HK-2. Many tumors (e.g. breast, colon, prostate, lung, bladder) show a decreased level of miR-145. Its role in controlling cell proliferation has been suggested, probably due to direct targeting *c-Myc* oncogene. It's probable that it also has a role in cell growth and invasion, so it has been proposed as a tumor suppressor (Sachdeva and Mo, 2010). Gan *et al.* reported the down-regulation of this miRNA and the corresponding up-regulation of some of its target genes in RCC samples, proposing a role of miR-145 in renal tumorigenesis (Gan *et al.*, 2010).
We confirmed by qPCR the up-regulation of the following supported target genes for miR-145: *ATM*, *CDC27*, *FER* and *GRB10*. We chose these genes because of their roles in many pathways such as: cell cycle, apoptosis, p53 signaling, DNA repair, cellular growth and proliferation, cellular assembly and organization, leukocyte extravasation signaling, post-translational modification, molecular transport and carbohydrate metabolism.
The *ATM* (ataxia-telangiectasia mutated) gene is mutated in ataxia-telangiectasia syndrome, which is a rare, autosomal recessive disorder characterized by cerebellar ataxia, neuro-degeneration, radiosensitivity, cell cycle checkpoint defects, genome instability and a predisposition to cancer. The ATM protein is a serine/threonine protein kinase and a member of the phosphoinositide 3-kinase-related protein kinase (PIKK) family, together with ATR (ATM and Rad3 related protein kinase), DNA-PKcs (DNA dependent protein kinase catalytic subunit) and mTOR (mammalian target of rapamycin). All PIKKs are involved in signaling following cellular stress. A number of studies have extensively demonstrated that *ATM* plays a role in cell cycle checkpoints, DNA double-strand breaks (the most cytotoxic lesions caused by ionizing radiation) repair, in chromosomal end-to-end fusion at telomeres in absence of the telomeric protection complex. It has been reported that following induction of DNA damage, or treatment with agents that alter chromatin

structure, *ATM* undergoes an intermolecular auto-phosphorylation on two serine residues, increasing its activity (Derheimer and Kastan, 2010). Also the exposure to hypoxia-induced replication arrest initiates a DNA damage response that includes both ATR- and ATM-mediated signaling. It has been shown that most solid tumors, including renal carcinoma, develop in an environment of below optimal oxygen concentration, which is hypoxia, and severe levels of hypoxia (<0,1% O_2) induce a specific hypoxic response implicating the unfolded protein response, cell death and DNA damage response (DDR). During DDR, signals, such as a double strand break, are detected by a group of proteins, including ATM. During hypoxia, ATM increases its auto-phosphorylation and phosphorylates Chk2 (cell cycle checkpoint kinase 2). Even though hypoxia doesn't lead to an accumulation of DNA damage, reoxygenation induces DNA damage at significant levels through the action of ROS (reactive oxygen species). Thus, the result of this damage is the ATM-Chk2-mediated G_2 arrest in order to allow repair (Olcina *et al.*, 2010). Therefore, it has been suggested that the repression of genes involved in DNA repair, such as *ATM*, may have an important role in increasing genomic instability in tumor cells, contributing to the aggressiveness of hypoxic tumors (Bristow and Hill, 2008). The involvement of *ATM* in many cell signaling processes, in cancer and especially in hypoxia could be very interesting in RCC field and in our RCC cell lines that showed a different level of HIF-1α protein, that has been shown to be involved in causing cell cycle arrest following moderate hypoxia by inhibition of *c-Myc* (Gordan *et al.*, 2007a).

CDC27 (cell division cycle 27 homolog) is a core subunit of the anaphase-promoting complex (APC), that is a ubiquitin ligase that initiates anaphase and mitotic exit. It has been reported that activation of APC is involved in the *TGF-β* signaling pathway (Wan and Kirschner, 2001a). *TGF-β* is an inhibitory growth factor for a variety of epithelial cells and loss of *TGF-β* growth inhibition is a hallmark for many types of human tumors. Zhang *et al.* demonstrated that the phosphorylation of *CDC27* serves as an important mechanism in activation of APC at a different level. Phosphorylated *CDC27* destroys SnoN, a proto-oncoprotein, repressor of transcription that is rapidly degraded upon stimulation by *TGF-β* in an ubiquitin-dependent manner, since over-expression of SnoN in *TGF-β* responsive cells blocks *TGF-β*-induced cell growth. On the other hand, *CDC27*, destroying SnoN, allows the transcription of genes necessary for growth inhibition. The authors suggested that it's likely that casein kinase II (CKII) is the responsive kinase that activates APC via phosphorylation of *CDC27* (Zhang *et al.*, 2011c). Moreover, multiple phosphorylation sites on *CDC27* have been suggested to be important in mitosis for its regulation (Kraft *et al.*, 2003). Thus, the alteration of *CDC27* expression level might affect the *TGF-β* signaling and the cell growth arrest in a variety of epithelial cells, as well as, in many types of human tumors.

FER (Fes-related protein) encodes a tyrosine kinase that is activated by cell-surface receptors, such as *EGFR* and *PDGFR*. Activated *FER* associates with and activates cellular protein containing SH2 domains. Recently, Guo and Stark reported that *FER* is on a pathway through which *EGF* activates *NF-kB* and that over-expression of *FER* activates *NF-kB*, conferring resistance to the *NF-kB* inhibitor quinacrine (Guo and Stark, 2011). The activation of *NF-kB* is important in tumors, since it induces the expression of *NF-kB*-dependent genes whose products inhibit apoptosis, promoting proliferation, inflammation and invasion (Baldwin, 1996). The exact function of *FER* is still unknown. Growth factors such as *EGF* and *PDGF* triggering signal transduction by their receptors activate *FER* which then interacts with proteins such as cortactin and p120Cas, implicated in the reorganization of the actin cytoskeleton (Kim and Wong, 1995,

1998). *FER* has also been implicated in the regulation of cell-cell and cell-matrix interactions that are mediated by adherens junctions and focal adhesions (Greer, 2002). *FER* is expressed ubiquitously in a variety of tissues and cells and is expressed at a high level in numerous malignant cell lines (Allard *et al.*, 2000a). According to literature, RCC cell lines showed a higher level of *FER* than in normal cells.

GRB10 encodes for a member of a super family of adapter proteins. This protein contains several interaction motifs. In fact, it has been reported that Grb10 protein interacts with tyrosine kinase receptors such as *PDGF* and *EGF*. Anyway, its function as an adapter molecule remains to be discovered. Peraldi *et al.* showed that Grb10 protein is a tyrosine phosphorylated in response to *VEGF*. Thus, *VEGF* increases the expression level of *GRB10*, and in turn Grb10 increases *KDR* (kinase insert domain containing receptor) molecules. *KDR* together with Flt-1 (Fms like tyrosine kinase) are two specific tyrosine kinase receptors expressed only on endothelial cells, that are activated by *VEGF*, that is involved in endothelial cell proliferation, angiogenesis. They suggested that Grb10 is involved in a positive feed-back loop in *VEGF* signaling, during neovascularization (Giorgetti-Peraldi *et al.*, 2001). Grb10 protein has been involved in the regulation of ligand-induced ubiquitination, internalization, and stability of the *IGF-IR* (insulin-like growth factor receptor) (Morrione, 2003).

The hub of the third big common network was miR-205, which was detected down-regulated in the three comparisons. miR-205 has been suggested as an important tumor suppressor miRNA in renal cancer, since it may be involved in cell proliferation, apoptosis, colony formation, migration and invasion in renal cancer cells (Majid *et al.*, 2011).

The down-regulation of miR-205 in RCC playing a role in inhibition of Src-mediated oncogenic pathways has been reported (Majid *et al.*, 2011). Furthermore, this miRNA may also have a role in epithelial to mesenchymal transition (Gregory *et al.*, 2008a; Tellez *et al.*, 2011). Among its predicted target genes, we chose to validate the following genes: *FER* (target gene in common with miR-145, as described above), *NT5E* and *RPS6KB1*. By qPCR, we confirmed the up-regulation of these supported target genes.

NT5E is implicated in cell cycle and nucleic acid metabolism; while *RPS6KB1* is involved in cell cycle, cellular growth and proliferation, cell signaling (e.g., mTOR signaling, PI3K/Akt signaling).

NT5E (ecto-5′-nucleotidase, also called *CD73*) encodes for a glycosyl-phosphatidylinositol (GPI)-linked, membrane protein found on the surface of a variety of cell types. It's thought to function as a co-signaling molecule on T lymphocytes, and as an adhesion molecule that is important for lymphocyte binding to endothelium. Recently, NT5E protein has been implicated in a variety of physiologic responses, e.g. epithelial ion and fluid transport, ischemic preconditioning, tissue injury, platelet function, hypoxia, and vascular leak (Colgan *et al.*, 2006; Sitkovsky *et al.*, 2008; Zhang, 2010b). A study reported that *NT5E* participates in cell-cell and cell-matrix interactions (Spychala, 2000). According to literature, we detected the up-regulation of *NT5E*, in fact, it's widely expressed in many cancer cell lines and is up-regulated in tumor tissues. Its over-expression has been associated with tumor neovascularization, invasiveness, and metastasis (Spychala, 2000). This up-regulation in cancerous tissues is accompanied by its high enzymatic activity, which can mediate the production of extracellular adenosine (Jin *et al.*, 2010), that impairs cellular antitumor immune responses at multiple levels, including T-cell activation, clonal expansion of tumor-specific T cells with helper and cytolytic effector function, tumor cell killing. Since the role of *NT5E* in tumor immune

escape via generation of adenosine, it has been suggested that targeted *NT5E* therapy is an important alternative approach to the effective control of tumor growth (Jin *et al.*, 2010; Zhang, 2010b).

RPS6KB1 (ribosomal protein S6 kinase) belongs to a family of proteins involved in numerous pathways, many of which are central to the carcinogenic process, such as regulation of cell growth, insulin and inflammation. *RPS6KB1* is a mitogen-activated protein kinase (MAPK) that regulates cell growth given its activation by growth factors such as *PDGF*, *EGF* and insulin through regulation by mTOR. *RPS6KB1* is a downstream effector of mTORC1 pathway in regulating cell growth by modulating many processes, including protein synthesis, ribosome biogenesis and autophagy. mTORC1 directly phosphorylates and activates *RPS6KB1*, which is an important regulator of cell size. *RPS6KB1* promotes protein synthesis and represses the phosphatidylinositol 3-kinase (PI3K)–Akt pathway by inhibiting *IRS1* (insulin receptor substrate 1) and *IRS2* expression (Sabatini, 2006). As mentioned in the introduction of this thesis, mTOR and PI3K-Akt signaling are relevant pathways that have been associated with RCC pathology (Tun *et al.*, 2010). *RPS6KB1* has been identified as a potential oncogene, since it is amplified in 8-10% of breast tumors and over-expressed in the majority of tumors with amplification (Sinclair *et al.*, 2003). *RPS6KB1* has three known functions: (1) protein synthesis by inducing selective translation of mRNAs that encode components of the translation apparatus and are essential for cell growth and proliferation (Dufner and Thomas, 1999); (2) cell cycle control by up-regulating cyclin D3, resulting in phosphorylation of pRb and E2F1 dependent entry of the cell into S phase (Feng *et al.*, 2000c); (3) cell migration by association with the Rac1 and Cdc42 GTPases that are involved in regulation of actin polymerization and cell migration (Lambert *et al.*, 2002).

By integrated analysis between miRNA and mRNA expression profiles in the three RCC cell lines compared to HK-2, we found interesting miRNA-gene regulatory networks. We focused our interest on relationships that exist within three wide common networks, composed by three miRNAs (one up-regulated and two down-regulated miRNAs) and their relative target genes that were already known to be associated with cancer and renal carcinoma by literature. In particular, by qPCR, we confirmed the expression levels of both these miRNAs and some of their supported target genes, thus, reporting their anti-correlation. However, to assess if a gene is a real target of a miRNA, thus, demonstrating their anti-correlation, functional validations are needed. We suggest that miRNA-target genes pairs such as miR-145 and its targets *ATM* and *GRB10*, miR-205 and *RPS6KB1*, miR-34a and *USP2*, could be of interest for functionally validation and further investigations in the RCC field.

6 CONCLUSIONS AND FUTURE PROSPECTS

In this PhD thesis, we described a comprehensive and integrated analysis between gene and miRNA expression profiles in three RCC cell lines compared to a normal renal tubular epithelial cell line.

Using Affymetrix high-density microarray technology, we performed whole-genome gene and miRNA expression analyses, thus identifying genes and miRNAs involved in functional processes and biological pathways associated with RCC biology. In agreement with already published data, we found many modulated genes and miRNAs known to be associated with RCC malignant progression. Additionally, we provided findings about novel genes and miRNAs potentially associated to clear cell RCC pathology. We found that the integration of gene and miRNA expression profiles allowed the identification of genes affected by miRNA post-transriptional regulation and their corresponding alterations, which could be of interest for RCC development and progression. Our results confirmed that immortalized RCC cell lines can be used as *in vitro* model for RCC pathology, since they showed gene and miRNA expression patterns resembling those of renal tumor tissues, thus maintaining the typical RCC signature. On the other hand, by comparing our results to already published data, we observed some discordances about some gene and miRNA modulations. Indeed, it should be noted that, whereas a cancerous tissue is characterized for being heterogeneous and composed by different cell populations, a tumor cell line is mostly enriched in tumoral component but it might accumulate different genomic alterations during *in vitro* culturing, thus explaining different results among distinct studies. Therefore, our study underlined that in order to carry out a functional analysis on specific pathways and miRNA-gene networks relevant for ccRCC pathology, the suitable number of RCC cell lines to be included should be properly evaluated.

In conclusion, we suggested that the integration of gene and miRNA expression profiles could help the identification of novel and complex functional relations between the whole transcriptome and miRNome that are potentially involved in renal carcinoma. Thus, the integration of various genomics data favours a deeper comprehension of RCC biology and the identification of functional processes and regulatory networks crucially important for tumorigenesis. This may represent a valuable resource to discover novel candidate biomarkers useful for diagnostic and prognostic clinical applications or for the development of novel targeted therapies.

Starting from the results here presented, we will plan further investigations addressing the functional validation of some miRNA-gene relationships using RNA interference approach on RCC cell lines. Alternatively, ccRCC primary cell cultures, could be used, since they are an optimal *in vitro* tumor model of RCC retaining the typical molecular features of parental RCC tissues and providing a greater cell homogeneity. Moreover, we are planning to study the role of these miRNA-gene networks in ccRCC etiopathogenesis and outcome using a clinical collection of well-characterized ccRCC tissue samples and taking into consideration their clinical phenotype and follow-up.

7 BIBLIOGRAPHY

Abe, Hideyuki, et al. "Possible role of the RhoC/ROCK pathway in progression of clear cell renal cell carcinoma." *Biomed Res* 29, no. 3 (2008): 155-161.

Albelda, S. M. "Role of integrins and other cell adhesion molecules in tumor progression and metastasis." *Lab Invest* 68, no. 1 (1993): 4-17.

Allard, P., et al. "Links between Fer tyrosine kinase expression levels and prostate cell proliferation." *Mol Cell Endocrinol* 159, no. 1-2 (2000a): 63-77.

Ambros, Victor. "MicroRNA pathways in flies and worms: growth, death, fat, stress, and timing." *Cell* 113, no. 6 (2003a): 673-676.

Ambros, Victor. "The functions of animal microRNAs." *Nature* 431, no. 7006 (2004): 350-355.

Ambros, Victor, and Rosalind C Lee. "Identification of microRNAs and other tiny noncoding RNAs by cDNA cloning." *Methods Mol Biol* 265 (2004a): 131-158.

Ambros, Victor, et al. "A uniform system for microRNA annotation." *RNA* 9, no. 3 (2003d): 277-279.

Ambros, Victor, Rosalind C Lee, Ann Lavanway, Peter T Williams, and David Jewell. "MicroRNAs and other tiny endogenous RNAs in C. elegans." *Curr Biol* 13, no. 10 (2003c): 807-818.

Anand, Sudarshan, and David A Cheresh. "MicroRNA-mediated regulation of the angiogenic switch." *Curr Opin Hematol* 18, no. 3 (2011): 171-176.

Baldewijns, Marcella M, Iris J H, Peter B Vermeulen, Patricia M M, Manon van Engeland, and Adriaan P de. "VHL and HIF signalling in renal cell carcinogenesis." *J Pathol* 221, no. 2 (2010): 125-138.

Baldwin, A. S. "The NF-kappa B and I kappa B proteins: new discoveries and insights." *Annu Rev Immunol* 14 (1996): 649-683.

Banks, Rosamonde E, et al. "Genetic and epigenetic analysis of von Hippel-Lindau (VHL) gene alterations and relationship with clinical variables in sporadic renal cancer." *Cancer Res* 66, no. 4 (2006): 2000-2011.

Banumathy, Gowrishankar, and Paul Cairns. "Signaling pathways in renal cell carcinoma." *Cancer Biol Ther* 10, no. 7 (2010): 658-664.

Barish, Grant D, Vihang A Narkar, and Ronald M Evans. "PPAR delta: a dagger in the heart of the metabolic syndrome." *J Clin Invest* 116, no. 3 (2006): 590-597.

Barker, Nick, and Hans Clevers. "Mining the Wnt pathway for cancer therapeutics." *Nat Rev Drug Discov* 5, no. 12 (2006): 997-1014.

Bartel, David P. "MicroRNAs: genomics, biogenesis, mechanism, and function." *Cell* 116, no. 2 (2004f): 281-297.

Bartels, Claudine L, and Gregory J Tsongalis. "MicroRNAs: novel biomarkers for human cancer." *Clin Chem* 55, no. 4 (2009a): 623-631.

Baskerville, Scott, and David P Bartel. "Microarray profiling of microRNAs reveals frequent coexpression with neighboring miRNAs and host genes." *RNA* 11, no. 3 (2005): 241-247.

Bentwich, Isaac, et al. "Identification of hundreds of conserved and non-conserved human microRNAs." *Nat Genet* 37, no. 7 (2005a): 766-770.

Beroukhim, Rameen, et al. "Patterns of gene expression and copy number alterations in von Hippel-Lindau disease-associated and sporadic clear cell carcinoma of the kidney." *Cancer Res* 69, no. 11 (2009): 4674-4681.

Bicciato, Silvio, et al. "A computational procedure to identify significant overlap of differentially expressed and genomic imbalanced regions in cancer datasets." *Nucleic Acids Res* 37, no. 15 (2009): 5057-5070.

Biswas, Swethajit, and Tim Eisen. "Immunotherapeutic strategies in kidney cancer when TKIs are not enough." *Nat Rev Clin Oncol* 6, no. 8 (2009b): 478-487.

Blower, Paul E, et al. "MicroRNA expression profiles for the NCI-60 cancer cell panel." *Mol Cancer Ther* 6, no. 5 (2007): 1483-1491.

Boer, J. M., et al. "Identification and classification of differentially expressed genes in renal cell carcinoma by expression profiling on a global human 31,500-element cDNA array." *Genome Res* 11, no. 11 (2001): 1861-1870.

Brannon, A. Rose, et al. "Meta-analysis of Clear Cell Renal Cell Carcinoma Gene Expression Defines a Variant Subgroup and Identifies Gender Influences on Tumor Biology." *Eur Urol*, 2011.

Brannon, A. Rose, et al. "Molecular Stratification of Clear Cell Renal Cell Carcinoma by Consensus Clustering Reveals Distinct Subtypes and Survival Patterns." *Genes Cancer* 1, no. 2 (2010): 152-163.

Brennecke, Julius, Alexander Stark, Robert B Russell, and Stephen M Cohen. "Principles of microRNA-target recognition." *PLoS Biol* 3, no. 3 (2005a): e85.

Brenner, Bruce M, and Daniel Rosenberg. "High-throughput SNP/CGH approaches for the analysis of genomic instability in colorectal cancer." *Mutat Res* 693, no. 1-2 (2010): 46-52.

Bristow, Robert G, and Richard P Hill. "Hypoxia and metabolism. Hypoxia, DNA repair and genetic instability." *Nat Rev Cancer* 8, no. 3 (2008): 180-192.

Cai, Xuezhong, Curt H Hagedorn, and Bryan R Cullen. "Human microRNAs are processed from capped, polyadenylated transcripts that can also function as mRNAs." *RNA* 10, no. 12 (2004): 1957-1966.

Calin, George A, and Carlo M Croce. "MicroRNA signatures in human cancers." *Nat Rev Cancer* 6, no. 11 (2006): 857-866.

Calin, George Adrian, et al. "A MicroRNA signature associated with prognosis and progression in chronic lymphocytic leukemia." *N Engl J Med* 353, no. 17 (2005): 1793-1801.

Calin, George Adrian, et al. "Frequent deletions and down-regulation of microRNA genes miR-15 and miR-16 at 13q14 in chronic lymphocytic leukemia." *Proc Natl Acad Sci U S A* 99, no. 24 (2002): 15524-15529.

Calin, George Adrian, et al. "Human microRNA genes are frequently located at fragile sites and genomic regions involved in cancers." *Proc Natl Acad Sci U S A* 101, no. 9 (2004b): 2999-3004.

Calin, George Adrian, et al. "MicroRNA profiling reveals distinct signatures in B cell chronic lymphocytic leukemias." *Proc Natl Acad Sci U S A* 101, no. 32 (2004): 11755-11760.

Chan, Jennifer A, Anna M Krichevsky, and Kenneth S Kosik. "MicroRNA-21 is an antiapoptotic factor in human glioblastoma cells." *Cancer Res* 65, no. 14 (2005): 6029-6033.

Chin, Lynda, William C Hahn, Gad Getz, and Matthew Meyerson. "Making sense of cancer genomic data." *Genes Dev* 25, no. 6 (2011): 534-555.

Choueiri, Toni K, et al. "von Hippel-Lindau gene status and response to vascular endothelial growth factor targeted therapy for metastatic clear cell renal cell carcinoma." *J Urol* 180, no. 3 (2008): 860--5; discussion 865-6.

Chow, Tsz-Fung F, et al. "Differential expression profiling of microRNAs and their potential involvement in renal cell carcinoma pathogenesis." *Clin Biochem* 43, no. 1-2 (2010): 150-158.

Chow, W. H., G. Gridley, J. F. Fraumeni, and B. Järvholm. "Obesity, hypertension, and the risk of kidney cancer in men." *N Engl J Med* 343, no. 18 (2000): 1305-1311.

Chow, Wong-Ho, Linda M Dong, and Susan S Devesa. "Epidemiology and risk factors for kidney cancer." *Nat Rev Urol* 7, no. 5 (2010a): 245-257.

Cifola, Ingrid, et al. "Genome-wide screening of copy number alterations and LOH events in renal cell carcinomas and integration with gene expression profile." *Mol Cancer* 7 (2008): 6.

Cimmino, Amelia, et al. "miR-15 and miR-16 induce apoptosis by targeting BCL2." *Proc Natl Acad Sci U S A* 102, no. 39 (2005): 13944-13949.

Cohen, A. J., et al. "Hereditary renal-cell carcinoma associated with a chromosomal translocation." *N Engl J Med* 301, no. 11 (1979d): 592-595.

Cohen, Herbert T, and Francis J McGovern. "Renal-cell carcinoma." *N Engl J Med* 353, no. 23 (2005a): 2477-2490.

Colgan, Sean P, Holger K Eltzschig, Tobias Eckle, and Linda F Thompson. "Physiological roles for ecto-5'-nucleotidase (CD73)." *Purinergic Signal* 2, no. 2 (2006): 351-360.

Cordes, Kimberly R, et al. "miR-145 and miR-143 regulate smooth muscle cell fate and plasticity." *Nature* 460, no. 7256 (2009): 705-710.

Cowey, C. Lance, and W. Kimryn Rathmell. "VHL gene mutations in renal cell carcinoma: role as a biomarker of disease outcome and drug efficacy." *Curr Oncol Rep* 11, no. 2 (2009): 94-101.

Cullen, Bryan R. "Transcription and processing of human microRNA precursors." *Mol Cell* 16, no. 6 (2004): 861-865.

da Silva, Sabrina Daniela, et al. "Clinicopathological significance of ubiquitin-specific protease 2a (USP2a), fatty acid synthase (FASN), and ErbB2 expression in oral squamous cell carcinomas." *Oral Oncol* 45, no. 10 (2009): e134--e139.

Dahinden, Corinne, et al. "Mining tissue microarray data to uncover combinations of biomarker expression patterns that improve intermediate staging and grading of clear cell renal cell cancer." *Clin Cancer Res* 16, no. 1 (2010b): 88-98.

Dalgliesh, Gillian L, et al. "Systematic sequencing of renal carcinoma reveals inactivation of histone modifying genes." *Nature* 463, no. 7279 (2010): 360-363.

Derheimer, Frederick A, and Michael B Kastan. "Multiple roles of ATM in monitoring and maintaining DNA integrity." *FEBS Lett* 584, no. 17 (2010): 3675-3681.

Doench, John G, Christian P Petersen, and Phillip A Sharp. "siRNAs can function as miRNAs." *Genes Dev* 17, no. 4 (2003): 438-442.

Du, Liqin, et al. "miR-93, miR-98, and miR-197 regulate expression of tumor suppressor gene FUS1." *Mol Cancer Res* 7, no. 8 (2009): 1234-1243.

Dufner, A., and G. Thomas. "Ribosomal S6 kinase signaling and the control of translation." *Exp Cell Res* 253, no. 1 (1999): 100-109.

Dulaimi, Essel, et al. "Promoter hypermethylation profile of kidney cancer." *Clin Cancer Res* 10, no. 12 Pt 1 (2004): 3972-3979.

Duns, Gerben, et al. "Histone methyltransferase gene SETD2 is a novel tumor suppressor gene in clear cell renal cell carcinoma." *Cancer Res* 70, no. 11 (2010): 4287-4291.

Dutta, Khokon Kumar, et al. "Association of microRNA-34a overexpression with proliferation is cell type-dependent." *Cancer Sci* 98, no. 12 (2007): 1845-1852.

Elkan-Miller, Tal, et al. "Integration of transcriptomics, proteomics, and microRNA analyses reveals novel microRNA regulation of targets in the mammalian inner ear." *PLoS One* 6, no. 4 (2011): e18195.

Enerly, Espen, et al. "miRNA-mRNA integrated analysis reveals roles for miRNAs in primary breast tumors." *PLoS One* 6, no. 2 (2011): e16915.

Enright, Anton J, Bino John, Ulrike Gaul, Thomas Tuschl, Chris Sander, and Debora S Marks. "MicroRNA targets in Drosophila." *Genome Biol* 5, no. 1 (2003): R1.

Erler, Janine T, and Amato J Giaccia. "Lysyl oxidase mediates hypoxic control of metastasis." *Cancer Res* 66, no. 21 (2006): 10238-10241.

Esch, F., et al. "Purification of a multipotent antideath activity from bovine liver and its identification as arginase: nitric oxide-independent inhibition of neuronal apoptosis." *J Neurosci* 18, no. 11 (1998): 4083-4095.

Esquela-Kerscher, Aurora, and Frank J Slack. "Oncomirs - microRNAs with a role in cancer." *Nat Rev Cancer* 6, no. 4 (2006): 259-269.

Estévez, Alvaro G, Mary Anne Sahawneh, Philipp S Lange, Narae Bae, Mariela Egea, and Rajiv R Ratan. "Arginase 1 regulation of nitric oxide production is key to survival of trophic factor-deprived motor neurons." *J Neurosci* 26, no. 33 (2006): 8512-8516.

Feng, L. X., N. Ravindranath, and M. Dym. "Stem cell factor/c-kit up-regulates cyclin D3 and promotes cell cycle progression via the phosphoinositide 3-kinase/p70 S6 kinase pathway in spermatogonia." *J Biol Chem* 275, no. 33 (2000c): 25572-25576.

Ferlay, J., D. M. Parkin, and E. Steliarova-Foucher. "Estimates of cancer incidence and mortality in Europe in 2008." *Eur J Cancer* 46, no. 4 (2010b): 765-781.

Finley, David S, Allan J Pantuck, and Arie S Belldegrun. "Tumor biology and prognostic factors in renal cell carcinoma." *Oncologist* 16 Suppl 2 (2011): 4-13.

Frew, Ian J, and Wilhelm Krek. "Multitasking by pVHL in tumour suppression." *Curr Opin Cell Biol* 19, no. 6 (2007): 685-690.

Fridman, Eddie, et al. "Accurate molecular classification of renal tumors using microRNA expression." *J Mol Diagn* 12, no. 5 (2010a): 687-696.

Fuhrman, S. A., L. C. Lasky, and C. Limas. "Prognostic significance of morphologic parameters in renal cell carcinoma." *Am J Surg Pathol* 6, no. 7 (1982): 655-663.

Furge, Kyle A, et al. "Detection of DNA copy number changes and oncogenic signaling abnormalities from gene expression data reveals MYC activation in high-grade papillary renal cell carcinoma." *Cancer Res* 67, no. 7 (2007): 3171-3176.

Gan, Boyi, et al. "FoxOs enforce a progression checkpoint to constrain mTORC1-activated renal tumorigenesis." *Cancer Cell* 18, no. 5 (2010): 472-484.

Gaur, Arti, et al. "Characterization of microRNA expression levels and their biological correlates in human cancer cell lines." *Cancer Res* 67, no. 6 (2007): 2456-2468.

Gentleman, Robert C, et al. "Bioconductor: open software development for computational biology and bioinformatics." *Genome Biol* 5, no. 10 (2004): R80.

Giampuzzi, Monia, Roberta Oleggini, Chris Albanese, Richard Pestell, and Armando Di Donato. "beta-catenin signaling and regulation of cyclin D1 promoter in NRK-49F cells transformed by down-regulation of the tumor suppressor lysyl oxidase." *Biochim Biophys Acta* 1745, no. 3 (2005): 370-381.

Gieseg, Michael A, Theresa Cody, Michael Z Man, Steven J Madore, Mark A Rubin, and Eric P Kaldjian. "Expression profiling of human renal carcinomas with functional taxonomic analysis." *BMC Bioinformatics* 3 (2002): 26.

Giorgetti-Peraldi, S., J. Murdaca, J. C. Mas, and E. Van Obberghen. "The adapter protein, Grb10, is a positive regulator of vascular endothelial growth factor signaling." *Oncogene* 20, no. 30 (2001): 3959-3968.

Godinot, Catherine, Elodie de Laplanche, Eric Hervouet, and Hélène Simonnet. "Actuality of Warburg's views in our understanding of renal cancer metabolism." *J Bioenerg Biomembr* 39, no. 3 (2007): 235-241.

Gordan, John D, Craig B Thompson, and M. Celeste Simon. "HIF and c-Myc: sibling rivals for control of cancer cell metabolism and proliferation." *Cancer Cell* 12, no. 2 (2007a): 108-113.

Gordan, John D, et al. "HIF-alpha effects on c-Myc distinguish two subtypes of sporadic VHL-deficient clear cell renal carcinoma." *Cancer Cell* 14, no. 6 (2008): 435-446.

Gordan, John D, Jessica A Bertout, Cheng-Jun Hu, J. Alan Diehl, e M. Celeste Simon. «HIF-2alpha promotes hypoxic cell proliferation by enhancing c-Myc transcriptional activity.» *Cancer Cell* 11, n. 4 (2007): 335-347.

Gotoh, T., and M. Mori. "Arginase II downregulates nitric oxide (NO) production and prevents NO-mediated apoptosis in murine macrophage-derived RAW 264.7 cells." *J Cell Biol* 144, no. 3 (1999): 427-434.

Gotoh, T., T. Sonoki, A. Nagasaki, K. Terada, M. Takiguchi, and M. Mori. "Molecular cloning of cDNA for nonhepatic mitochondrial arginase (arginase II) and comparison of its induction with nitric oxide synthase in a murine macrophage-like cell line." *FEBS Lett* 395, no. 2-3 (1996): 119-122.

Gottardo, Fedra, et al. "MicroRNA profiling in kidney and bladder cancers." *Urol Oncol* 25, no. 5 (2007): 387-392.

Graner, Edgard, et al. "The isopeptidase USP2a regulates the stability of fatty acid synthase in prostate cancer." *Cancer Cell* 5, no. 3 (2004): 253-261.

Greer, Peter. "Closing in on the biological functions of Fps/Fes and Fer." *Nat Rev Mol Cell Biol* 3, no. 4 (2002): 278-289.

Gregory, Philip A, Cameron P Bracken, Andrew G Bert, and Gregory J Goodall. "MicroRNAs as regulators of epithelial-mesenchymal transition." *Cell Cycle* 7, no. 20 (2008): 3112-3118.

Gregory, Philip A, et al. "The miR-200 family and miR-205 regulate epithelial to mesenchymal transition by targeting ZEB1 and SIP1." *Nat Cell Biol* 10, no. 5 (2008a): 593-601.

Griffiths-Jones, Sam. "miRBase: microRNA sequences and annotation." *Curr Protoc Bioinformatics* Chapter 12 (2010): Unit 12.9.1-Unit 12.910.

Griffiths-Jones, Sam. "The microRNA Registry." *Nucleic Acids Res* 32, no. Database issue (2004): D109-D111.

Griffiths-Jones, Sam, Harpreet Kaur Saini, Stijn van Dongen, and Anton J Enright. "miRBase: tools for microRNA genomics." *Nucleic Acids Res* 36, no. Database issue (2008): D154--D158.

Grosshans, Helge, Ted Johnson, Kristy L Reinert, Mark Gerstein, and Frank J Slack. "The temporal patterning microRNA let-7 regulates several transcription factors at the larval to adult transition in *C. elegans*." *Dev Cell* 8, no. 3 (2005): 321-330.

Guinan, P., et al. "TNM staging of renal cell carcinoma: Workgroup No. 3. Union International Contre le Cancer (UICC) and the American Joint Committee on Cancer (AJCC)." *Cancer* 80, no. 5 (1997): 992-993.

Guo, Canhui, and George R Stark. "FER tyrosine kinase (FER) overexpression mediates resistance to quinacrine through EGF-dependent activation of NF-kappaB." *Proc Natl Acad Sci U S A* 108, no. 19 (2011): 7968-7973.

Ha, Eunyoung, Ji-Hye Bang, Jung N Son, Ho-Chan Cho, and Kyo-Chul Mun. "Carbamylated albumin stimulates microRNA-146, which is increased in human renal cell carcinoma." *Mol Med Report* 3, no. 2 (2010): 275-279.

Hansel, D. E. «Genetic alterations and histopathologic findings in familial renal cell carcinoma.» *Histol Histopathol* 21, n. 4 (2006): 437-444.

Havelange, Violaine, et al. "Functional implications of microRNAs in acute myeloid leukemia by integrating microRNA and messenger RNA expression profiling." *Cancer*, 2011a.

He, Lin, et al. "A microRNA polycistron as a potential human oncogene." *Nature* 435, no. 7043 (2005a): 828-833.

He, Xingyue, Lin He, and Gregory J Hannon. "The guardian's little helper: microRNAs in the p53 tumor suppressor network." *Cancer Res* 67, no. 23 (2007a): 11099-11101.

Heinzelmann, Joana, et al. "Specific miRNA signatures are associated with metastasis and poor prognosis in clear cell renal cell carcinoma." *World J Urol* 29, no. 3 (2011): 367-373.

Higgins, T, J, P, et al. "Gene expression patterns in renal cell carcinoma assessed by complementary DNA microarray." *Am J Pathol* 162, no. 3 (2003b): 925-932.

Huang, Da Wei, Brad T Sherman, and Richard A Lempicki. "Bioinformatics enrichment tools: paths toward the comprehensive functional analysis of large gene lists." *Nucleic Acids Res* 37, no. 1 (2009): 1-13.

Huang, Jim C, et al. "Using expression profiling data to identify human microRNA targets." *Nat Methods* 4, no. 12 (2007): 1045-1049.

Huang, Xin, et al. "Hypoxia-inducible miR-210 regulates normoxic gene expression involved in tumor initiation." *Mol Cell* 35, no. 6 (2009b): 856-867.

Huang, Xin, Quynh-Thu Le, and Amato J Giaccia. "MiR-210-micromanager of the hypoxia pathway." *Trends Mol Med* 16, no. 5 (2010): 230-237.

Huang, Y., et al. "Microarray analysis of microRNA expression in renal clear cell carcinoma." *Eur J Surg Oncol* 35, no. 10 (2009j): 1119-1123.

Hunt, Jay D, Olga L van, Garnett P McMillan, Paolo Boffetta, and Paul Brennan. "Renal cell carcinoma in relation to cigarette smoking: meta-analysis of 24 studies." *Int J Cancer* 114, no. 1 (2005b): 101-108.

Hyman, Elizabeth, et al. "Impact of DNA amplification on gene expression patterns in breast cancer." *Cancer Res* 62, no. 21 (2002): 6240-6245.

Imamura, F., M. Mukai, M. Ayaki, and H. Akedo. "Y-27632, an inhibitor of rho-associated protein kinase, suppresses tumor cell invasion via regulation of focal adhesion and focal adhesion kinase." *Jpn J Cancer Res* 91, no. 8 (2000): 811-816.

Inoki, Ken, et al. "TSC2 integrates Wnt and energy signals via a coordinated phosphorylation by AMPK and GSK3 to regulate cell growth." *Cell* 126, no. 5 (2006): 955-968.

Iorio, Marilena V, et al. "MicroRNA gene expression deregulation in human breast cancer." *Cancer Res* 65, no. 16 (2005): 7065-7070.

Ioshikhes, Ilya, Sashwati Roy, and Chandan K Sen. "Algorithms for mapping of mRNA targets for microRNA." *DNA Cell Biol* 26, no. 4 (2007): 265-272.

Irizarry, Rafael A, et al. "Exploration, normalization, and summaries of high density oligonucleotide array probe level data." *Biostatistics* 4, no. 2 (2003): 249-264.

Iwai, K., et al. "Identification of the von Hippel-Lindau tumor suppressor protein as part of an active E3 ubiquitin ligase complex." *Proc Natl Acad Sci U S A* 96, no. 22 (1999): 12436-12441.

Jansen, A., S. Lewis, V. Cattell, and H. T. Cook. "Arginase is a major pathway of L-arginine metabolism in nephritic glomeruli." *Kidney Int* 42, no. 5 (1992): 1107-1112.

Jeffers, M., et al. "Activating mutations for the met tyrosine kinase receptor in human cancer." *Proc Natl Acad Sci U S A* 94, no. 21 (1997): 11445-11450.

Jin, Dachuan, et al. "CD73 on tumor cells impairs antitumor T-cell responses: a novel mechanism of tumor-induced immune suppression." *Cancer Res* 70, no. 6 (2010): 2245-2255.

John, Bino, Anton J Enright, Alexei Aravin, Thomas Tuschl, Chris Sander, and Debora S Marks. "Human MicroRNA targets." *PLoS Biol* 2, no. 11 (2004): e363.

Jones, Jon, et al. "Gene signatures of progression and metastasis in renal cell cancer." *Clin Cancer Res* 11, no. 16 (2005c): 5730-5739.

Juan, David, et al. "Identification of a microRNA panel for clear cell kidney cancer." *Urology* 75, no. 4 (2010): 835-841.

Juengel, E., et al. "Alterations of the gene expression profile in renal cell carcinoma after treatment with the histone deacetylase-inhibitor valproic acid and interferon-alpha." *World J Urol* 29, no. 6 (2011): 779-786.

Jung, Monika, et al. "MicroRNA profiling of clear cell renal cell cancer identifies a robust signature to define renal malignancy." *J Cell Mol Med* 13, no. 9B (2009): 3918-3928.

Jung, Monika, et al. "Robust microRNA stability in degraded RNA preparations from human tissue and cell samples." *Clin Chem* 56, no. 6 (2010): 998-1006.

Kabat, G. C., S. A Navarro, A. B. Miller, e T. E. Rohan. «A cohort study of reproductive and hormonal factors and renal cell cancer risk in women.» *Br J Cancer* 96, n. 5 (2007): 845-849.

Karube, Yoko, et al. "Reduced expression of Dicer associated with poor prognosis in lung cancer patients." *Cancer Sci* 96, no. 2 (2005): 111-115.

Kashyap, M. K., et al. "Biochemical and molecular markers in renal cell carcinoma: an update and future prospects." *Biomarkers* 10, no. 4 (2005): 258-294.

Kelsh, Michael A, Dominik D Alexander, Pamela J Mink, and Jeffrey H Mandel. "Occupational trichloroethylene exposure and kidney cancer: a meta-analysis." *Epidemiology* 21, no. 1 (2010): 95-102.

Kertesz, Michael, Nicola Iovino, Ulrich Unnerstall, Ulrike Gaul, and Eran Segal. "The role of site accessibility in microRNA target recognition." *Nat Genet* 39, no. 10 (2007): 1278-1284.

Khvorova, Anastasia, Angela Reynolds, and Sumedha D Jayasena. "Functional siRNAs and miRNAs exhibit strand bias." *Cell* 115, no. 2 (2003): 209-216.

Kim, L., and T. W. Wong. "Growth factor-dependent phosphorylation of the actin-binding protein cortactin is mediated by the cytoplasmic tyrosine kinase FER." *J Biol Chem* 273, no. 36 (1998): 23542-23548.

Kim, L., and T. W. Wong. "The cytoplasmic tyrosine kinase FER is associated with the catenin-like substrate pp120 and is activated by growth factors." *Mol Cell Biol* 15, no. 8 (1995): 4553-4561.

Kim, Taewan, et al. "p53 regulates epithelial mesenchymal transition through microRNAs targeting ZEB1 and ZEB2." *J Exp Med* 208, no. 5 (2011a): 875-883.

Kim, V. Narry. "MicroRNA biogenesis: coordinated cropping and dicing." *Nat Rev Mol Cell Biol* 6, no. 5 (2005): 376-385.

Kiriakidou, Marianthi, et al. "A combined computational-experimental approach predicts human microRNA targets." *Genes Dev* 18, no. 10 (2004): 1165-1178.

Kirschmann, Dawn A, et al. "A molecular role for lysyl oxidase in breast cancer invasion." *Cancer Res* 62, no. 15 (2002): 4478-4483.

Kitano, Kentaro, et al. "CpG island methylation of microRNAs is associated with tumor size and recurrence of non-small-cell lung cancer." *Cancer Sci* 102, no. 12 (2011): 2126-2131.

Kluger, Harriet M, et al. "Classification of renal cell carcinoma based on expression of VEGF and VEGF receptors in both tumor cells and endothelial cells." *Lab Invest* 88, no. 9 (2008): 962-972.

Kosari, Farhad, et al. "Clear cell renal cell carcinoma: gene expression analyses identify a potential signature for tumor aggressiveness." *Clin Cancer Res* 11, no. 14 (2005): 5128-5139.

Kovacs, G. «Molecular cytogenetics of renal cell tumors.» *Adv Cancer Res* 62 (1993c): 89-124.

Kraft, Claudine, et al. "Mitotic regulation of the human anaphase-promoting complex by phosphorylation." *EMBO J* 22, no. 24 (2003): 6598-6609.

Krek, Azra, et al. "Combinatorial microRNA target predictions." *Nat Genet* 37, no. 5 (2005): 495-500.

Krishnamachary, Balaji, et al. "Hypoxia-inducible factor-1-dependent repression of E-cadherin in von Hippel-Lindau tumor suppressor-null renal cell carcinoma mediated by TCF3, ZFHX1A, and ZFHX1B." *Cancer Res* 66, no. 5 (2006): 2725-2731.

Kulshreshtha, Ritu, et al. "A microRNA signature of hypoxia." *Mol Cell Biol* 27, no. 5 (2007a): 1859-1867.

Lagos-Quintana, M., R. Rauhut, W. Lendeckel, and T. Tuschl. "Identification of novel genes coding for small expressed RNAs." *Science* 294, no. 5543 (2001): 853-858.

Lai, Eric C. "microRNAs: runts of the genome assert themselves." *Curr Biol* 13, no. 23 (2003): R925--R936.

Lambert, John M, Antoine E Karnoub, Lee M Graves, Sharon L Campbell, and Channing J Der. "Role of MLK3-mediated activation of p70 S6 kinase in Rac1 transformation." *J Biol Chem* 277, no. 7 (2002): 4770-4777.

Landgraf, Pablo, et al. "A mammalian microRNA expression atlas based on small RNA library sequencing." *Cell* 129, no. 7 (2007a): 1401-1414.

Latif, F., et al. "Identification of the von Hippel-Lindau disease tumor suppressor gene." *Science* 260, no. 5112 (1993b): 1317-1320.

Lau, N. C., L. P. Lim, E. G. Weinstein, and D. P. Bartel. "An abundant class of tiny RNAs with probable regulatory roles in Caenorhabditis elegans." *Science* 294, no. 5543 (2001): 858-862.

Le Beau, M. M., R. S. Lemons, R. Espinosa, R. A. Larson, N. Arai, and J. D. Rowley. "Interleukin-4 and interleukin-5 map to human chromosome 5 in a region encoding growth factors and receptors and are deleted in myeloid leukemias with a del(5q)." *Blood* 73, no. 3 (1989): 647-650.

Lee, Inhan, et al. "New class of microRNA targets containing simultaneous 5'-UTR and 3'-UTR interaction sites." *Genome Res* 19, no. 7 (2009): 1175-1183.

Lee, R. C., R. L. Feinbaum, and V. Ambros. "The *C. elegans* heterochronic gene lin-4 encodes small RNAs with antisense complementarity to lin-14." *Cell* 75, no. 5 (1993): 843-854.

Lee, Yoontae, et al. "MicroRNA genes are transcribed by RNA polymerase II." *EMBO J* 23, no. 20 (2004): 4051-4060.

Levi, Fabio, et al. «The changing pattern of kidney cancer incidence and mortality in Europe.» *BJU Int* 101, n. 8 (2008h): 949-958.

Lewis, Benjamin P, Christopher B Burge, and David P Bartel. "Conserved seed pairing, often flanked by adenosines, indicates that thousands of human genes are microRNA targets." *Cell* 120, no. 1 (2005a): 15-20.

Lewis, Benjamin P, I hung Shih, Matthew W Jones-Rhoades, David P Bartel, and Christopher B Burge. "Prediction of mammalian microRNA targets." *Cell* 115, no. 7 (2003): 787-798.

Li, C., and W. Hung Wong. "Model-based analysis of oligonucleotide arrays: model validation, design issues and standard error application." *Genome Biol* 2, no. 8 (2001): RESEARCH0032.

Li, Jordan Yz, Tuck Y Yong, Michael Z Michael, and Jonathan M Gleadle. "Review: The role of microRNAs in kidney disease." *Nephrology (Carlton)* 15, no. 6 (2010a): 599-608.

Li, Wei, and Kangcheng Ruan. "MicroRNA detection by microarray." *Anal Bioanal Chem* 394, no. 4 (2009d): 1117-1124.

Lim, Lee P, et al. "Microarray analysis shows that some microRNAs downregulate large numbers of target mRNAs." *Nature* 433, no. 7027 (2005): 769-773.

Lim, Lee P, et al. "The microRNAs of *Caenorhabditis elegans*." *Genes Dev* 17, no. 8 (2003): 991-1008.

Lin, Ken-Yu, et al. "Ectopic expression of vascular cell adhesion molecule-1 as a new mechanism for tumor immune evasion." *Cancer Res* 67, no. 4 (2007): 1832-1841.

Lin, Ming, Lee-Jen Wei, William R Sellers, Marshall Lieberfarb, Wing Hung Wong, and Cheng Li. "dChipSNP: significance curve and clustering of SNP-array-based loss-of-heterozygosity data." *Bioinformatics* 20, no. 8 (2004): 1233-1240.

Linehan, W. Marston, Jeffrey S Rubin, and Donald P Bottaro. "VHL loss of function and its impact on oncogenic signaling networks in clear cell renal cell carcinoma." *Int J Biochem Cell Biol* 41, no. 4 (2009a): 753-756.

Linehan, W. Marston, Ramaprasad Srinivasan, and Laura S Schmidt. "The genetic basis of kidney cancer: a metabolic disease." *Nat Rev Urol* 7, no. 5 (2010): 277-285.

Lionetti, Marta, et al. "Identification of microRNA expression patterns and definition of a microRNA/mRNA regulatory network in distinct molecular groups of multiple myeloma." *Blood* 114, no. 25 (2009): e20--e26.

Liou, Louis S, et al. "Microarray gene expression profiling and analysis in renal cell carcinoma." *BMC Urol* 4 (2004): 9.

Liu, Chang-Gong, et al. "An oligonucleotide microchip for genome-wide microRNA profiling in human and mouse tissues." *Proc Natl Acad Sci U S A* 101, no. 26 (2004): 9740-9744.

Liu, Huiqing, et al. "Identifying mRNA targets of microRNA dysregulated in cancer: with application to clear cell Renal Cell Carcinoma." *BMC Syst Biol* 4 (2010a): 51.

Liu, Wennuan, et al. "Comprehensive assessment of DNA copy number alterations in human prostate cancers using Affymetrix 100K SNP mapping array." *Genes Chromosomes Cancer* 45, no. 11 (2006): 1018-1032.

Liu, Wennuan, et al. "Homozygous deletions and recurrent amplifications implicate new genes involved in prostate cancer." *Neoplasia* 10, no. 8 (2008): 897-907.

Liu, Xiqiang, et al. "Deregulation of manganese superoxide dismutase (SOD2) expression and lymph node metastasis in tongue squamous cell carcinoma." *BMC Cancer* 10 (2010b): 365.

Liu, Yu-Huei, Chang-Yueh Lin, Wei-Chou Lin, Sai-Wen Tang, Ming-Kuen Lai, and Jung-Yaw Lin. "Up-regulation of vascular endothelial growth factor-D expression in clear cell renal cell carcinoma by CD74: a critical role in cancer cell tumorigenesis." *J Immunol* 181, no. 9 (2008a): 6584-6594.

Ljungberg, Börje, et al. «The epidemiology of renal cell carcinoma.» *Eur Urol* 60, n. 4 (2011): 615-621.

Lu, Jun, et al. "MicroRNA expression profiles classify human cancers." *Nature* 435, no. 7043 (2005c): 834-838.

Lu, Ming, et al. "An analysis of human microRNA and disease associations." *PLoS One* 3, no. 10 (2008): e3420.

Maher, E. R., and W. G. Kaelin. "von Hippel-Lindau disease." *Medicine (Baltimore)* 76, no. 6 (1997): 381-391.

Majid, Shahana, et al. "MicroRNA-205 inhibits Src-mediated oncogenic pathways in renal cancer." *Cancer Res* 71, no. 7 (2011): 2611-2621.

Matsuda, Daisuke, et al. "Identification of copy number alterations and its association with pathological features in clear cell and papillary RCC." *Cancer Lett*, 2008.

Mejean, Arnaud, et al. "Prognostic factors for the survival of patients with papillary renal cell carcinoma: meaning of histological typing and multifocality." *J Urol* 170, no. 3 (2003a): 764-767.

Meloni-Ehrig, Aurelia M. "Renal cancer: cytogenetic and molecular genetic aspects." *Am J Med Genet* 115, no. 3 (2002): 164-172.

Mestdagh, Pieter, et al. "The microRNA body map: dissecting microRNA function through integrative genomics." *Nucleic Acids Res* 39, no. 20 (2011): e136.

Metzig, Marie, et al. "An RNAi screen identifies USP2 as a factor required for TNF-α-induced NF-kB signaling." *Int J Cancer* 129, no. 3 (2011): 607-618.

Michael, Michael Z, Susan M O', Nicholas G van, Graeme P Young, and Robert J James. "Reduced accumulation of specific microRNAs in colorectal neoplasia." *Mol Cancer Res* 1, no. 12 (2003): 882-891.

Min, Hyeyoung, and Sungroh Yoon. "Got target? Computational methods for microRNA target prediction and their extension." *Exp Mol Med* 42, no. 4 (2010a): 233-244.

Miyanaka, K., et al. "Immunohistochemical localization of arginase II and other enzymes of arginine metabolism in rat kidney and liver." *Histochem J* 30, no. 10 (1998): 741-751.

Morrione, Andrea. "Grb10 adapter protein as regulator of insulin-like growth factor receptor signaling." *J Cell Physiol* 197, no. 3 (2003): 307-311.

Motzer, Robert J, and Ana M Molina. "Targeting renal cell carcinoma." *J Clin Oncol* 27, no. 20 (2009b): 3274-3276.

Mourelatos, Zissimos, et al. "miRNPs: a novel class of ribonucleoproteins containing numerous microRNAs." *Genes Dev* 16, no. 6 (2002): 720-728.

Muoio, Deborah M, et al. "Peroxisome proliferator-activated receptor-alpha regulates fatty acid utilization in primary human skeletal muscle cells." *Diabetes* 51, no. 4 (2002): 901-909.

Nakada, C., et al. "Genome-wide microRNA expression profiling in renal cell carcinoma: significant down-regulation of miR-141 and miR-200c." *J Pathol* 216, no. 4 (2008): 418-427.

Nakada, Chisato, et al. "Overexpression of miR-210, a downstream target of HIF-1α, causes centrosome amplification in renal carcinoma cells." *J Pathol* 224, no. 2 (2011): 280-288.

Neal, Calida S, Michael Z Michael, Lesley H Rawlings, Mark B Van, and Jonathan M Gleadle. "The VHL-dependent regulation of microRNAs in renal cancer." *BMC Med* 8 (2010): 64.

Nishizuka, Satoshi, et al. "Proteomic profiling of the NCI-60 cancer cell lines using new high-density reverse-phase lysate microarrays." *Proc Natl Acad Sci U S A* 100, no. 24 (2003): 14229-14234.

Noon, Aidan P, et al. "Combined p53 and MDM2 biomarker analysis shows a unique pattern of expression associated with poor prognosis in patients with renal cell carcinoma undergoing radical nephrectomy." *BJU Int*, 2011.

Noon, Aidan P, et al. "p53 and MDM2 in renal cell carcinoma: biomarkers for disease progression and future therapeutic targets?" *Cancer* 116, no. 4 (2010): 780-790.

Nouh, A, Mohammed A, et al. «Renal cell carcinoma in patients with end-stage renal disease: relationship between histological type and duration of dialysis.» *BJU Int* 105, n. 5 (2010): 620-627.

Nunez-Iglesias, Juan, Chun-Chi Liu, Todd E Morgan, Caleb E Finch, and Xianghong Jasmine Zhou. "Joint genome-wide profiling of miRNA and mRNA expression in Alzheimer's disease cortex reveals altered miRNA regulation." *PLoS One* 5, no. 2 (2010): e8898.

Nymark, Penny, et al. "Integrative analysis of microRNA, mRNA and aCGH data reveals asbestos- and histology-related changes in lung cancer." *Genes Chromosomes Cancer* 50, no. 8 (2011): 585-597.

Olcina, Monica, Philip S Lecane, and Ester M Hammond. "Targeting hypoxic cells through the DNA damage response." *Clin Cancer Res* 16, no. 23 (2010): 5624-5629.

Park, Sun-Mi, Arti B Gaur, Ernst Lengyel, and Marcus E Peter. "The miR-200 family determines the epithelial phenotype of cancer cells by targeting the E-cadherin repressors ZEB1 and ZEB2." *Genes Dev* 22, no. 7 (2008): 894-907.

Parker, Alexander S, James R Cerhan, Carol A Janney, Charles F Lynch, and Kenneth P Cantor. "Smoking cessation and renal cell carcinoma." *Ann Epidemiol* 13, no. 4 (2003a): 245-251.

Perego, RA, Bianchi C, Corizzato M, Eroini B, Torsello B, Valsecchi C,Di Fonzio A, Cordani N, Favini P, Ferrero S, Pitto M, Sarto C, Magni F, Rocco F and Mocarelli P. "Primary cell cultures arising from normal kidney and renal cell carcinoma retain the proteomic profile of corresponding tissues. " *J Prot Res* 4, (2005):1503–1510.

Perske, Christina, Nitza Lahat, Sharon Sheffy Levin, Haim Bitterman, Bernhard Hemmerlein, and Michal Amit Rahat. "Loss of inducible nitric oxide synthase expression in the mouse renal cell carcinoma cell line RENCA is mediated by microRNA miR-146a." *Am J Pathol* 177, no. 4 (2010): 2046-2054.

Petillo, David, Eric J Kort, John Anema, Kyle A Furge, Ximing J Yang, and Bin Tean Teh. "MicroRNA profiling of human kidney cancer subtypes." *Int J Oncol* 35, no. 1 (2009): 109-114.

Piqueras, Laura, et al. "Activation of PPARbeta/delta induces endothelial cell proliferation and angiogenesis." *Arterioscler Thromb Vasc Biol* 27, no. 1 (2007): 63-69.

Powers, Martin P, Karla Alvarez, Hyun-Jung Kim, and Federico A Monzon. "Molecular classification of adult renal epithelial neoplasms using microRNA expression and virtual karyotyping." *Diagn Mol Pathol* 20, no. 2 (2011): 63-70.

Rajewsky, Nikolaus. "microRNA target predictions in animals." *Nat Genet* 38 Suppl (2006a): S8--13.

Redova, Martina, Marek Svoboda, and Ondrej Slaby. "MicroRNAs and their target gene networks in renal cell carcinoma." *Biochem Biophys Res Commun* 405, no. 2 (2011): 153-156.

Renehan, Andrew G, Margaret Tyson, Matthias Egger, Richard F Heller, and Marcel Zwahlen. "Body-mass index and incidence of cancer: a systematic review and meta-analysis of prospective observational studies." *Lancet* 371, no. 9612 (2008): 569-578.

Ribal, Maria J. "Molecular profiling of renal cancer: the journey to clinical application." *Eur Urol* 59, no. 5 (2011): 731-733.

Richards, F. M. "Molecular pathology of von Hippel-Lindau disease and the VHL tumour suppressor gene." *Expert Rev Mol Med* 2001 (2001): 1-27.

Rodriguez, Antony, Sam Griffiths-Jones, Jennifer L Ashurst, and Allan Bradley. "Identification of mammalian microRNA host genes and transcription units." *Genome Res* 14, no. 10A (2004): 1902-1910.

Roschke, Anna V, et al. "Karyotypic complexity of the NCI-60 drug-screening panel." *Cancer Res* 63, no. 24 (2003): 8634-8647.

Ryan, M. J., G. Johnson, J. Kirk, S. M. Fuerstenberg, R. A. Zager, and B. Torok-Storb. "HK-2: an immortalized proximal tubule epithelial cell line from normal adult human kidney." *Kidney Int* 45, no. 1 (1994): 48-57.

Sabatini, David M. "mTOR and cancer: insights into a complex relationship." *Nat Rev Cancer* 6, no. 9 (2006): 729-734.

Sachdeva, Mohit, and Yin-Yuan Mo. "miR-145-mediated suppression of cell growth, invasion and metastasis." *Am J Transl Res* 2, no. 2 (2010): 170-180.

Sales, Gabriele, Alessandro Coppe, Andrea Bisognin, Marta Biasiolo, Stefania Bortoluzzi, and Chiara Romualdi. "MAGIA, a web-based tool for miRNA and Genes Integrated Analysis." *Nucleic Acids Res* 38 Suppl (2010): W352--W359.

Sarver, Aaron L, Lihua Li, and Subbaya Subramanian. "MicroRNA miR-183 functions as an oncogene by targeting the transcription factor EGR1 and promoting tumor cell migration." *Cancer Res* 70, no. 23 (2010): 9570-9580.

Sato, Fumiaki, Soken Tsuchiya, Kazuya Terasawa, and Gozoh Tsujimoto. "Intra-platform repeatability and inter-platform comparability of microRNA microarray technology." *PLoS One* 4, no. 5 (2009): e5540.

Schmidt, L., et al. "Germline and somatic mutations in the tyrosine kinase domain of the MET proto-oncogene in papillary renal carcinomas." *Nat Genet* 16, no. 1 (1997): 68-73.

Schraml, P., et al. "CDKNA2A mutation analysis, protein expression, and deletion mapping of chromosome 9p in conventional clear-cell renal carcinomas: evidence for a second tumor suppressor gene proximal to CDKN2A." *Am J Pathol* 158, no. 2 (2001): 593-601.

Schuetz, Audrey N, et al. "Molecular classification of renal tumors by gene expression profiling." *J Mol Diagn* 7, no. 2 (2005): 206-218.

Semenza, G. L. "Defining the role of hypoxia-inducible factor 1 in cancer biology and therapeutics." *Oncogene* 29, no. 5 (2010a): 625-634.

Shen, Ronglai, Adam B Olshen, and Marc Ladanyi. "Integrative clustering of multiple genomic data types using a joint latent variable model with application to breast and lung cancer subtype analysis." *Bioinformatics* 25, no. 22 (2009): 2906-2912.

Shioi, Ko ichi, et al. "Vascular cell adhesion molecule 1 predicts cancer-free survival in clear cell renal carcinoma patients." *Clin Cancer Res* 12, no. 24 (2006): 7339-7346.

Silva, Elisabete, and Patrício Soares da Silva. "Reactive oxygen species and the regulation of renal Na+-K+-ATPase in opossum kidney cells." *Am J Physiol Regul Integr Comp Physiol* 293, no. 4 (2007): R1764--R1770.

Simão, Sónia, et al. "Age-related changes in renal expression of oxidant and antioxidant enzymes and oxidative stress markers in male SHR and WKY rats." *Exp Gerontol* 46, no. 6 (2011): 468-474.

Sinclair, Colleen S, Matthew Rowley, Ali Naderi, and Fergus J Couch. "The 17q23 amplicon and breast cancer." *Breast Cancer Res Treat* 78, no. 3 (2003): 313-322.

Sitkovsky, Michail V, Jorgen Kjaergaard, Dmitriy Lukashev, and Akio Ohta. "Hypoxia-adenosinergic immunosuppression: tumor protection by T regulatory cells and cancerous tissue hypoxia." *Clin Cancer Res* 14, no. 19 (2008): 5947-5952.

Skubitz, Keith M, and Amy P N. "Differential gene expression in renal-cell cancer." *J Lab Clin Med* 140, no. 1 (2002): 52-64.

Skubitz, Keith M, Wolfgang Zimmermann, Wolfgang Zimmerman, Robert Kammerer, Stefan Pambuccian, and Amy P N. "Differential gene expression identifies subgroups of renal cell carcinoma." *J Lab Clin Med* 147, no. 5 (2006): 250-267.

Smalheiser, Neil R. "EST analyses predict the existence of a population of chimeric microRNA precursor-mRNA transcripts expressed in normal human and mouse tissues." *Genome Biol* 4, no. 7 (2003): 403.

Smith, T. F., and M. S. Waterman. "Identification of common molecular subsequences." *J Mol Biol* 147, no. 1 (1981a): 195-197.

Søkilde, Rolf, et al. "Global microRNA analysis of the NCI-60 cancer cell panel." *Mol Cancer Ther* 10, no. 3 (2011): 375-384.

Spychala, J. "Tumor-promoting functions of adenosine." *Pharmacol Ther* 87, no. 2-3 (2000): 161-173.

Stark, Alexander, Julius Brennecke, Robert B Russell, and Stephen M Cohen. "Identification of Drosophila MicroRNA targets." *PLoS Biol* 1, no. 3 (2003): E60.

Stassar, M. J., et al. "Identification of human renal cell carcinoma associated genes by suppression subtractive hybridization." *Br J Cancer* 85, no. 9 (2001): 1372-1382.

Stillebroer, Alexander B, Peter F A, Otto C Boerman, Wim J G, and Egbert Oosterwijk. "Carbonic anhydrase IX in renal cell carcinoma: implications for prognosis, diagnosis, and therapy." *Eur Urol* 58, no. 1 (2010): 75-83.

Sturgeon, Catharine M, et al. "National Academy of Clinical Biochemistry Laboratory Medicine Practice Guidelines for use of tumor markers in clinical practice: quality requirements." *Clin Chem* 54, no. 8 (2008a): e1-e10.

Su, Ren-Wei, et al. "The integrative analysis of microRNA and mRNA expression in mouse uterus under delayed implantation and activation." *PLoS One* 5, no. 11 (2010): e15513.

Su, Wan-Lin, Robert R Kleinhanz, and Eric E Schadt. "Characterizing the role of miRNAs within gene regulatory networks using integrative genomics techniques." *Mol Syst Biol* 7 (2011): 490.

Sültmann, Holger, et al. "Gene expression in kidney cancer is associated with cytogenetic abnormalities, metastasis formation, and patient survival." *Clin Cancer Res* 11, no. 2 Pt 1 (2005): 646-655.

't Hoen, C, P, A, et al. "Deep sequencing-based expression analysis shows major advances in robustness, resolution and inter-lab portability over five microarray platforms." *Nucleic Acids Res* 36, no. 21 (2008): e141.

Takahashi, M., et al. "Gene expression profiling of clear cell renal cell carcinoma: gene identification and prognostic classification." *Proc Natl Acad Sci U S A* 98, no. 17 (2001g): 9754-9759.

Takahashi, Masayuki, et al. "Molecular subclassification of kidney tumors and the discovery of new diagnostic markers." *Oncogene* 22, no. 43 (2003): 6810-6818.

Takamizawa, Junichi, et al. "Reduced expression of the let-7 microRNAs in human lung cancers in association with shortened postoperative survival." *Cancer Res* 64, no. 11 (2004): 3753-3756.

Tanabe, K., et al. "Molecular regulation of intercellular adhesion molecule 1 (ICAM-1) expression in renal cell carcinoma." *Urol Res* 25, no. 4 (1997a): 231-238.

Team, R Core Development. "R: A Language and Environment for Statistical Computing." 2009.

Tellez, Carmen S, et al. "EMT and stem cell-like properties associated with miR-205 and miR-200 epigenetic silencing are early manifestations during carcinogen-induced transformation of human lung epithelial cells." *Cancer Res* 71, no. 8 (2011): 3087-3097.

Thoenes, W., S. Störkel, and H. J. Rumpelt. "Histopathology and classification of renal cell tumors (adenomas, oncocytomas and carcinomas). The basic cytological and histopathological elements and their use for diagnostics." *Pathol Res Pract* 181, no. 2 (1986): 125-143.

Tsuruta, Tomohiko, et al. "miR-152 is a tumor suppressor microRNA that is silenced by DNA hypermethylation in endometrial cancer." *Cancer Res* 71, no. 20 (2011): 6450-6462.

Tun, Han W, et al. "Pathway signature and cellular differentiation in clear cell renal cell carcinoma." *PLoS One* 5, no. 5 (2010): e10696.

Urbich, Carmen, Angelika Kuehbacher, and Stefanie Dimmeler. "Role of microRNAs in vascular diseases, inflammation, and angiogenesis." *Cardiovasc Res* 79, no. 4 (2008): 581-588.

van Vlodrop, H, I, J, et al. "Prognostic significance of Gremlin1 (GREM1) promoter CpG island hypermethylation in clear cell renal cell carcinoma." *Am J Pathol* 176, no. 2 (2010): 575-584.

Varela, Ignacio, et al. "Exome sequencing identifies frequent mutation of the SWI/SNF complex gene PBRM1 in renal carcinoma." *Nature* 469, no. 7331 (2011): 539-542.

Vasselli, James R, et al. "Predicting survival in patients with metastatic kidney cancer by gene-expression profiling in the primary tumor." *Proc Natl Acad Sci U S A* 100, no. 12 (2003): 6958-6963.

Velickovic, Marija, Brett Delahunt, Bryan McIver, and Stefan K G. "Intragenic PTEN/MMAC1 loss of heterozygosity in conventional (clear cell) renal cell carcinoma is associated with poor patient prognosis." *Mod Pathol* 15, no. 5 (2002): 479-485.

Vogt, Markus, et al. "Frequent concomitant inactivation of miR-34a and miR-34b/c by CpG methylation in colorectal, pancreatic, mammary, ovarian, urothelial, and renal cell carcinomas and soft tissue sarcomas." *Virchows Arch* 458, no. 3 (2011): 313-322.

Volinia, Stefano, et al. "A microRNA expression signature of human solid tumors defines cancer gene targets." *Proc Natl Acad Sci U S A* 103, no. 7 (2006): 2257-2261.

Volinia, Stefano, et al. "Reprogramming of miRNA networks in cancer and leukemia." *Genome Res* 20, no. 5 (2010): 589-599.

Wan, Y., and M. W. Kirschner. "Identification of multiple CDH1 homologues in vertebrates conferring different substrate specificities." *Proc Natl Acad Sci U S A* 98, no. 23 (2001a): 13066-13071.

Wang, Huixia, et al. "Comparative analysis and integrative classification of NCI-60 cell lines and primary tumors using gene expression profiling data." *BMC Genomics* 7 (2006b): 166.

Wendt, Michael K, Tressa M Allington, and William P Schiemann. "Mechanisms of the epithelial-mesenchymal transition by TGF-beta." *Future Oncol* 5, no. 8 (2009): 1145-1168.

Weng, Lihong, et al. "MicroRNA profiling of clear cell renal cell carcinoma by whole-genome small RNA deep sequencing of paired frozen and formalin-fixed, paraffin-embedded tissue specimens." *J Pathol* 222, no. 1 (2010): 41-51.

Whaley, J. M., et al. "Germ-line mutations in the von Hippel-Lindau tumor suppressor gene are similar to somatic von Hippel-Lindau aberrations in sporadic renal cell carcinoma." *Am J Hum Genet* 55, no. 6 (1994): 1092-1102.

White A, N, M, and George M Yousef. "MicroRNAs: exploring a new dimension in the pathogenesis of kidney cancer." *BMC Med* 8 (2010): 65.

White, A, N, M, et al. "miRNA profiling for clear cell renal cell carcinoma: biomarker discovery and identification of potential controls and consequences of miRNA dysregulation." *J Urol* 186, no. 3 (2011b): 1077-1083.

Wullschleger, Stephan, Robbie Loewith, and Michael N Hall. "TOR signaling in growth and metabolism." *Cell* 124, no. 3 (2006): 471-484.

Yao, Masahiro, et al. "A three-gene expression signature model to predict clinical outcome of clear cell renal carcinoma." *Int J Cancer* 123, no. 5 (2008): 1126-1132.

Yi, Zhengjun, Yurong Fu, Shushu Zhao, Xuguang Zhang, and Chuanxiang Ma. "Differential expression of miRNA patterns in renal cell carcinoma and non-tumorous tissues." *J Cancer Res Clin Oncol* 136, no. 6 (2010): 855-862.

Young, A. N., et al. "Expression profiling of renal epithelial neoplasms: a method for tumor classification and discovery of diagnostic molecular markers." *Am J Pathol* 158, no. 5 (2001): 1639-1651.

Youssef, Youssef M, et al. "Accurate molecular classification of kidney cancer subtypes using microRNA signature." *Eur Urol* 59, no. 5 (2011): 721-730.

Zhang, Aimin, Yi Liu, Yizhen Shen, Youhe Xu, and Xiangtie Li. "miR-21 modulates cell apoptosis by targeting multiple genes in renal cell carcinoma." *Urology* 78, no. 2 (2011b): 474.e13--474.e19.

Zhang, Bin. "CD73: a novel target for cancer immunotherapy." *Cancer Res* 70, no. 16 (2010b): 6407-6411.

Zhang, Jifeng, et al. "Peroxisome proliferator-activated receptor delta is up-regulated during vascular lesion formation and promotes post-confluent cell proliferation in vascular smooth muscle cells." *J Biol Chem* 277, no. 13 (2002b): 11505-11512.

Zhang, Liyong, Takeo Fujita, George Wu, Xiao Xiao, and Yong Wan. "Phosphorylation of the anaphase-promoting complex/Cdc27 is involved in TGF-beta signaling." *J Biol Chem* 286, no. 12 (2011c): 10041-10050.

Zhang, Shihua, Qingjiao Li, Juan Liu, and Xianghong Jasmine Zhou. "A novel computational framework for simultaneous integration of multiple types of genomic data to identify microRNA-gene regulatory modules." *Bioinformatics* 27, no. 13 (2011): i401-i409.

Zhang, Zhan, et al. "MicroRNA miR-210 modulates cellular response to hypoxia through the MYC antagonist MNT." *Cell Cycle* 8, no. 17 (2009): 2756-2768.

Zhang, Zhong-Fa, et al. "A comparison study reveals important features of agreement and disagreement between summarized DNA and RNA data obtained from renal cell carcinoma." *Mutat Res* 657, no. 1 (2008): 77-83.

Zhao, Hongjuan, Börje Ljungberg, Kjell Grankvist, Torgny Rasmuson, Robert Tibshirani, and James D Brooks. "Gene expression profiling predicts survival in conventional renal cell carcinoma." *PLoS Med* 3, no. 1 (2006f): e13.

Zhou, Grace X, Joanna Ireland, Patricia Rayman, James Finke, and Ming Zhou. "Quantification of carbonic anhydrase IX expression in serum and tissue of renal cell carcinoma patients using enzyme-linked immunosorbent assay: prognostic and diagnostic potentials." *Urology* 75, no. 2 (2010): 257-261.

Zhou, Liang, et al. "Integrated profiling of microRNAs and mRNAs: microRNAs located on Xq27.3 associate with clear cell renal cell carcinoma." *PLoS One* 5, no. 12 (2010a): e15224.

Zhou, Xiaofeng, Samuel C Mok, Zugen Chen, Yang Li, and David T W. "Concurrent analysis of loss of heterozygosity (LOH) and copy number abnormality (CNA) for oral premalignancy progression using the Affymetrix 10K SNP mapping array." *Hum Genet* 115, no. 4 (2004): 327-330.

8 GLOSSARY OF ABBREVIATIONS

4E-BP1	4E-binding protein 1
aCGH	array-comparative genomic hybridization
Ago	Argonaute
AJCC	American Joint Committee on Cancer
AML	acute myeloid leukemia
ANXA4	annexin A4
APC	adenomatosis polyposis coli protein
ARE	antioxidant response elements
ARG2	Arginase 2
ASK1	apoptosis signal regulating kinase 1
ATCC	American Type Culture Collection
ATM	ataxia-telangiectasia, mutated
ATR	ATM and Rad3 related protein kinase
bFGF	basic fibroblast growth factor
BMPs	bone morphogenetic proteins
BP	biological processes
CAIX	carbonic anhydrase IX
cAlb	carbamylated albumin
CAV1	caveolin-1
CCND1	cyclin D1
ccRCC	clear cell renal cell carcinoma
CDC27	cell division cycle 27 homolog
CDF	custom definition file
CDH1	E-cadherin
CDKN2A	cyclin-dependent kinase inhibitor 2A
Chk2	cell cycle checkpoint kinase 2
chr	chromosome
chRCC	chromofobe renal cell carcinoma
CK1	casein kinase 1
CLL	chronic lymphocytic leukemia
CN	copy number
CNA	copy number alteration
COSMIC	Catalogue Of Somatic Mutations In Cancer
COX-2	cyclooxygenase-2
CXCR	chemochine receptors
DAVID	Database for Annotation, Visualization and Integrated Discovery
DDR	DNA damage response
DEGs	differential expressed genes
DEMs	differentially espresse miRNAs
DNA-PKcs	DNA dependent protein kinase catalytic subunit
ECM	extracellular matrix
EGFR	epidermal growth factor
ELOSA	Enzyme Linked Oligosorbent Assay
EMT	epithelial to mesenchymal transition
ENG	endoglin
EPO	erythropoietin
FAS	fatty acid synthase
FDA	Food and Drug Administration
FER	Fes-related protein
FFPE	formalin-fixed paraffin-embedded
GLUT-1	glucose transporter
GO	Gene Ontology
GREM1	gremlin1
GSK-3β	glycogen synthase kinase 3β
H_2O_2	hydrogen peroxide
HAF	hypoxia-associated factor
HGF	hepatocyte growth factor
HIF	hypoxia-inducible factor
HK-2	human kidney 2
HMDD	Human MicroRNA & Disease Database
HPRC	hereditary papillary renal carcinoma
HRE	hypoxia-response element
HSP90	heat shock protein 90
ICAM-1	intercellular adhesion molecule-1

IFNα	interferon α
IGF	insulin-like growth factor
IL-2	interleukin-2
iNOS	inducible nitric oxide synthase
ITGA	integrin
IVT	*in vitro* transcription
JARID1C	lysine (K)-specific demethylase 5C
LEF-TCF	lymphoid enhancer-binding factor 1-T cell specific transcription factor 7
LMW	low molecular weight
LOH	loss of heterozygosity
LOX	lysyl oxidase
MAGIA	MiRNA and Genes Integrated Analysis
MAPK	miogeno-activated protein kinase
MET	mesenchymal to epithelial transitino
MF	molecular function
miRISC	miRNA-containing RNA-induced silencing complex
miRNA	microRNA
MM	multiple myeloma
MMP	metalloproteinase
mTOR	mammalian target of rapamycin
MUC1	mucin 1
NCI	National Cancer Institute
NF-kB	nuclear factor-kappa B
NO	nitric oxide
NOS	nitric oxide synthase
Nrf2	Nuclear factor-erythroid 2-related factor 2
NT5E	ecto-5′-nucleotidase
PBRM1	polybromo 1
PDGF	platelet-derived growth factor
PDK1	pyruvate dehydrogenase kinase 1
PFKM	6-phosphofructokinase 1
PHDs	prolyl hydroxylases
PID	Pathway Interaction Database
PIP3	phosphatidylinositol-3,4,5-triphosphate
PLGF	placental growth factor
PM	perfect match
PPARD	peroxisomal proliferators-activated receptor-delta
pRCC	papillary renal cell carcinoma
PTEN	phosphatase and tensin homolog
qPCR	quantitative PCR
RACK1	receptor for activated C-kinase 1
RCC	renal cell carcinoma
RIN	RNA Integrity Number
RMA	Robust Multi-array Average
ROCK1	Rho-kinase 1
ROS	reactive oxygen species
RP	Rank Product
RPS6KB1	ribosomal protein S6 kinase
RT	reverse transcription
SCF	VHL skp-cullin-F-box protein
SDF1	stromal cell-derived factor 1
SETD2	SET domain containing 2
SFK	Src family of protein kinases
SOD2	superoxide dismutase 2
TGF-α	transforming growth factor-α
TNF-α	tumor necrosis factor-α
TNM	tumor, node, metastasis
UICC	Union for International Cancer Control
USP2	ubiquitin-specific protease 2
UTR	untranslated region
UTX	lysine (K)-specific demethylase 6A
VCAM1	vascular cell adhesion molecule1
VEGF	vascular epithelial growth factor
VHL	von Hippel-Lindau
VIM	Vimentin
WHO	World Health Organization

9 APPENDIX

Table 1. List of the 154 genes included in the VHL and HIF pathways by PID (Pathway Interaction Database).

Entrez ID	Gene	Entrez ID	Gene	Entrez ID	Gene	Entrez ID	Gene
25	*ABL1*	2321	*VEGFR1*	5045	*FURIN*	7033	TFF3
52	*ACP1*	2324	*VEGFR3*	5054	*PAI*	7037	TFR
123	*ADRP*	2534	*FYN*	5155	*PDGFB*	7157	TP53
133	*ADM*	2549	*GAB1*	5159	*PDGFRB*	7319	UBE2A
207	*AKT1*	2624	*GATA2*	5170	*PDK1*	7410	VAV2
226	*ALDOA*	2645	*GCK*	5209	*PFKFB3*	7414	VCL
387	*RHOA*	2885	*GRB2*	5211	*PFKL*	7422	VEGFA
405	*ARNT*	2886	*GRB7*	5230	*PGK1*	7423	VEGFB
444	*ASPH*	2887	*GRB10*	5236	*PGM1*	7428	VHL
472	*ATM*	3090	*HIC1*	5243	*MDR1*	7525	YES1
581	*BAX*	3091	*HIF-1A*	5315	*PKM*	7852	CXCR4
664	*BNIP3*	3098	*HK1*	5335	*PLCG1*	8260	ARD1
768	*CAIX*	3099	*HK2*	5566	*PRKACA*	8553	BHLHE40
808	*CAM*	3162	*HMOX1*	5578	*PKKCA*	8648	SRC-1
867	*CBL*	3172	*HNF4*	5580	*PRKCD*	8826	IQGAP1
998	*CDC42*	3265	*HRAS*	5600	*MAPK11*	8828	NRP2
1003	*CDH5*	3303	*HSP70*	5606	*MKK3*	8829	NRP1
1026	*CDKN1A*	3315	*HSP27*	5728	*PTEN*	8877	SPHK1
1029	*CDKN2A*	3320	*HSP90*	5747	*FAK1*	9047	TSAD
1356	*CP*	3398	*ID2*	5770	*PTPN1*	9175	MLK
1385	*CREB1*	3484	*IGFBP1*	5771	*PTPN2*	9429	ABCG2
1445	*CSK*	3486	*IGFBP3*	5777	*SHP1*	9564	BCAR1
1499	*CTNNB1*	3689	*ITGB2*	5781	*SHP2*	10370	CITED2
1647	*GADD45A*	3725	*JUN*	5795	*DEP1*	10397	NDRG1
1785	*DNM2*	3791	*VEGFR2*	5829	*PXN*	10499	TIF2
1796	*DOK1*	3939	*LDHA*	5879	*RAC1*	10603	APS
1901	*S1PR1*	3952	*LEP*	5921	*RASGAP*	10818	FRS2
1906	*EDN1*	4035	*LRP1*	6093	*ROCK1*	10987	JAB1
2022	*ENG*	4170	*MCL1*	6095	*RORA4*	23607	CD2AP
2023	*ENO1*	4193	*MDM2*	6387	*CXCL12*	25759	SHC2
2033	*EP300*	4609	*MYC*	6461	*SHB*	29907	SNX15
2034	*HIF-2A*	4690	*NCK1*	6464	*SHC*	51564	HDAC7
2056	*EPO*	4734	*NEDD4*	6503	*SLAP*	54583	PHD2
2113	*ETS1*	4793	*NFKBIB*	6513	*GLUT1*	64344	IPAS
2185	*PYK2*	4843	*NOS2*	6648	*SOD2*	79365	BHLHE41
2235	*FECH*	4846	*ENOS*	6667	SP1	112399	PHD3
2241	*FER*	4869	*NPM1*	6714	SRC	171221	HSP40
2242	*FES*	4907	*NT5E*	7015	TERT		
2274	*FHL2*	5034	*P4HB*	7018	TF		

*Table 2. The top 50 down-regulated and up-regulated genes in Caki-1 vs HK-2, obtained by Rank Product analysis. *Expression values are reported in log_2 fold-change.*

Entrez ID	Gene Symbol	log_2FC*	Entrez ID	Gene Symbol	log_2FC*
6588	*SLN*	-7.07	10584	*COLEC10*	7.10
100033435	*SNORD116-24*	-6.57	54578	*UGT1A6*	7.05
2239	*GPC4*	-6.42	6288	*SAA1*	6.86
100128252	*LOC100128252*	-6.16	5552	*SRGN*	6.52
6578	*SLCO2A1*	-6.15	6594	*SMARCA1*	6.21
100033420	*SNORD116-8*	-5.83	216	*ALDH1A1*	6.18
91851	*CHRDL1*	-5.79	6372	*CXCL6*	5.96
4494	*MT1F*	-5.54	84740	*LOC84740*	5.77
83716	*CRISPLD2*	-5.41	1646	*AKR1C2*	5.74
255743	*NPNT*	-5.32	23743	*BHMT2*	5.71
729642	*NA*	-5.29	9615	*GDA*	5.60
4493	*MT1E*	-5.18	414899	*BLID*	5.50
100033413	*SNORD116-1*	-5.15	3910	*LAMA4*	5.49
26810	*SNORD41*	-5.13	91607	*SLFN11*	5.47
8519	*IFITM1*	-5.13	7412	*VCAM1*	5.43
26585	*GREM1*	-5.11	22998	*LIMCH1*	5.16
4642	*MYO1D*	-5.11	330	*BIRC3*	5.14
9118	*INA*	-5.10	11167	*FSTL1*	5.14
100033426	*SNORD116-14*	-4.92	80243	*PREX2*	4.97
677840	*SNORA71D*	-4.90	57020	*C16orf62*	4.94
6090	*RNY5*	-4.87	85477	*SCIN*	4.92
5080	*PAX6*	-4.85	23532	*PRAME*	4.76
894	*CCND2*	-4.83	8644	*AKR1C3*	4.65
100033427	*SNORD116-15*	-4.78	79745	*CLIP4*	4.65
4935	*GPR143*	-4.78	8754	*ADAM9*	4.65
100033434	*SNORD116-23*	-4.76	290	*ANPEP*	4.59
89944	*GLB1L2*	-4.69	2919	*CXCL1*	4.56
3772	*KCNJ15*	-4.66	653	*BMP5*	4.54
677807	*SNORA22*	-4.64	29103	*DNAJC15*	4.52
4501	*MT1X*	-4.59	1645	*AKR1C1*	4.48
1152	*CKB*	-4.55	79339	*OR51B4*	4.44
83543	*AIF1L*	-4.54	57016	*AKR1B10*	4.40
10734	*STAG3*	-4.47	10346	*TRIM22*	4.31
100033418	*SNORD116-6*	-4.46	837	*CASP4*	4.25
8357	*HIST1H3H*	-4.42	440712	*C1orf186*	4.21
10406	*WFDC2*	-4.38	344887	*LOC344887*	4.19
7351	*UCP2*	-4.37	5125	*PCSK5*	4.09
5730	*PTGDS*	-4.35	761	*CA3*	4.09
4060	*LUM*	-4.29	50484	*RRM2B*	4.09
7012	*TERC*	-4.27	51316	*PLAC8*	4.07
9365	*KL*	-4.23	6374	*CXCL5*	4.06
79887	*PLBD1*	-4.23	8411	*EEA1*	3.97
8291	*DYSF*	-4.23	7169	*TPM2*	3.97
283596	*SNHG10*	-4.22	2564	*GABRE*	3.97
164312	*LRRN4*	-4.20	401494	*PTPLAD2*	3.96
2348	*FOLR1*	-4.16	313	*AOAH*	3.96
677801	*SNORA14A*	-4.11	91351	*DDX60L*	3.91
6591	*SNAI2*	-4.08	80008	*TMEM156*	3.90
121504	*HIST4H4*	-4.05	9982	*FGFBP1*	3.90
1634	*DCN*	-4.04	4982	*TNFRSF11B*	3.89

Figure 1. Caki-1 vs HK-2: DAVID enrichment analysis on GO Biological Process terms for the 951 down-regulated genes (panel A) and the 1003 up-regulated genes (panel B). On the X-axis, the log(p-value) of DAVID enrichment test is reported.

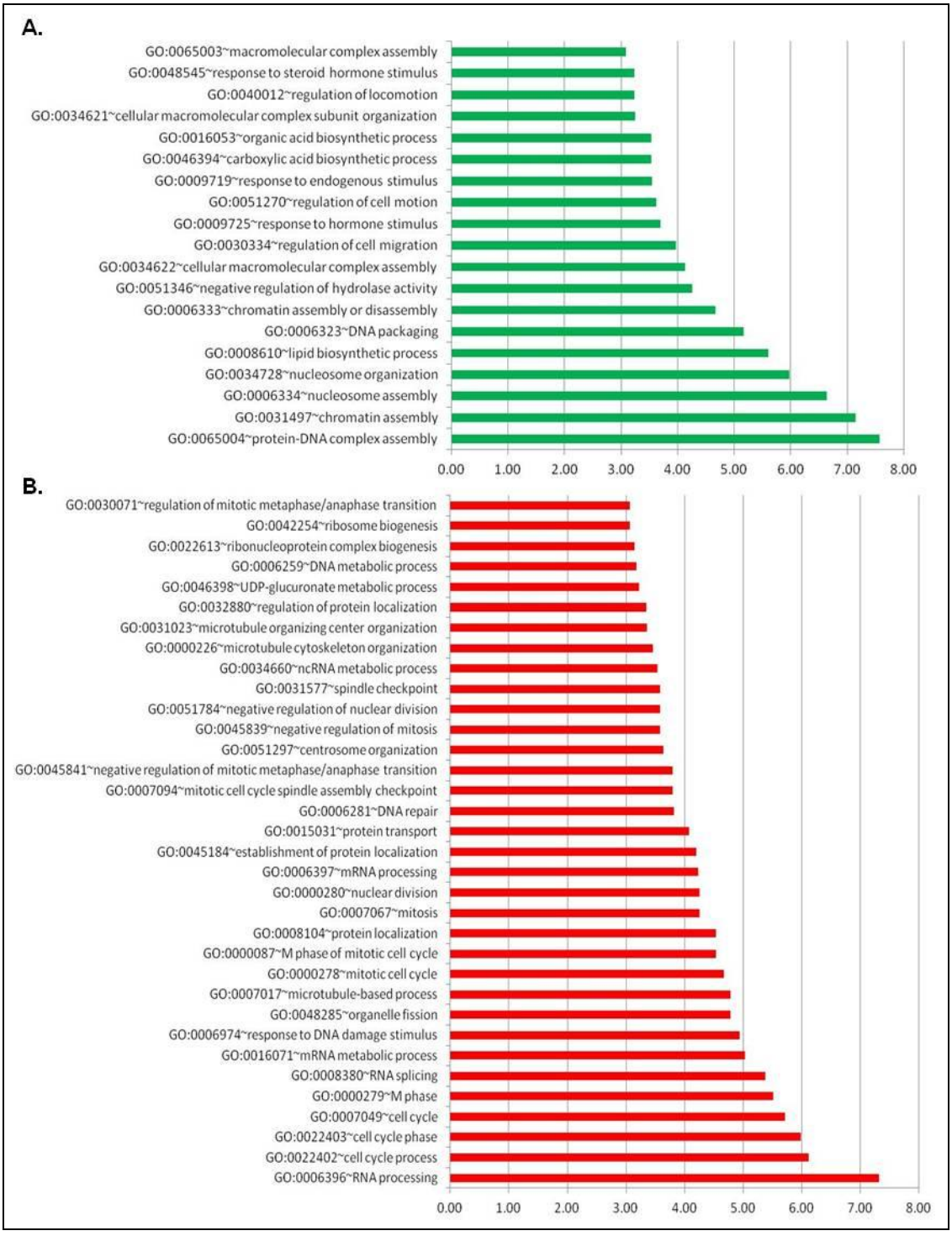

*Table 3. The top 50 down-regulated and up-regulated genes in Caki-2 vs HK-2, obtained by Rank Product analysis. *Expression values are reported in log_2 fold-change.*

Entrez ID	Gene Symbol	log_2FC*	Entrez ID	Gene Symbol	log_2FC*
3955	*LFNG*	-2.68	1645	*AKR1C1*	8.14
718	*C3*	-2.68	57016	*AKR1B10*	8.13
10266	*RAMP2*	-2.67	216	*ALDH1A1*	8.03
79814	*AGMAT*	-2.67	1646	*AKR1C2*	7.79
5010	*CLDN11*	-2.67	54600	*UGT1A9*	7.71
57462	*KIAA1161*	-2.67	54578	*UGT1A6*	6.94
10148	*EBI3*	-2.66	10149	*GPR64*	6.57
84952	*CGNL1*	-2.66	57834	*CYP4F11*	6.38
26805	*SNORD45A*	-2.65	6750	*SST*	6.36
4833	*NME4*	-2.65	22998	*LIMCH1*	6.33
10591	*C6orf108*	-2.65	1244	*ABCC2*	6.11
441246	*RPL35P5*	-2.64	5552	*SRGN*	6.11
79899	*PRR5L*	-2.64	5125	*PCSK5*	6.04
81888	*HYI*	-2.64	8653	*DDX3Y*	5.97
115123	*MARCH3*	-2.64	8644	*AKR1C3*	5.96
196740	*C10orf72*	-2.64	10686	*CLDN16*	5.87
6515	*SLC2A3*	-2.63	266977	*GPR110*	5.86
6136	*RPL12*	-2.63	1470	*CST2*	5.83
388282	*LOC388282*	-2.63	79745	*CLIP4*	5.82
7117	*TMSL3*	-2.63	9615	*GDA*	5.80
23452	*ANGPTL2*	-2.61	80243	*PREX2*	5.73
11147	*HHLA3*	-2.61	5268	*SERPINB5*	5.64
56911	*C21orf7*	-2.60	2877	*GPX2*	5.62
11337	*GABARAP*	-2.60	80008	*TMEM156*	5.58
23635	*SSBP2*	-2.59	256764	*WDR72*	5.57
5050	*PAFAH1B3*	-2.58	4051	*CYP4F3*	5.53
6446	*SGK1*	-2.58	8942	*KYNU*	5.51
8722	*CTSF*	-2.57	57020	*C16orf62*	5.51
29933	*GPR132*	-2.57	7348	*UPK1B*	5.45
4881	*NPR1*	-2.57	344887	*LOC344887*	5.37
26801	*SNORD48*	-2.56	54575	*UGT1A10*	5.26
2275	*FHL3*	-2.56	928	*CD9*	5.26
633	*BGN*	-2.56	7447	*VSNL1*	5.22
23371	*TENC1*	-2.55	29953	*TRHDE*	5.21
124976	*SPNS2*	-2.55	5144	*PDE4D*	5.21
25915	*NDUFAF3*	-2.55	767	*CA8*	5.17
3009	*HIST1H1B*	-2.54	64208	*POPDC3*	5.13
997	*CDC34*	-2.54	56923	*NMUR2*	5.09
54478	*FAM64A*	-2.54	771	*CA12*	5.00
9099	*USP2*	-2.54	6594	*SMARCA1*	4.94
27122	*DKK3*	-2.54	23657	*SLC7A11*	4.94
79883	*PODNL1*	-2.54	55790	*CSGALNACT1*	4.91
6297	*SALL2*	-2.53	23743	*BHMT2*	4.78
2947	*GSTM3*	-2.52	23532	*PRAME*	4.72
25864	*ABHD14A*	-2.52	9086	*EIF1AY*	4.72
79897	*RPP21*	-2.52	79695	*GALNT12*	4.71
8092	*ALX1*	-2.52	51313	*C4orf18*	4.70
256227	*MGC87042*	-2.52	1469	*CST1*	4.70
93145	*OLFM2*	-2.51	330	*BIRC3*	4.68
79966	*SCD5*	-2.51	23266	*LPHN2*	4.67

Figure 2. Caki-2 vs HK-2: DAVID enrichment analysis on GO Biological Process terms for the 951 down-regulated genes (panel A) and the 1007 up-regulated genes (panel B). On the X-axis, the log(p-value) of DAVID enrichment test is reported.

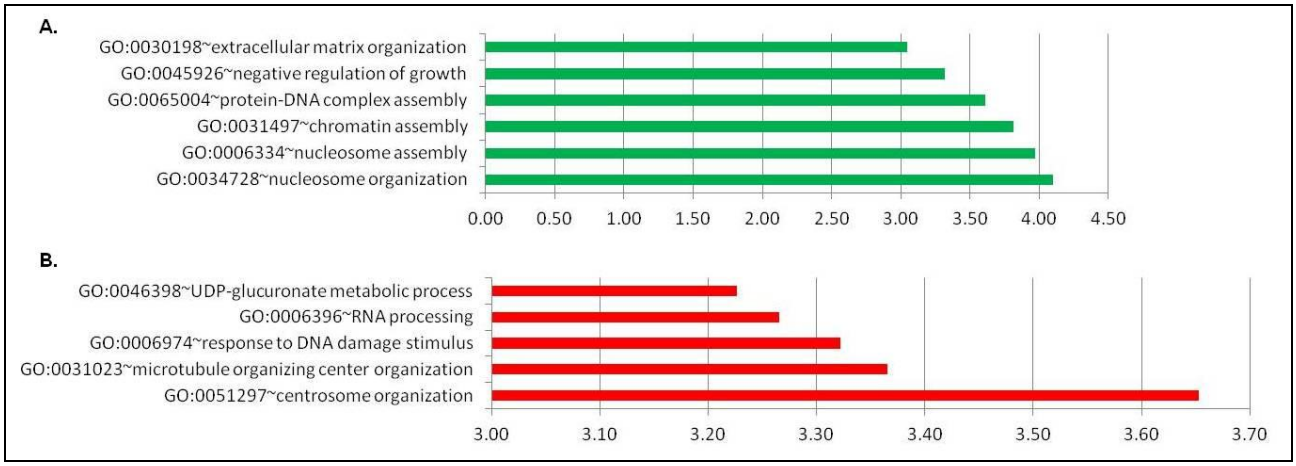

*Table 4. The top 50 down-regulated and up-regulated genes in A498 vs HK-2, obtained by Rank Product analysis. *Expression values are reported in log_2 fold-change.*

Entrez ID	Gene Symbol	log_2FC*	Entrez ID	Gene Symbol	log_2FC*
3303	*HSPA1A*	-7.63	216	*ALDH1A1*	7.61
1004	*CDH6*	-7.48	10686	*CLDN16*	6.37
6588	*SLN*	-7.23	10584	*COLEC10*	6.21
7345	*UCHL1*	-6.03	6594	*SMARCA1*	6.05
100128252	*LOC100128252*	-6.01	79745	*CLIP4*	5.88
91663	*MYADM*	-5.90	51702	*PADI3*	5.64
29015	*SLC43A3*	-5.88	91607	*SLFN11*	5.57
26585	*GREM1*	-5.59	57020	*C16orf62*	5.51
8355	*HIST1H3G*	-5.56	85477	*SCIN*	5.38
4060	*LUM*	-5.48	5919	*RARRES2*	5.31
729642	*NA*	-5.30	8754	*ADAM9*	5.21
684	*BST2*	-5.30	6335	*SCN9A*	5.12
3009	*HIST1H1B*	-5.18	5341	*PLEK*	5.11
677840	*SNORA71D*	-5.09	928	*CD9*	5.05
2239	*GPC4*	-5.06	837	*CASP4*	5.05
26810	*SNORD41*	-5.02	164781	*WDR69*	5.03
8342	*HIST1H2BM*	-5.00	10060	*ABCC9*	4.75
3772	*KCNJ15*	-5.00	7070	*THY1*	4.69
4935	*GPR143*	-5.00	23266	*LPHN2*	4.58
3018	*HIST1H2BB*	-4.98	10346	*TRIM22*	4.56
4316	*MMP7*	-4.82	64881	*PCDH20*	4.53
5730	*PTGDS*	-4.80	5649	*RELN*	4.48
8357	*HIST1H3H*	-4.76	346389	*MACC1*	4.38
2202	*EFEMP1*	-4.73	23532	*PRAME*	4.37
8519	*IFITM1*	-4.72	23230	*VPS13A*	4.33
4494	*MT1F*	-4.69	64097	*EPB41L4A*	4.32
89944	*GLB1L2*	-4.68	5144	*PDE4D*	4.25
100033420	*SNORD116-8*	-4.65	3676	*ITGA4*	4.17
10653	*SPINT2*	-4.49	9723	*SEMA3E*	4.16
7351	*UCP2*	-4.47	4065	*LY75*	4.13
6090	*RNY5*	-4.45	54809	*SAMD9*	4.11
100033434	*SNORD116-23*	-4.36	6568	*SLC17A1*	4.04
8904	*CPNE1*	-4.32	3113	*HLA-DPA1*	4.01
10734	*STAG3*	-4.31	2170	*FABP3*	4.00
8368	*HIST1H4L*	-4.27	55031	*USP47*	3.99
677801	*SNORA14A*	-4.26	50484	*RRM2B*	3.99
4995	*OR3A2*	-4.25	84740	*LOC84740*	3.98
100127980	*LOC100127980*	-4.19	440706	*NA*	3.95
2878	*GPX3*	-4.19	343450	*KCNT2*	3.94
8354	*HIST1H3I*	-4.18	55075	*UACA*	3.92
6920	*TCEA3*	-4.18	100129762	*NA*	3.92
3383	*ICAM-1*	-4.15	158471	*PRUNE2*	3.91
100033435	*SNORD116-24*	-4.15	219285	*SAMD9L*	3.90
10457	*GPNMB*	-4.13	79780	*CCDC82*	3.89
1634	*DCN*	-4.13	120892	*LRRK2*	3.84
100033413	*SNORD116-1*	-4.13	50940	*PDE11A*	3.82
7851	*MALL*	-4.10	51747	*LUC7L3*	3.81
90649	*ZNF486*	-4.06	7130	*TNFAIP6*	3.81
8356	*HIST1H3J*	-4.01	10111	*RAD50*	3.80
7102	*TSPAN7*	-4.01	132671	*SPATA18*	3.80

Figure 3. A498 vs HK-2: DAVID enrichment analysis on GO Biological Process terms for the 971 down-regulated genes (panel A) and the 997 up-regulated genes (panel B). On the X-axis, the log(p-value) of DAVID enrichment test is reported.

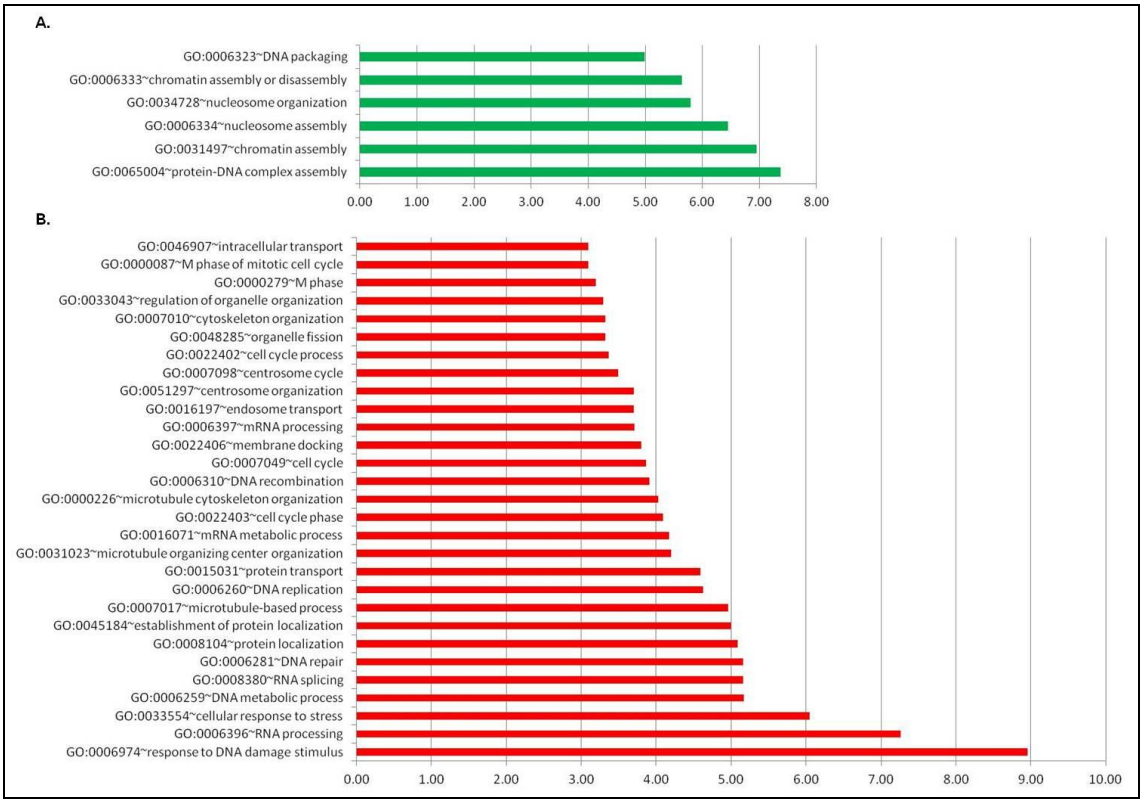

Table 5. List of qPCR TaqMan® MicroRNA Expression Assays (purchased from Applied Biosystems, Life Technologies, Inc. Carlsbad, CA, USA). RNU48 was used as endogenous control to normalize miRNA expression levels.

TaqMan® MicroRNA Assay	Assay ID
hsa-miR-21	000397
hsa-miR-34a	000426
hsa-miR-143	002249
hsa-miR-145	002278
hsa-miR-146a	000468
hsa-miR-149	002255
hsa-miR-152	000475
hsa-miR-183	002269
hsa-miR-205	000509
hsa-miR-210	000512
hsa-miR-221	000524
RNU48	001006

*Table 6. List of down-regulated (24) and up-regulated (26) miRNAs in Caki-1 vs HK-2, obtained by Rank Product analysis. *Expression values are reported in log_2 fold-change.*

MIRNA	log_2FC*	MIRNA	log_2FC*
hsa-miR-205	-4.68	hsa-miR-100	5.59
hsa-miR-182	-3.40	hsa-miR-125b	5.41
hsa-miR-335	-2.84	hsa-miR-146a	3.58
hsa-miR-129-star	-2.81	hsa-miR-494	2.93
hsa-miR-103	-2.47	hsa-let-7a	2.73
hsa-miR-130b	-2.32	hsa-miR-146b-5p	2.69
hsa-miR-129-3p	-2.23	hsa-miR-99a	2.65
hsa-miR-107	-2.11	hsa-miR-224	2.57
hsa-miR-145	-2.09	hsa-miR-125b-1-star	2.55
hsa-miR-576-3p	-2.03	hsa-let-7f	2.50
hsa-miR-93	-1.84	hsa-miR-29b-1-star	2.43
hsa-miR-342-3p	-1.71	hsa-miR-1207-5p	2.11
hsa-miR-183	-1.71	hsa-miR-663b	1.97
hsa-miR-19b	-1.60	hsa-let-7g	1.86
hsa-miR-132	-1.60	hsa-miR-574-5p	1.85
hsa-miR-708	-1.57	hsa-let-7c	1.74
hsa-miR-106b	-1.56	hsa-miR-34a	1.58
hsa-miR-197	-1.48	hsa-miR-675	1.53
hsa-miR-16	-1.43	hsa-miR-196a	1.48
hsa-miR-99b	-1.43	hsa-miR-27a-star	1.39
hsa-miR-574-3p	-1.43	hsa-miR-29a	1.25
hsa-miR-17	-1.34	hsa-miR-128	1.19
hsa-miR-606	-1.32	hsa-miR-1303	1.08
hsa-miR-143	-1.31	hsa-miR-181d	1.05
		hsa-miR-484	1.01
		hsa-miR-23a	0.98

*Table 7. List of down-regulated (30) and up-regulated (32) miRNAs in Caki-2 vs HK-2, obtained by Rank Product analysis. *Expression values are reported in log_2 fold-change.*

MIRNA	log_2FC*	MIRNA	log_2FC*
hsa-miR-205	-4.57	hsa-miR-100	2.31
hsa-miR-155	-3.91	hsa-miR-34a	2.30
hsa-miR-21	-3.40	hsa-miR-210	2.19
hsa-miR-25	-2.90	hsa-miR-185	2.18
hsa-miR-28-3p	-2.88	hsa-miR-663	2.09
hsa-miR-19b	-2.87	hsa-miR-23a-star	2.03
hsa-miR-1826	-2.86	hsa-miR-138	1.92
hsa-miR-193a-5p	-2.68	hsa-miR-486-5p	1.84
hsa-miR-708	-2.62	hsa-miR-193b-star	1.84
hsa-miR-30a-star	-2.53	hsa-miR-378	1.81
hsa-miR-27b	-2.39	hsa-miR-320d	1.79
hsa-miR-29a	-2.10	hsa-miR-140-3p	1.70
hsa-miR-221	-2.04	hsa-miR-30c-2-star	1.70
hsa-miR-26a	-2.02	hsa-miR-423-5p	1.67
hsa-miR-145	-1.90	hsa-miR-324-5p	1.66
hsa-miR-183	-1.84	hsa-miR-423-3p	1.64
hsa-miR-197	-1.83	hsa-miR-31	1.54
hsa-miR-152	-1.83	hsa-miR-24	1.41
hsa-miR-149	-1.82	hsa-miR-193b	1.41
hsa-miR-182	-1.78	hsa-miR-1228-star	1.38
hsa-miR-200b	-1.71	hsa-miR-149-star	1.37
hsa-miR-30c	-1.62	hsa-miR-638	1.37
hsa-miR-20a	-1.56	hsa-miR-629	1.37
hsa-miR-132	-1.54	hsa-miR-125b	1.34
hsa-let-7i	-1.53	hsa-miR-146a	1.34
hsa-miR-28-5p	-1.50	hsa-miR-320a	1.32
hsa-miR-130a	-1.48	hsa-miR-320b	1.32
hsa-miR-181b	-1.41	hsa-miR-671-5p	1.28
hsa-let-7f	-1.33	hsa-miR-625-star	1.26
hsa-miR-342-3p	-1.23	hsa-miR-17-star	1.25
		hsa-miR-151-5p	1.24
		hsa-miR-720	1.23

*Table 8. List of down-regulated (36) and up-regulated (18) miRNAs in Caki-2 vs HK-2, obtained by Rank Product analysis. *Expression values are reported in log_2 fold-change.*

MIRNA	log_2FC*	MIRNA	log_2FC*
hsa-miR-31	-4.88	hsa-miR-127-3p	2.71
hsa-miR-205	-4.73	hsa-miR-194	2.08
hsa-miR-345	-2.27	hsa-miR-29a	2.07
hsa-miR-125a-5p	-2.17	hsa-miR-192	2.01
hsa-miR-145	-2.12	hsa-miR-34a	1.93
hsa-miR-574-3p	-2.05	hsa-miR-34c-5p	1.54
hsa-miR-210	-1.87	hsa-miR-134	1.28
hsa-miR-99b	-1.82	hsa-miR-29b-1-star	1.22
hsa-miR-197	-1.80	hsa-miR-34c-3p	1.20
hsa-miR-28-5p	-1.74	hsa-miR-27a	1.18
hsa-let-7e	-1.48	hsa-miR-548a-3p	1.14
hsa-miR-149	-1.45	hsa-miR-20a	1.11
hsa-miR-361-5p	-1.44	hsa-miR-379	1.08
hsa-miR-130b	-1.43	hsa-miR-132-star	1.05
hsa-miR-532-5p	-1.42	hsa-miR-1288	1.05
hsa-miR-152	-1.41	hsa-miR-30a	0.99
hsa-miR-15b	-1.36	hsa-miR-1280	0.96
hsa-miR-193a-5p	-1.36	hsa-miR-484	0.88
hsa-miR-362-5p	-1.35		
hsa-miR-132	-1.29		
hsa-miR-28-3p	-1.29		
hsa-miR-342-3p	-1.28		
hsa-miR-183	-1.26		
hsa-miR-92b	-1.24		
hsa-miR-23b	-1.24		
hsa-miR-500	-1.22		
hsa-miR-143	-1.15		
hsa-miR-1307	-1.15		
hsa-miR-146a	-1.14		
hsa-miR-107	-1.10		
hsa-miR-625	-1.10		
hsa-miR-20b	-1.10		
hsa-miR-221	-1.09		
hsa-miR-103	-1.07		
hsa-miR-744	-1.06		
hsa-miR-106b-star	-1.03		

Table 9. List of qPCR TaqMan® Gene Expression Assays (purchased from Applied Biosystems, Life Technologies, Inc. Carlsbad, CA, USA). ACTB was used as housekeeping gene (endogenous control) to normalize gene expression.

TaqMan® Gene Expression Assay	Assay ID
ATM	Hs01112307_m1
CDC27	Hs00265810_m1
FER	Hs01099028_m1
GRB10	Hs00193409_m1
NT5E	Hs01573922_m1
PPARD	Hs00987011_m1
RPS6KB1	Hs00177357_m1
USP2	Hs00275859_m1
ACTB	Hs99999903_m1

Table 10. Counts of predicted target genes for each DEM as calculated by MAGIA tool.

MIRNA	No. PREDICTED TARGET GENES	MIRNA	No. PREDICTED TARGET GENES
hsa-miR-145	280	hsa-miR-15b	11
hsa-miR-205	237	hsa-miR-103	10
hsa-miR-34a	217	hsa-miR-194	10
hsa-miR-1228*	153	hsa-miR-183	9
hsa-miR-663	126	hsa-miR-324-5p	9
hsa-miR-143	76	hsa-miR-23a	9
hsa-miR-31	58	hsa-miR-196a	8
hsa-miR-30a*	48	hsa-miR-224	8
hsa-miR-125b-1*	46	hsa-miR-146b-5p	8
hsa-miR-210	44	hsa-miR-125b	8
hsa-miR-25	42	hsa-miR-29a	7
hsa-miR-24	41	hsa-miR-130a	6
hsa-miR-345	37	hsa-miR-125a-5p	6
hsa-miR-26a	37	hsa-miR-342-3p	6
hsa-miR-155	35	hsa-miR-181d	5
hsa-miR-29b-1*	32	hsa-miR-130b	5
hsa-miR-127-3p	31	hsa-miR-100	4
hsa-miR-193b	30	hsa-miR-379	4
hsa-miR-185	30	hsa-miR-34c-5p	4
hsa-miR-28-3p	29	hsa-let-7f	4
hsa-let-7a	28	hsa-miR-99a	3
hsa-miR-197	27	hsa-miR-193a-5p	3
hsa-miR-423-3p	26	hsa-miR-19b	3
hsa-miR-221	24	hsa-miR-192	2
hsa-miR-106b	23	hsa-miR-671-5p	2
hsa-miR-138	23	hsa-miR-1207-5p	2
hsa-miR-181b	23	hsa-miR-28-5p	2
hsa-miR-27b	21	hsa-miR-128	2
hsa-miR-320d	19	hsa-miR-335	1
hsa-miR-23b	19	hsa-miR-1303	1
hsa-miR-200b	19	hsa-miR-484	1
hsa-miR-708	17	hsa-miR-149	1
hsa-miR-486-5p	17	hsa-miR-500	1
hsa-miR-17	16	hsa-miR-574-3p	1
hsa-miR-20a	16	hsa-miR-606	1
hsa-miR-107	14	hsa-miR-625	1
hsa-miR-16	13	hsa-miR-132	1
hsa-let-7e	13	hsa-miR-629	1
hsa-miR-146a	13	hsa-miR-134	1
hsa-miR-151-5p	13	hsa-miR-27a*	1
hsa-miR-23a*	12	hsa-miR-1826	1
hsa-let-7i	12	hsa-miR-720	1
hsa-let-7c	12	hsa-miR-744	1
hsa-miR-182	11	hsa-miR-152	1
		Tot. = 88	Tot. = 2236

10 ACKNOWLEDGEMENTS

This work and PhD fellowships have been supported by grants from the Doctoral School of Molecular Medicine (University of Milan), from CARIPLO Foundation TOSCA Project, from CISI (Centro Interdipartimentale Studi biomolecolari e applicazioni Industriali) and from the Italian Ministry of University and Research (MIUR): FIRB 2003 (RBLA03ER38_004), PRIN 2008 (WY2TY9_002), FIRB 2007 (RBRN07BMCT, Rete nazionale per lo studio del proteoma umano).

A special acknowledgement to Prof.ssa Cristina Battaglia (Dept. Biomedical Sciences and Technologies, University of Milan) for supervision and coordination of study design, data analysis, data interpretation and writing of this thesis; Dott. Gianluca De Bellis (ITB-CNR, Milan) for supporting the research project; Prof. Roberto Perego and Dott.ssa Cristina Bianchi (University of Milano-Bicocca) for cell cultures; Prof.ssa Rosanna Asselta (University of Milan) for providing the DNA Sequencer ABI 3130XL instrument; Dott.ssa Stefania Bortoluzzi and Dott.ssa Marta Biasiolo (University of Padua) for integrative genomic data analysis.

I would like to sincerely thank my lab team: Dott.ssa Ingrid Cifola (ITB-CNR, Milan), Dott.ssa Eleonora Mangano (ITB-CNR, Milan), Dott.ssa Maria Carla Proverbio (University of Milan), for their precious help and expertise, and Dott. Fabio Frascati for statistical data analysis.

A special thanks goes to Marco Pellegrini for his precious help in thesis formatting.

Finally, I would like to gratefully thank my family and Enzo for their constant support and encouragement.

11 SCIENTIFIC PRODUCTS

“Gene expression profiling of A549 cells exposed to Milan PM2.5”. M. Gualtieri, E. Longhin, M. Mattioli, P. Mantecca, **V. Tinaglia**, E. Mangano, M.C. Proverbio, M. Camatini and C. Battaglia. *Toxicology Letters* (in press).

“Molecular portrait of clear cell renal cell carcinoma: an integrative analysis of gene expression profiling and genomic copy number”. C. Battaglia, E. Mangano, S. Bicciato, F. Frascati, S. Nuzzo, **V. Tinaglia**, C. Bianchi, R.A. Perego and I. Cifola. Book: *Emerging research and treatments in renal cell carcinoma*, ISBN 978-953-307-841-0 (in press).

“Differential expression of microRNAs in subjects exposed to metal rich particulate matter”. L. Angelici, V. Motta, F. Nordio, F. Frascati, **V. Tinaglia**, V. Bollati, P.A. Bertazzi, C, Battaglia and A. Baccarelli. (Poster: ISEE 2011 Conference, Barcellona, 13-16 September 2011).

“Integrated genomics analysis of gene and miRNA expression profiles in clear cell renal carcinoma cell lines”. **V. Tinaglia**, I. Cifola, F. Frascati, E. Mangano, M. Biasolo, M.C. Proverbio, S. Bortoluzzi, V. Di Stefano, C. Bianchi, R. Perego and C. Battaglia. (Poster: CNIO Frontiers Meeting 2011 Madrid, 28-30 March 2011).

“Reconstruction and study of post-transcriptional regulatory networks governing tumour development and progression by integrated analysis of miRNAs and targets expression profiles”. M. Biasiolo, G. Sales, A. Coppe, A. Bisognin, **V. Tinaglia**, I. Cifola, F. Frascati, E. Mangano, M. Lionetti, L. Agnelli, A. Neri, C. Battaglia, C. Romualdi and S. Bortoluzzi. (Poster: AIBGXII, Trento, 8-9 September 2010).

“Integration of gene and miRNA expression profiles in clear cell renal carcinoma cell lines and relationship with *VHL* gene status” C. Battaglia, **V. Tinaglia**, I. Cifola, F. Frascati, E. Mangano, M. Biasiolo, S. Bortoluzzi, S. Bombelli, C. Bianchi and R. Perego. Meeting Abstract: *EJC SUPPLEMENTS*, 8 (5): 206-206 817 June 2010.

“Integration of gene and miRNA expression profiles in clear cell renal carcinoma cell lines and relationship with VHL gene status”. C. Battaglia, **V. Tinaglia**, I. Cifola, F. Frascati, E. Mangano, M. Biasiolo, S. Bortoluzzi, S. Bombelli, C. Bianchi and R. Perego. (Poster: EACR21 Oslo, 26-29 June 2010).